The Fluctuating Gap Model

Dissertation
zur
Erlangung des Doktorgrades (Dr. rer. nat.)
der
Mathematisch-Naturwissenschaftlichen Fakultät
der
Rheinischen Friedrich-Wilhelms-Universität Bonn

vorgelegt von
Xiaobin Cao

aus
Jiangsu, China

Bonn, January 2011

Angefertigt mit Genehmigung der Mathematisch-Naturwissenschaftlichen Fakultät der
Rheinischen Friedrich-Wilhelms-Universität Bonn

1. Gutachter: Prof. Dr. Hartmut Monien

2. Gutachter: Prof. Dr. Carsten Urbach

Tag der Promotion: 25.01.2011

Erscheinungsjahr: 2011

Abstract

The quasi-one-dimensional systems exhibit some unusual phenomenon, such as the Peierls instability [1], the pseudogap phenomena [2] and the absence of a Fermi-Dirac distribution function line shape in the photoemission spectroscopy [3]. Ever since the discovery of materials with highly anisotropic properties, it has been recognized that fluctuations play an important role above the three-dimensional phase transition. This regime where the precursor fluctuations are presented can be described by the so called fluctuating gap model (FGM) which was derived from the Fröhlich Hamiltonian to study the low energy physics of the one-dimensional electron-phonon system. Not only is the FGM of great interest in the context of quasi-one-dimensional materials [1, 2], liquid metal [4] and spin waves above T_c in ferromagnets [5], but also in the semiclassical approximation of superconductivity, it is possible to replace the original three-dimensional problem by a directional average over effectively one-dimensional problem [6] which in the weak coupling limit is described by the FGM [7, 8]. In this work, we investigate the FGM in a wide temperature range with different statistics of the order parameter fluctuations. We derive a formally exact solution to this problem and calculate the density of states, the spectral function and the optical conductivity. In our calculation, we show that a Dyson singularity appears in the low energy density of states for Gaussian fluctuations in the commensurate case. In the incommensurate case, there is no such kind of singularity, and the zero frequency density of states varies differently as a function of the correlation lengths for different statistics of the order parameter fluctuations. Using the density of states we calculated with non-Gaussian order parameter fluctuations, we are able to calculate the static spin susceptibility which agrees with the experimental data very well. In the calculation of the spectral functions, we show that as the correlation increases, the quasi-particle peak broadens and splits into two bands, which indicates a break down of the Fermi liquid picture. The comparison between our results and those obtained using the second-order Born approximation shows that the perturbation theory is unreliable near the Fermi surface. Also with our non-Gaussian fluctuations, our calculation of spectral functions can explain the experimental angle-resolved photoemission spectroscopy (ARPES) data in a reasonable way. At last, the optical conductivity calculation confirms a zero dc conductivity in our model, and suggests that a finite dc conductivity obtained in a former calculation is just an artifact of the perturbation theory.

Acknowledgments

First of all, I would like to express my deepest gratitude to my supervisor Professor Dr. Hartmut Monien, who in the first place gave me the great opportunity to work with him. I could not have finished this work without his support and patience. I can always count on his profound knowledge in physics and rich research experience whenever I came up against problems in my work. Other than that, his broad knowledge in various areas makes even a casual conversation with him beneficial. I have learned so much from him not only in physics but also in many other aspects.

I am also grateful to my colleagues whom I have spent most of my time with in Germany. The discussions with them are always pleasant and fruitful. Special thanks would go to my former colleague Gang Li, who is also a very good friend. He never failed to give me great encouragement and suggestion. Also his help to my personal life made the living in Germany much easier.

Furthermore, I would like to extend my thanks to Dr. Andreas Wisskirchen who has been taking care of all the computers and keep many things going on in our institute. I troubled him quit a lot of times about my financial support, and he never complained. I also would like to thank Mrs Dagmar Fassbender and Patricia Zündorf for their help in various situations.

Last but not least, I would like to thank my parents, who support me all the way from the very beginning of my study. I am also thankful to all my friends for their support and encouragement.

Contents

Chapter 1

The Fluctuating Gap Model

1.1 Introduction

A large number of organic and inorganic compounds have crystal structure in which the fundamental structure units form a linear chain. The overlap of the electronic wavefunctions in a specific direction leads to strongly anisotropic electron bands. These kind of compounds which have characteristic one-dimensional metallic behavior are usually called quasi-one-dimensional or low-dimensional materials. As the temperature is lowered, they undergo a Peierls transition and develop a charge density wave (CDW) [1]. A qualitative understanding of the Peierls instability can already be gained by coupling independent electrons to phonons and treating the phonon filed which can be identified as the order parameter field in a mean-field picture. This mean-field solution leads to a finite transition temperature T_c^{MF} at which long-range order develops. The transition is due to their quasi-one-dimensional nature which results in a (perfectly) nested Fermi surface. However, this is just an artifact of the mean-field approximation. As is well known, a strictly one-dimensional system with only short-range interaction does not develop a long-range order at any finite temperature. The phase transition to the charge density wave which would break a continuous symmetry is then prevented by the fluctuations of the order parameters. Real quasi-one-dimensional materials are highly anisotropic three-dimensional system. As the temperature is lowered, the electronic interchain Coulomb interaction and tunneling results a finite transition temperature T_{3D} below which the three-dimensional long-range order occurs. For weak interchain coupling, we usually have $T_{3D} \approx T_c^{MF}/4$ [2]. The region below T_c^{MF} is characterized by one-dimensional fluctuations which at some temperature $T^* > T_{3D}$, crossover to fluctuations with two- or three- dimensional character. T^* is the temperature at which the transverse correlation length becomes comparable to the interchain spacing.

Besides the Peierls instability, the quasi-one-dimensional materials exhibit many other unusual phenomena such as pseudogaps which can be observed in various experiments like the spin susceptibility [9], specific heat and optical conductivity [10, 11, 12]. The pseudogap phenomenon was first explained by considering the one-dimensional fluctuations precursor to the real CDW phase transition. Ever since the discovery of quasi-one-dimensional materials, it has been recognized that fluctuation effects play an important role above the three-dimensional transition temperature T_{3D} since the reduction of phase space from three dimension to one dimension makes fluctuations very important. At low

temperature, the order parameter fluctuations vary slowly in space and time, therefore has significant amplitude to back scatter electrons. The back scattering will tend to open a gap but will not do so completely because the order is not perfect. In 1973, Lee, Rice and Anderson introduced the one-dimensional so-called fluctuating gap model (FGM), in which fluctuations of the phonon field are described by a static disorder potential, to study the regime above the phase transition where precursor fluctuations are presented [2]. They argued that one need only consider the leading perturbative one-boson-exchange diagram for the self-energy, and resulted in a suppression of the low energy density of states. The density of states was suppressed from the non-interacting value by a factor proportional to the inverse of the correlation length of the scattering. Later on, a lot of effort has been made and various approximations and methods have been used to solve the problem. Method based on solving a stationary Fokker-Planck equation [13] can only obtain the exact result for the density of states for Gaussian order parameter fluctuations in the white-noise limit. A few years later, Sadovskii [14, 15] obtained a continued-fraction expansion of the single-particle Green's function, which was often regarded as the one and only exact solution of the FGM for Gaussian order parameter fluctuations with finite correlation lengths [16, 17, 18]. However a recent paper by Tchernyshyov [19] showed that a class of diagrams was neglected by Sadovskii and therefore the results were totally unphysical. Numerical calculation based on exact diagonalization methods [20] or the phase formalism [21, 22, 23] gave exact result for the density of states for Gaussian order parameter fluctuations. Both calculations showed that Gaussian order parameter fluctuations are inapplicable at low temperature where even a modest suppression of the density of states requires an enormous correlation length and also, since the amplitude fluctuations got frozen out, a hard gap should appear in the limit $T \to 0$ if the quantum fluctuations are neglected. On the other hand, models taking into account phase fluctuations only [22] tend to overestimate the suppression of the electronic density at the Fermi surface and cannot describe the right physics above the mean-field phase transition. Using a standard Ginzburg-Landau theory, Monien [24] was able to numerically calculate the density of states for the crossover regime to non-Gaussian order parameter fluctuations. In the same manner, Bartosch has put forward the so called stochastic method originated by Halperin [25] to get formally exact results for different electronic properties [26, 27].

The FGM is of great interest not only in the context of quasi-one-dimensional materials [2, 28, 29, 30], but also of liquid metals [4] and spin waves above T_c in ferromagnets [5]. Recently, the pseudogaps observed in the underdoped phase of high temperature superconductors have been proven to be similar to that found in the charge density wave materials [31, 32, 33]. The non-Fermi liquid behavior of the quasi-one-dimensional systems revealed by the high-quality Angle-Resolved Photoemission Spectroscopy (ARPES) data obtained from various materials [3, 34, 35, 36, 37, 38, 39] has some common features to those observed in the high-T_c superconductors. In the semiclassical approximation of superconductivity, it is possible to replace the original three-dimensional problem by a directional average over effectively one-dimensional problem [6] which in the weak coupling limit are described by the FGM. And also a generalization of the FGM towards higher dimensions to describe the phase above the phase-transition in underdoped high temperature superconductors by anti-ferromagnetic short-range order fluctuations was considered in Refs. [17] and [18]. The connection between pseudogaps observed in quasi-one-dimensional systems and underdoped phase of high temperature superconductors makes the better

understanding of the pseudogap phase more interesting and has drawn great attention on the fluctuating gap model [16, 17, 18]. Under this circumstance, it is really necessary to do a complete survey on the FGM, and in this work, we are going to investigate electronic properties such as the density of states, the spectral function and also the optical conductivity in a wide temperature range.

This work is organized as follows: In Chapter 1, we first introduce the Frölich Hamiltonian [40] which was proposed to describe the one-dimensional electron-phone system. Using the Euclidean functional integral approach, we obtain an action which after integrating out the fermionic degree of freedom can be approximated by a static free energy functional of the phonon field. Expanding this functional for small field and keeping only the relevant term, we are left with the famous Ginzburg-Landau functional to describe the static phonon field which is identified as the order parameter field. Then we introduce the Fluctuating Gap Model as an effective model to describe the low energy physics of quasi one-dimensional materials. We solve this model in the mean-field case and show that a charge-density wave appears below the phase transition temperature T_c^{MF}.

Chapter 2 will focus on the order parameter fluctuations described by the Ginzburg-Landau functional. When the temperature is relatively high, the second order term dominates, and the order parameter fluctuations show a Gaussian characteristic behavior. Using the Ornstein-Uhlenbeck process we can generate fluctuating order parameters with required correlation length and expectation value of the square of the order parameters. At very low temperature, the amplitude fluctuations get frozen out and only the phase fluctuations play a role. For a fixed finite correlation length, we will show that the phase fluctuations can be described by a simple Wiener process. In between, close to the transition temperature, we need to consider the higher order term in the Ginzburg-Landau functional. By using the transfer matrix method, we will derive a general Langevin equation to generate configurations of the order parameters. The drift term in the Langevin equation is approximated by a polynomial in $|\Delta|$.

In Chapter 3, we start to investigate the FGM with some approximated methods. In the perturbation theory, we introduce the second order Born approximation, which was first used by Lee, Rice and Anderson [2] to explain the pseudogap phase. To go beyond the perturbative calculation, we will also examine the method based on solving a Fokker-Planck equation. We show that some exact results can be obtained but just for some special realization of the order parameter fluctuations. In the last part of this chapter, we then put forward the stochastic method first proposed by Halperin [25] and derive a formally exact method to calculate electronic properties including the density of states, the spectral function and the optical conductivity. The method is applicable to all kinds of order parameter fluctuations, no mater Gaussian or non-Gaussian.

In Chapter 4. the numerical results are presented. We use finite element method (FEM) to solve a set of Fokker-Planck equations. Once we have the stationary solutions to these equations, by using the numerical integration, we can finally get all the electronic properties we want. We present our calculation of the density of states, the spectral function and the optical conductivity for different statistics of the order parameter fluctuations. They are compared with those results obtained using other methods. In addition some experimental accessible quantities such as the static spin susceptibility and angle-resolved photoemission spectroscopy (ARPES) lines are calculated using our results of the density of states and the spectral function. Both results show very good agreement with

the experimental data. Finally we make our conclusion in the last chapter.

1.2 Fröhlich Hamiltonian and Euclidean Action

The Frölich Hamiltonian was proposed by Fröhlich [40] in 1954 to describe a one-dimensional electron-phonon system. The Hamiltonian is

$$H = \sum_{k,\sigma} \epsilon_k c^\dagger_{k,\sigma} c_{k,\sigma} + \sum_q \omega_q b^\dagger_q b_q + \sum_q \frac{g_q}{\sqrt{L}} \hat{\rho}^\dagger_q (b_{q+K(q)} + b^\dagger_{-q-K(q)}), \tag{1.1}$$

where $c^\dagger_{k,\sigma}$ ($c_{k,\sigma}$) creates (annihilates) an electron with energy ϵ_k and spin σ. Their anti-commutators are

$$\{c_{k,\sigma}, c_{k',\sigma'}\} = 0, \{c_{k,\sigma}, c^\dagger_{k',\sigma'}\} = \delta_{\sigma,\sigma'}\delta_{k,k'}. \tag{1.2}$$

$b^\dagger_q$ and b_q are creation and annihilation operators of the phonons with phonon dispersion ω_q, which satisfy the commutation relations

$$[b_q, b_{q'}] = 0, [b_q, b^\dagger_{q'}] = \delta_{q,q'}. \tag{1.3}$$

The third term in the Hamiltonian is the interaction between electrons and phonons. The electron density is defined as

$$\hat{\rho}^\dagger_q \equiv \sum_{k,\sigma} c^\dagger_{k+q,\sigma} c_{k,\sigma}. \tag{1.4}$$

The phonons are linearly coupled to the electrons via the coupling constant g_q, and L is the length of the system.

It is very difficult to solve this problem directly. Fortunately functional integral provides a powerful tool for the study of many-particle systems and the resulting action provides a very good starting point for further approximations. By using the Euclidean functional integral approach, we convey the Fröhlich Hamiltonian into the action

$$S\{\Psi^*, \Psi; \phi\} = S_{el}\{\Psi^*, \Psi\} + S_{ph}\{\phi\} + S_{int}\{\Psi^*, \Psi; \phi\}, \tag{1.5}$$

with

$$S_{el}\{\Psi^*, \Psi\} = \beta \sum_{k,\tilde{\omega}_n,\sigma} \Psi^*_{k,\tilde{\omega}_n,\sigma} \left[i\tilde{\omega}_n - \tilde{\epsilon}_k \right] \Psi_{k,\tilde{\omega}_n,\sigma}, \tag{1.6}$$

$$S_{ph}\{\phi\} = \frac{1}{2}\beta L \sum_{q,\omega_m} \frac{1}{|g_q|^2} \phi^*_{q,\omega_m} \left[\frac{\omega_m^2 + \omega_q^2}{\omega_q} \right] \phi_{q,\omega_m}, \tag{1.7}$$

$$S_{int}\{\Psi^*, \Psi; \phi\} = \beta \sum_{q,\omega_m} \left(\sum_{k,\tilde{\omega}_n} \Psi^*_{k+q,\tilde{\omega}_n+\omega_m} \Psi_{k,\tilde{\omega}_n} \right) \phi_{q,\omega_m}, \tag{1.8}$$

which correspond to the three terms in the original Hamiltonian respectively. Here we have defined two auxiliary variables

$$\phi_{q,\omega_m} \equiv \frac{g_q}{\sqrt{L}} \left(b_{q,\omega_m} + b^*_{-q,-\omega_m} \right), \tag{1.9}$$

$$\eta_{q,\omega_m} \equiv -i \frac{g_q}{\sqrt{L}} \left(b_{q,\omega_m} - b^*_{-q,-\omega_m} \right). \tag{1.10}$$

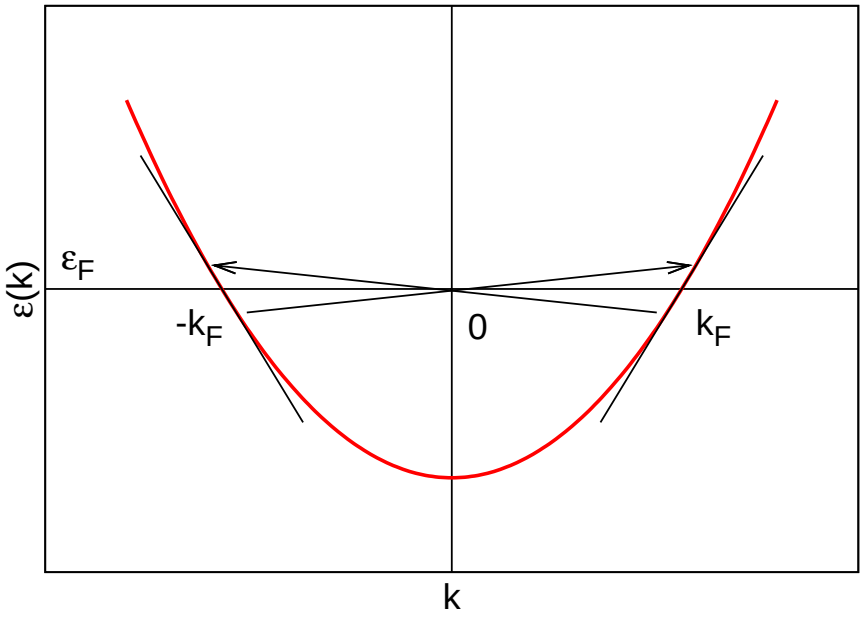

Figure 1.1: Linearized dispersion relation around two Fermi points.

Since the original action is Gaussian in η, we have already integrated it out to get the above results.

In the expression given above, $\beta = 1/k_B T$ is the inverse temperature and $\tilde{\epsilon}_k \equiv \epsilon_k - \mu$ is the energy dispersion reduced by the chemical potential μ. $\Psi_{k,\tilde{\omega}_n}$ and $\Psi^*_{k,\tilde{\omega}_n}$ are conjugated Grassmann variables which describe electrons with momentum k and fermionic Matsubara frequency $\tilde{\omega}_n \equiv (2n+1)\,\pi/\beta$. b_{q,ω_m} and b^*_{q,ω_m} are complex phonon field with momentum q and bosonic Matsubara frequency $\omega_m \equiv 2\pi m/\beta$.

For a detailed derivation, see Negele and Orland [41] and the dissertation of Lorenz Bartosch [42].

1.3 Approximations

So far, no approximation has been made. In the following we will introduce some approximations in order to proceed. The resulted model should contain all the physics we are interested in and be easier to solve than the original one.

1.3.1 Linear Dispersion

If we just consider the low-energy physics, which means only the electrons that in the vicinity of the Fermi energy are involved, in this case we can linearize the energy dispersion of the electrons around two Fermi points, as shown in Fig. (1.1):

$$\tilde{\epsilon}_k = v_F \left(|k| - k_F \right). \tag{1.11}$$

Here v_F and k_F are the Fermi velocity and Fermi momentum respectively, and the energy is measured from the Fermi level.

We can separate the electrons from left-moving and right-moving branches, where the left-moving branch represents the electrons near the Fermi point $-k_F$ and the right-moving branch represents electrons around k_F. The spinor field can be defined by

$$\bar{\Psi}_{k,\tilde{\omega}_n,\sigma} \equiv \begin{pmatrix} \Psi_{+,k,\tilde{\omega}_n,\sigma} \\ \Psi_{-,k,\tilde{\omega}_n,\sigma} \end{pmatrix} \equiv \begin{pmatrix} \Psi_{k_F+k,\tilde{\omega}_n,\sigma} \\ \Psi_{-k_F+k,\tilde{\omega}_n,\sigma} \end{pmatrix}. \tag{1.12}$$

People should notice here the momentum k is measured relative to the Fermi points.

Using the linear dispersion relation Eq. (1.11), we can see that the electronic part of the action can easily be written in terms of these spinor fields and the inverse non-interacting Matsubara Green's function

$$\mathbf{G}_0^{-1}(k,\tilde{\omega}_n) \equiv \begin{pmatrix} i\tilde{\omega}_n - v_F k & 0 \\ 0 & i\tilde{\omega}_n + v_F k \end{pmatrix}. \tag{1.13}$$

1.3.2 Commensurability

Since the momentum transfer of the phonon is either small compared with the Fermi momentum (forward scattering) or approximately $2k_F$ (backward scattering), we can decompose ϕ_{q,ω_m} accordingly

$$\mathbf{V}_{q,\omega_m} \equiv \begin{pmatrix} V_{q,\omega_m} & \Delta_{q,\omega_m} \\ \Delta^*_{-q,-\omega_m} & V_{q,\omega_m} \end{pmatrix} \equiv \begin{pmatrix} \phi_{q,\omega_m} & \phi_{q+2k_F,\omega_m} \\ \phi_{q-2k_F,\omega_m} & \phi_{q,\omega_m} \end{pmatrix}. \tag{1.14}$$

From Eq.(1.9) we can directly show that

$$\phi^*_{q,\omega_m} = \frac{g_q}{\sqrt{L}}\left(b^*_{q,\omega_m} + b_{-q,-\omega_m}\right) = \phi_{-q,-\omega_m}. \tag{1.15}$$

It is followed directly by

$$V^*_{q,\omega_m} = V_{-q,-\omega_m} \tag{1.16}$$

However there is no such simple relation for Δ_{q,ω_m}. Since

$$\Delta_{q,\omega_m} = \phi_{q+2k_F,\omega_m}, \tag{1.17}$$

then

$$\Delta^*_{-q,-\omega_m} = \frac{g_q}{\sqrt{L}}\left(b^*_{-q+2k_F,-\omega_m} + b_{q-2k_F,\omega_m}\right) = \Delta_{q-4k_F,\omega_m}. \tag{1.18}$$

So if it satisfies $4k_F a = 2n\pi$ or $n\pi/a = 2k_F, n = 1, 2, 3\ldots$, where a is the lattice spacing, we will have $\Delta_{q-4k_F,\omega_m} = \Delta_{q,\omega_m}$, and therefor $\Delta_{q,\omega_m} = \Delta^*_{-q,-\omega_m}$. We refer to this case as the commensurate case. In the incommensurate case, then all Δ^*_{q,ω_m} and $\Delta_{-q',-\omega'_m}$ are independent.

1.3.3 Phonon Statistics

Defining the matrices $\mathbf{G}_0^{-1}$ and $\mathbf{V}$ by

$$\left(\mathbf{G}_0^{-1}\right)_{k,k',\tilde{\omega}_n,\tilde{\omega}_{n'}} \equiv \delta_{k,k'}\delta_{\tilde{\omega}_n,\tilde{\omega}_{n'}}\mathbf{G}_0^{-1}(k,\tilde{\omega}_n), \tag{1.19}$$

$$\left(\mathbf{V}\right)_{k,k',\tilde{\omega}_n,\tilde{\omega}_{n'}} \equiv \mathbf{V}_{k-k',\tilde{\omega}_n-\tilde{\omega}_{n'}}, \tag{1.20}$$

then the action Eq. (1.5) can be written in the following form

$$S\{\bar{\Psi}^\dagger,\bar{\Psi};V,\Delta,\Delta^*\} = S_{el-ph}\{\bar{\Psi}^\dagger,\bar{\Psi};V,\Delta,\Delta^*\} + S_{ph}\{V,\Delta,\Delta^*\}, \tag{1.21}$$

with

$$S_{el-ph}\{\bar{\Psi}^\dagger,\bar{\Psi};V,\Delta,\Delta^*\} = \beta \sum_{k,k',\tilde{\omega}_n,\tilde{\omega}_{n'},\sigma} \bar{\Psi}^\dagger_{k,\tilde{\omega}_n,\sigma} \left(\mathbf{G}_0^{-1} - \mathbf{V}\right)_{k,k',\tilde{\omega}_n,\tilde{\omega}_{n'}} \bar{\Psi}_{k',\tilde{\omega}_{n'},\sigma} \tag{1.22}$$

$$\begin{aligned} S_{ph}\{V,\Delta,\Delta^*\} &= \frac{1}{2}\beta L \sum_{q,\omega_m} \frac{1}{|g_q|^2}\left[\frac{\omega_m^2+\omega_q^2}{\omega_q}\right] V^*_{q,\omega_m} V_{q,\omega_m} \\ &\quad + \frac{1}{c}\beta L \sum_{q,\omega_m} \frac{1}{|g_{2k_F+q}|^2}\left[\frac{\omega_m^2+\omega_{2k_F+q}^2}{\omega_{2k_F+q}}\right] \Delta^*_{q,\omega_m}\Delta_{q,\omega_m} \end{aligned} \tag{1.23}$$

where $c=2$ in the commensurate case and $c=1$ in the incommensurate case.

To determine the phonon statistics, we further integrate out the fermionic fields, and the bosonic action becomes:

$$S\{V,\Delta,\Delta^*\} = S\{V\} + S\{\Delta,\Delta^*\}, \tag{1.24}$$

with

$$S\{V\} = \frac{1}{2}\beta L \sum_{q,\omega_m} \frac{1}{|g_q|^2}\left[\frac{\omega_m^2+\omega_{ren}^2(q,\omega_m)}{\omega_q}\right] V^*_{q,\omega_m} V_{q,\omega_m}, \tag{1.25}$$

$$\begin{aligned} S\{\Delta,\Delta^*\} &= \frac{1}{c}\beta L \sum_{q,\omega_m} \frac{1}{|g_{2k_F+q}|^2}\left[\frac{\omega_m^2+\left(\omega_{ren}^{2k_F}(q,\omega_m)\right)^2}{\omega_{2k_F+q}}\right] \Delta^*_{q,\omega_m}\Delta_{q,\omega_m} \\ &\quad + \frac{s}{2}\beta L {\sum_{q_i,\omega_{m_i}}}' U_4\left(q_i,\omega_{m_i}\right) \Delta^*_{-q_4,-\omega_{m_4}} \Delta^*_{-q_3,-\omega_{m_3}} \Delta_{q_2,\omega_{m_2}} \Delta_{q_1,\omega_{m_1}}, \end{aligned} \tag{1.26}$$

where $s=2$ for fermions with spin $1/2$ and $s=1$ for spinless fermions, $\omega_{ren}\left(q,\omega_m\right)$ and $\omega_{ren}^{2k_F}\left(q,\omega_m\right)$ are renormalized phonon frequencies:

$$\omega_{ren}^2(q,\omega_m) \equiv \omega_q^2\left[1 - s\left(|g_q|^2/\omega_q\right)\Pi_0(q,\omega_m)\right], \tag{1.27}$$

$$\left(\omega_{ren}^{2k_F}(q,\omega_m)\right)^2 \equiv \omega_{2k_F+q}^2\left[1 - cs\left(|g_{2k_F+q}|^2/\omega_{2k_F+q}\right)\Pi_0^{2k_F}(q,\omega_m)\right], \tag{1.28}$$

and

$$\Pi_0(q,\omega_m) \equiv -\frac{1}{\beta L}\sum_{\alpha}\sum_{k,\tilde{\omega}_n} G_0^\alpha(k,\tilde{\omega}_n) G_0^\alpha(k+q,\tilde{\omega}_n+\omega_m), \tag{1.29}$$

$$\Pi_0^{2k_F}(q,\omega_m) \equiv -\frac{1}{\beta L}\sum_{k,\tilde{\omega}_n} G_0^-(k,\tilde{\omega}_n) G_0^+(k+q,\tilde{\omega}_n+\omega_m). \tag{1.30}$$

The prime on the last sum in Eq. (1.26) denotes that the sums over q_i and ω_{m_i} are restricted to $\sum_{i=1}^4 q_i = 0$ and $\sum_{i=1}^4 \omega_{m_i} = 0$. In the following we will only consider the leading term of $U_4(q_i,\omega_{m_i})$, which means we only consider $U_4 \equiv U_4(0,0)$:

$$U_4 \equiv U_4(0,0) = \frac{1}{\beta L}\sum_{k,\tilde{\omega}_n} \frac{1}{\left[i\tilde{\omega}_n + v_F k\right]^2\left[i\tilde{\omega}_n - v_F k\right]^2}. \tag{1.31}$$

1.3.4 Static Approximation

Finally, to get a time-independent Ginzburg-Landau functional, we will ignore quantum fluctuations, which means we drop out all finite bosonic frequencies ω_m. In thermal field theory, this corresponds to a classical approximation, in which the typical frequency of a boson is much less than the temperature, and the occupation number of that mode greatly exceeds one. As long as this does not lead to an ultraviolet catastrophe, it appears to be a reasonable approximation. Then the action $S\{V,\Delta,\Delta^*\}$ turns into the free energy functional $\beta F\{V,\Delta,\Delta^*\}$, with

$$\begin{aligned} F\{V,\Delta,\Delta^*\} &= F\{V\}+F\{\Delta,\Delta^*\}, && (1.32)\\ F\{V\} &= \frac{1}{2}L\sum_q \frac{1}{|g_q|^2}\left[\frac{\omega^2_{ren}(q,\omega_m)}{\omega_q}\right]V_q^*V_q, && (1.33)\\ F\{\Delta,\Delta^*\} &= \frac{1}{c}L\sum_q \frac{1}{|g_{2k_F+q}|^2}\left[\frac{\left(\omega^{2k_F}_{ren}(q,\omega_m)\right)^2}{\omega_{2k_F+q}}\right]\Delta_q^*\Delta_q \\ &\quad +\frac{s}{2}L\sum_{q_i}U_4\left(q_i\right)\Delta^*_{-q_4}\Delta^*_{-q_3}\Delta_{q_2}\Delta_{q_1}. && (1.34)\end{aligned}$$

Since $F\{V\}$ is Gaussian in V, the electron-phonon coupling only leads to slightly renormalized phonon statistics for small q. We are more interested in the back-scattering potential $\Delta(x)$, and from now on, we only consider $F\{\Delta,\Delta^*\}$.

1.4 Ginzburg-Landau Functional

We now concentrate on the truncated free energy functional $F\{\Delta,\Delta^*\}$, expanding $\Pi_0^{2k_F}\equiv\Pi_0^{2k_F}(q,0)$ up to terms of second order in q, we obtain

$$\Pi_0^{2k_F}(q)=\Pi_0^{2k_F}(0)-Cv_F^2q^2, \tag{1.35}$$

where

$$C=\frac{q}{\beta L}\sum_{k,\tilde{\omega}_n}\frac{1}{\left[i\tilde{\omega}_n+v_Fk\right]\left[i\tilde{\omega}_n-v_Fk\right]^3}. \tag{1.36}$$

$\Pi_0^{2k_F}(0)$ can be calculated as follows:

$$\begin{aligned}\Pi_0^{2k_F} &= -\frac{1}{\beta L}\sum_{k,\tilde{\omega_n}}G_0^-(k,\tilde{\omega_n})G_0^+(k,\tilde{\omega_n})\\ &= -\int_{-k_0}^{k_0}\frac{dk}{2\pi}\frac{f(v_Fk)-f(-v_Fk)}{2v_Fk}\\ &= \int_{-k_0}^{k_0}\frac{dk}{2\pi}\frac{\tanh(\beta v_Fk/2)}{2v_Fk}\\ &= \frac{\rho_0}{2}\int_0^{\epsilon_0/2k_BT}du\frac{\tanh u}{u}, && (1.37)\end{aligned}$$

where k_0 and ϵ_0 are momentum and energy cutoff. For $\epsilon_0/k_BT\gg 1$, the last integral depends logarithmically on $\epsilon_0/2k_BT$.

$$\int_0^x du\frac{\tanh u}{u}=\ln(x)-\int_0^\infty du\frac{\ln u}{\cosh^2 u}+O(e^{-x})=\ln(4e^\gamma x/\pi)+O(e^{-x}), \tag{1.38}$$

with

$$\gamma \equiv \lim_{N\leftarrow\infty}\left(\sum_{n=1}^{N}\frac{1}{n}-\ln(N)\right)=0.577215664\ldots. \tag{1.39}$$

is the Euler's constant. Then we have for $\Pi_0^{2k_F}(0)$

$$\Pi_0^{2k_F}(0)=\rho_0/2\ln\left[(2e^{\gamma}/\pi)\,\epsilon_0/k_BT\right]. \tag{1.40}$$

Plugging Eq. (1.40) into the definition of the renormalized phonon frequency Eq. (1.28) and setting it to be zero, we can get the mean-field transition temperature

$$k_BT_c^{MF}=1.134\epsilon_0\exp(-1/\lambda), \tag{1.41}$$

where

$$\lambda\equiv cs\frac{\rho_0|g_q|^2}{2\omega_q} \tag{1.42}$$

is the dimensionless coupling constant.

To calculate C and U_4 we consider the general expression

$$C_{\nu_1,\nu_2}=\frac{1}{\beta L}\sum_{k,\tilde{\omega}_n}\frac{1}{\left[i\tilde{\omega}_n+v_Fk\right]^{\nu_1}\left[i\tilde{\omega}_n-v_Fk\right]^{\nu_2}}, \tag{1.43}$$

which vanishes if $\nu_1+\nu_2$ is odd and greater then two. Turning the k-summation into an integral and using the residue theorem, it follows for even $\nu\equiv\nu_1+\nu_2\geq 4$

$$\begin{aligned}
C_{\nu_1,\nu_2} &= \frac{2}{\beta}\sum_{\tilde{\omega}_n>0}\int\frac{du}{2\pi v_F}\frac{1}{\left[i\tilde{\omega}_n+u\right]^{\nu_1}\left[i\tilde{\omega}_n-u\right]^{\nu_2}}\\
&= -\frac{\rho_0}{2}\frac{4\pi i}{\beta}\sum_{\tilde{\omega}_n>0}\frac{1}{(\nu_1-1)!}\left(\frac{d}{du}\right)^{\nu_1-1}\frac{1}{\left[i\tilde{\omega}_n-u\right]^{\nu_2}}\Big|_{u=-i\tilde{\omega}_n}\\
&= -\frac{\rho_0}{2}\frac{4\pi i}{\beta}\frac{(\nu-2)(\nu-3)\cdots\nu_2}{(\nu_1-1)!}\sum_{\tilde{\omega}_n>0}\frac{1}{\left[2i\tilde{\omega}_n\right]^{\nu-1}}\\
&= \frac{\rho_0}{2}(-1)^{\nu/2}\left(\frac{\beta}{4\pi}\right)^{\nu-2}\begin{pmatrix}\nu-2\\ \nu_1-1\end{pmatrix}\left(2^{\nu-1}-1\right)\xi(\nu-1),
\end{aligned} \tag{1.44}$$

where in the last step we have used

$$\begin{aligned}
\sum_{\tilde{\omega}_n}\frac{1}{\left[2i\tilde{\omega}-n\right]^{\nu-1}} &= \left(\frac{\beta}{2\pi i}\right)^{\nu-1}\sum_{nodd}\frac{1}{n^{\nu-1}}\\
&= \left(\frac{\beta}{2\pi i}\right)^{\nu-1}\left(\sum_{n=1}^{\infty}\frac{1}{n^{\nu-1}}-\sum_{n=1}^{\infty}\frac{1}{(2n)^{\nu-1}}\right)\\
&= \left(\frac{\beta}{2\pi i}\right)^{\nu-1}\left(2^{\nu-1}-1\right)\xi(\nu-1),
\end{aligned} \tag{1.45}$$

here

$$\xi(\nu)\equiv\sum_{n=1}^{\infty}\frac{1}{n^{\nu}} \tag{1.46}$$

is the Riemann zeta-function. Then it follows that

$$U_4 = 2C = \rho_0 \left(\frac{\beta}{4\pi}\right)^2 7\xi(3). \tag{1.47}$$

With the above approximation and the calculated results, we can write the truncated free energy functional as

$$F\{\Delta,\Delta^*\} = \frac{s\rho_0 L}{2}\left[a(T)\sum_q \Delta_q^*\Delta_q + b(T)\sum_{q_i}{}' \Delta^*_{-q_4}\Delta^*_{-q_3}\Delta_{q_2}\Delta_{q_1} + c(T)\sum_q q^2\Delta_q^*\Delta_q\right]. \tag{1.48}$$

Here the temperature dependent coefficients $a(T)$, $b(T)$ and $c(T)$ are

$$a(T) = \ln\frac{T}{T_c^{MF}}, k_B T_c^{MF} = 1.134\epsilon_0\exp(-1/\lambda), \tag{1.49}$$

$$b(T) = \left(\frac{1}{4\pi k_B T}\right)^2 7\zeta(3), \tag{1.50}$$

$$c(T) = \left(\frac{v_F}{4\pi k_B T}\right)^2 7\zeta(3). \tag{1.51}$$

We Define the order parameter field $\Delta(x)$ as the Fourier transform of Δ_q:

$$\Delta(x) = \sum_q e^{iqx}\Delta_q. \tag{1.52}$$

Since in the commensurate case, we have $\Delta_q^* = \Delta_{-q}$, then the order parameter field $\Delta(x)$ is real. In the incommensurate case, $\Delta_q^* = \Delta_{-q}$ does not hold and $\Delta(x)$ is complex. In terms of $\Delta(x)$, the truncated free energy functional turns into

$$F[\Delta(x)] = \frac{1}{\pi v_F}\int_0^L dx(a(T)|\Delta(x)|^2 + b(T)|\Delta(x)|^4 + c(T)|\partial_x\Delta(x)|^2). \tag{1.53}$$

1.5 Fluctuating Gap Model

Having discussed the statistics of the phonon field, we now come back to the electronic part of the action. From Eq. (1.22) we can see that for a specific realization of the order parameters, the electronic part of the Hamiltonian reads

$$\mathbf{H} = \sum_{k,k'}\left(c^\dagger_{+,k}, c^\dagger_{-,k}\right) H_{k,k'}\begin{pmatrix} c_{+,k'} \\ c_{-,k'}\end{pmatrix}, \tag{1.54}$$

where

$$H_{k,k'} = \begin{pmatrix} v_F k\delta_{k,k'} & \Delta_{k-k'} \\ \Delta^*_{-(k-k')} & -v_F k\delta_{k,k'}\end{pmatrix}. \tag{1.55}$$

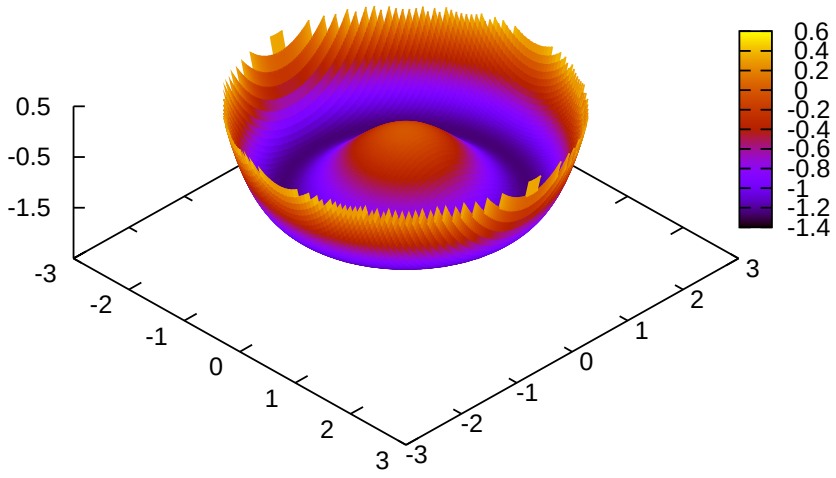

Figure 1.2: The minimum of the Ginzburg-Landau function in the incommensurate case for $a(T) < 0$.

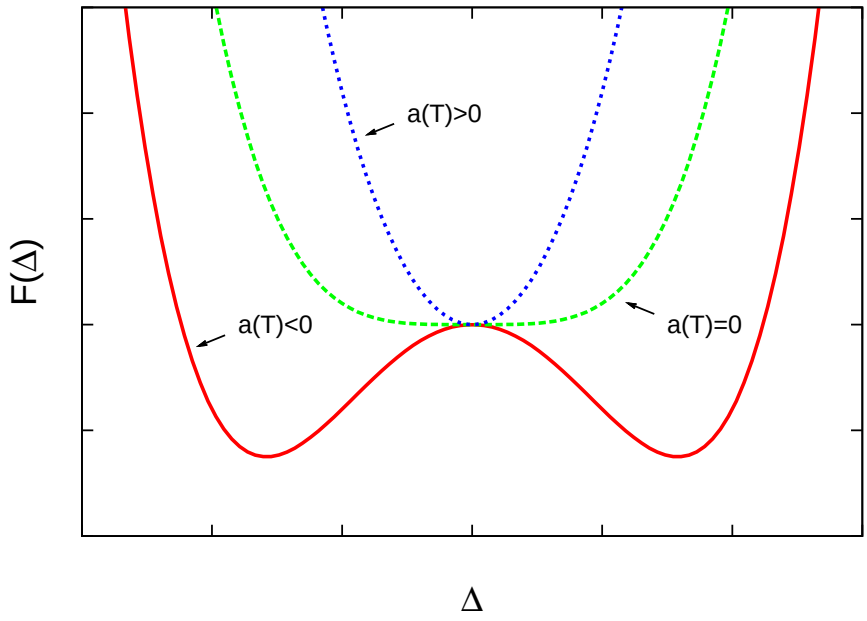

Figure 1.3: The minimum of the Ginzburg-Landau function in the commensurate case for different $a(T)$.

Here, $c^{\dagger}_{\pm,k}$ and $c_{\pm,k}$ are creation and annihilation operators of right- or left-moving electrons with momentum k measured relative to the Fermi wave vector. A Fourier transformation leads to

$$\hat{H}(x,-i\partial_x) = \begin{pmatrix} -iv_F\partial_x & \Delta(x) \\ \Delta^*(x) & iv_F\partial_x \end{pmatrix}. \tag{1.56}$$

This is the Hamiltonian of the FGM.

1.5.1 Mean-Field Theory

Now we consider the mean field approximation, i.e. we ignore fluctuations of the order parameter field and set $\Delta(x)$ to be spatially constant. Since the fluctuating order parameters are described by the Ginzburg-Landau functional [Eq. (1.53)], in the mean-field approximation the gradient term vanishes, we can get the Free energy function

$$F(\Delta) = \frac{s\rho_0 L}{2}\left(a(T)|\Delta|^2 + b(T)|\Delta|^4\right). \tag{1.57}$$

In this case, $F(\Delta)$ is minimized at $\Delta = \Delta_0 e^{i\vartheta}$. As showed in Fig. (1.2), in the incommensurate case, the order parameters are complex, then its minimum is the bottom of a potential well, that means it has fixed amplitude Δ_0 but an arbitrary phase ϑ. In the commensurate case Fig. (1.3), on the other hand, the phase value is only allowed to be either 0 or π, that means $\Delta = \Delta_0 e^{i\vartheta} = \pm\Delta_0$, with

$$\Delta_0(T) = \left(\frac{|a(T)|}{2b(T)}\right)^{1/2}, T \le T_c^{MF}. \tag{1.58}$$

Since at $T \le T_c^{MF}$, we can set $a(T) = (T - T_c^{MF})/T_c^{MF}$ and $b(T)$ to be the value at the transition temperature $b(T_c^{MF})$, thus we have

$$\Delta_0(T) = \frac{4\pi k_B T_c^{MF}}{(2\cdot 7\zeta(3))^{1/2}}\left(\frac{T_c^{MF}-T}{T_c^{MF}}\right)^{1/2}, T \le T_c^{MF}. \tag{1.59}$$

Energy Gap

Since $\Delta_0(T)$ rises continuously from zero at $T = T_c^{MF}$, the system undergoes a second order phase transition. The critical exponent 1/2 is the typical mean-field exponent. A more accurate solution to $\Delta_o(T)$ can be obtained by solving the BCS gap equation [43]

$$\frac{1}{\lambda} = \frac{2\pi}{\beta}\sum_{0<\tilde{\omega}_n<\epsilon_0}\frac{1}{\sqrt{\tilde{\omega}_n^2 + \Delta_0^2(T)}}, \tag{1.60}$$

where as usual λ is the dimensionless coupling constant and ϵ_0 is the energy cutoff.

At $T = T_c^{MF}$, we have $\Delta_0(T) = 0$. At zero temperature, where $\beta \to \infty$, the sum over Matsubara frequencies in Eq. (1.60) turns into an integral

$$\begin{aligned} F_{T=0}(\Delta) &= s\rho_0 L\left(-\int_0^{\epsilon_0} dE\left[\sqrt{E^2+|\Delta|^2} - E\right] + \frac{|\Delta|^2}{2\lambda}\right) \\ &= \frac{s\rho_0}{2} L\left(-\epsilon_0\sqrt{\epsilon_0^2+|\Delta|^2} + \epsilon_0^2 - |\Delta|^2 \ln\frac{\epsilon_0 + \sqrt{\epsilon_0^2+|\Delta|^2}}{|\Delta|} + \frac{|\Delta|^2}{\lambda}\right). \end{aligned} \tag{1.61}$$

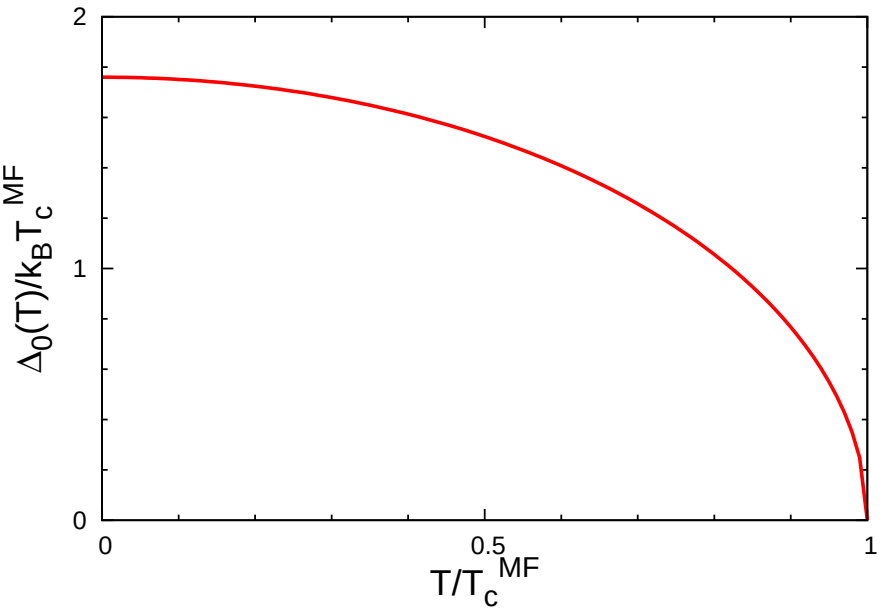

Figure 1.4: The mean-field energy gap $\Delta_0(T)$ as a function of the temperature.

In the weak coupling assumption where $|\Delta| \ll \epsilon_0$, we ignore terms of order $|\Delta|^2/\epsilon_0^2$, such that

$$F_{T=0}(\Delta) = -\frac{s\rho_0}{2} L|\Delta|^2 \left(\frac{1}{2} + \ln\left(\frac{2\epsilon_0}{|\Delta|}\right) - \frac{1}{\lambda}\right). \tag{1.62}$$

Setting the derivative of this equation with respect to Δ equal to zero, we obtain for the minimized free energy

$$F_{T=0}(\Delta_0(0)) = -\frac{s\rho_0 L}{2}\frac{\Delta_0^2(0)}{2}. \tag{1.63}$$

Now $\Delta_0(0)$ is given by, in the weak coupling limit,

$$\Delta_0(0) = 2\epsilon_0 e^{-1/\lambda}. \tag{1.64}$$

Expressing λ in terms of the mean-field transition temperature T_c^{MF}, we have

$$\Delta_0(0) = 1.764 k_B T_c^{MF}. \tag{1.65}$$

So we can use the following mean-field approximation for the energy gap at any finite temperature $T < T_c^{MF}$

$$\Delta_0(T) = 1.76 k_B T_c^{MF} \left(\frac{T_c^{MF} - T}{T_c^{MF}}\right)^{1/2}, T \leq T_c^{MF}, \tag{1.66}$$

which reproduces the value for the gap at zero temperature.

Bogoliubov Transformation

In the mean-field approximation, the Hamiltonian reads

$$H_k = \begin{pmatrix} v_F k & \Delta_0 e^{i\vartheta} \\ \Delta_0 e^{-i\vartheta} & -v_F k \end{pmatrix}. \tag{1.67}$$

Where Δ_0 is just the energy gap we calculated above. This Hamiltonian can be diagonalized by the Bogoliubov transformation

$$\begin{pmatrix} c_{+,k} \\ c_{-,k} \end{pmatrix} = U_k \begin{pmatrix} a_{+,k} \\ a_{-,k} \end{pmatrix}, \tag{1.68}$$

where U_k is a two by two matrix. For the new fermion operators $a^\dagger_{\pm,k}$ and $a_{\pm,k}$ to satisfy the anticommutation relations

$$\{a_{\alpha,k}, a_{\alpha',k'}\} = 0, \{a_{\alpha,k}, a^\dagger_{\alpha',k'}\} = \delta_{\alpha,\alpha'}\delta_{k,k'}, \tag{1.69}$$

we need to have for the elements of the transformation matrix U_k

$$|U_{++,k}|^2 + |U_{+-,k}|^2 = 1, \tag{1.70}$$

and

$$U_{--,k} = U^*_{++,k}, U_{-+,k} = -U^*_{+-,k}. \tag{1.71}$$

Energy Dispersion

The eigenvalues of H_k can be obtained easily by diagonalizing the above matrix, and the results are $\pm E_k$, where

$$E_k = \mathrm{sgn}(k)\sqrt{v_F^2 k^2 + \Delta_0^2}. \tag{1.72}$$

Then the matrix U_k is just

$$U_k = \frac{1}{\sqrt{2}} \begin{pmatrix} (1 + v_F k/E_k)^{1/2} e^{i\vartheta/2} & -\mathrm{sgn}(k)\,(1 - v_F k/E_k)^{1/2} e^{i\vartheta/2} \\ \mathrm{sgn}(k)\,(1 - v_F k/E_k)^{1/2} e^{-i\vartheta/2} & (1 + v_F k/E_k)^{1/2} e^{-i\vartheta/2} \end{pmatrix}. \tag{1.73}$$

In terms of the new fermion operators, the electronic part of the mean-field Hamiltonian can be written in the form

$$H^{MF}_{el} = \sum_{\alpha,k} \alpha E_k a^\dagger_{\alpha,k} a_{\alpha,k}. \tag{1.74}$$

Density of States

The density of states is given by

$$\begin{aligned} \rho^{MF}(\omega) &= \int_{-\infty}^{+\infty} \frac{dk}{2\pi} \sum_\alpha \delta(\omega - \alpha E_k) \\ &= \rho_0 \frac{|\omega|}{\sqrt{\omega^2 - \Delta_0^2}} \theta(\omega^2 - \Delta_0^2). \end{aligned} \tag{1.75}$$

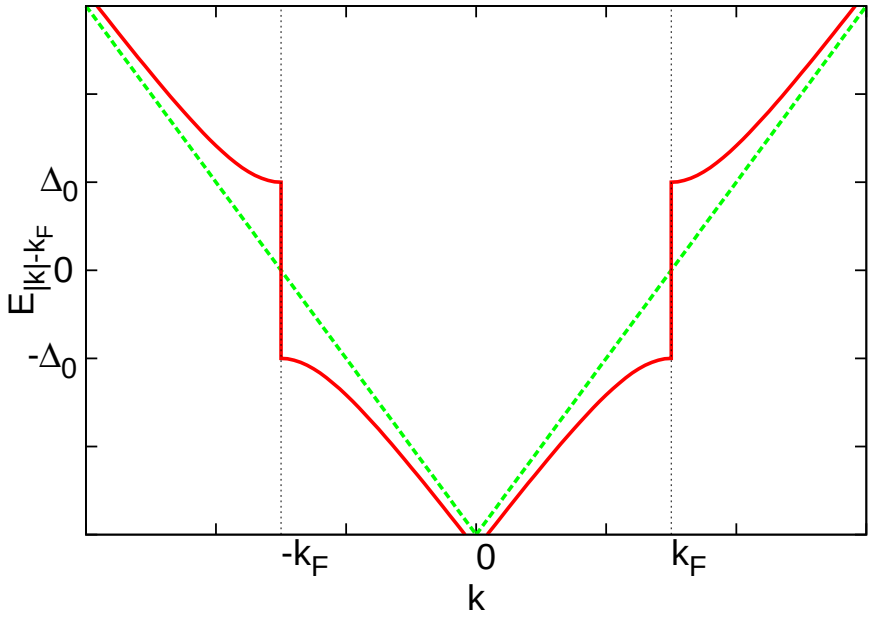

Figure 1.5: Energy dispersion $E_{|k|-k_F}$ relative to the Fermi level of the mean-field Hamiltonian. The green dashed line represents the linearized dispersion relation.

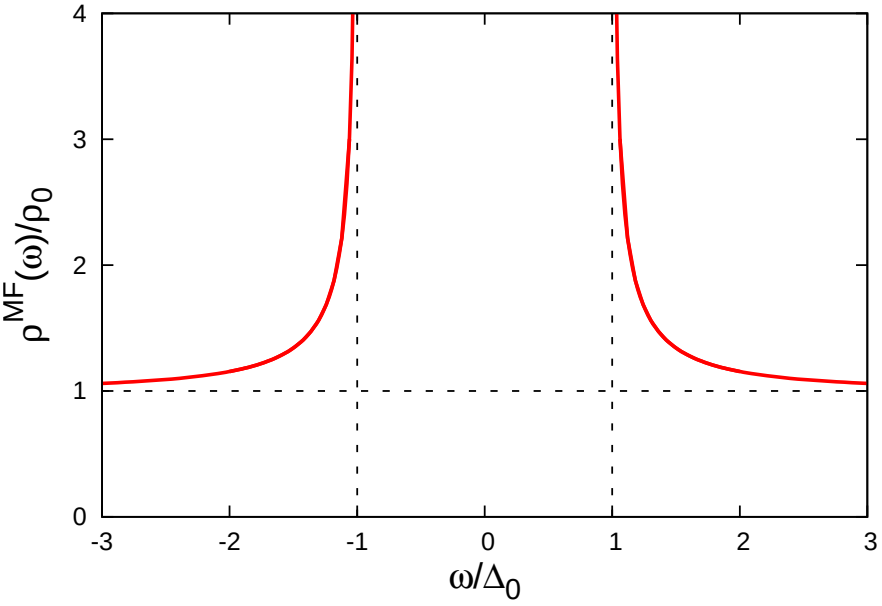

Figure 1.6: Plot of the density of states in the mean-field approximation.

where

$$\rho_0 = \frac{1}{\pi v_F} \tag{1.76}$$

is the density of states of free fermions with a linearized energy dispersion.

We plot the energy dispersion and the density of states in Fig. (1.5) and Fig. (1.6) respectively. Both figures show that a single particle gap has opened at energy $\omega = \Delta_0$.

1.5.2 Charge-Density Wave

Static Lattice Distortion

The phonon operators $b_q^\dagger$ and b_q are related to the operators of the normal coordinates u_q of the lattice system by

$$u_q = \left(\frac{1}{2M\omega_q}\right)^{1/2} \left(b_q + b_{-q}^\dagger\right). \tag{1.77}$$

Here, M is the ionic mass and ω_q is the phonon dispersion. So the lattice displacement operator of the ions at $x_n = na$ are given by the Fourier transformation

$$u(x_n) = \sum_q e^{iqx_n} \left(\frac{1}{2NM\omega_q}\right)^{1/2} \left(b_q + b_{-q}^\dagger\right), \tag{1.78}$$

and the expectation value of the lattice displacement is just

$$\langle u(x_n)\rangle = \sum_q e^{iqx_n} \left(\frac{1}{2NM\omega_q}\right)^{1/2} \left(\langle b_q\rangle + \langle b_{-q}^\dagger\rangle\right). \tag{1.79}$$

Within the mean-field approximation, we have

$$\langle \Delta(x)\rangle = \Delta_0 e^{i\vartheta}, \tag{1.80}$$

and the Fourier transformation shows that only the $q = 0$ component survives. Along with the definition of Δ_q, and do the same for the conjugated form, we therefor have

$$\frac{|g_{2k_F}|}{\sqrt{L}} \left(\langle b_{2k_F}\rangle + \langle b_{-2k_F}^\dagger\rangle\right) = \Delta_0 e^{i\vartheta}, \tag{1.81}$$

$$\frac{|g_{2k_F}|}{\sqrt{L}} \left(\langle b_{-2k_F}\rangle + \langle b_{2k_F}^\dagger\rangle\right) = \Delta_0 e^{-i\vartheta}. \tag{1.82}$$

Inserting them into Eq. (1.79), we can get

$$\langle u(x_n)\rangle = \left(\frac{2a}{M\omega_{2k_F}|g_{2k_F}|^2}\right)^{1/2} \Delta_0 \cos(2k_F x_n + \vartheta). \tag{1.83}$$

Below the Peierls transition $\Delta_0 > 0$, and the system develops a static lattice distortion with wave vector $2k_F$ whose amplitude is proportional to the order parameter $\langle\Delta(x)\rangle$. In the case of a half-filled band, $k_F = \pi/2a$, such that all ions are displaces by the same amount but in alternating directions.

Charge-Density Wave

An direct result from the static lattice distortion discussed above is the redistribution of the ion charge, which also form a wave-like patten. This can be seen by considering the ground state. Since all energy levels below the Fermi surface are occupied, that means for the new Fermi operators, the expectation values satisfy

$$\langle a_{\alpha,k} a_{\alpha',k'} \rangle = 0, \langle a_{\alpha,k} a^{\dagger}_{\alpha',k'} \rangle = \delta_{\alpha,\alpha'} \delta_{k,k'} \theta(-\alpha k). \tag{1.84}$$

The density operator is defined as

$$\hat{\rho}(x) = \Psi^{\dagger}(x) \Psi(x), \tag{1.85}$$

where

$$\Psi(x) = \frac{1}{\sqrt{L}} \sum_{k} e^{ikx} c_k = \frac{1}{\sqrt{L}} \sum_{\alpha,k} e^{i(\alpha k_F + k)x} c_{\alpha,k}. \tag{1.86}$$

Recalling that $c_{\alpha,k} = \sum_{\alpha'} U_{\alpha\alpha',k} a_{\alpha',k}$, it follows

$$\hat{\rho}(x) = \frac{1}{L} \sum_{\alpha,\alpha'',k} \sum_{\alpha',\alpha''',k'} U^{*}_{\alpha\alpha'',k} U_{\alpha'\alpha''',k'} e^{-i(\alpha k_F + k)x} e^{i(\alpha' k_F + k')x} a^{\dagger}_{\alpha'',k} a_{\alpha''',k'}. \tag{1.87}$$

Taking the ground state expectation value and making use of Eqs. (1.70) and (1.84), we get

$$\begin{aligned} \langle \hat{\rho}(x) \rangle &= \frac{1}{L} \sum_{\alpha\alpha'\alpha''} \sum_{k<0} U^{*}_{\alpha\alpha'',k} U_{\alpha'\alpha'',k} e^{-i(\alpha-\alpha')k_F x} \\ &= \frac{1}{L} \sum_{k>0} \Big[1 + \left(U^{*}_{+-,k} U_{--,k} + U^{*}_{++,k} U_{-+,k} \right) e^{-2ik_F x} \\ &\quad + \left(U^{*}_{--,k} U_{+-,k} + U^{*}_{-+,k} U_{++,k} \right) e^{2ik_F x} \Big]. \end{aligned} \tag{1.88}$$

Since $U^{*}_{+-,k} = U_{-+,k}$, we end up with

$$\langle \hat{\rho}(x) \rangle = \tilde{\rho}_0 - \tilde{\rho}_1 \cos(2k_F x + \vartheta), \tag{1.89}$$

where $\tilde{\rho}_0 = \pi/k_0$ is the charge-density for $\Delta_0 = 0$ and

$$\tilde{\rho}_1 = \frac{4}{L} \sum_{0<k<k_0} \left(1 - \frac{v_F^2 k^2}{E_k^2} \right)^{1/2} \sim \frac{\Delta_0}{\pi v_F^2 \lambda} \tag{1.90}$$

Below the Peierls transition the system exhibits a charge-density wave with wave vector $2k_F$ and amplitude proportional to the absolute value of the order parameter $|\langle \Delta(x) \rangle| = \Delta_0$.

1.5.3 Beyond The Mean-Field Theory

In the above calculation, we have shown that the system undergoes a mean-field phase transition at a critical temperature T_c^{MF}. As temperature is lowered, an energy gap forms and a density wave develops which breaks the continuous symmetry. However,

this is an artifact of the mean-field approximation, the existence of the order parameter fluctuations prevents all these from happening. The Mermin-Wagner theorem states that the fluctuations lead to the absence of long-range order in a strictly one-dimensional system at any finite temperature [44]. Real quasi-one-dimensional materials, however, are highly anisotropic three-dimensional systems with interchain interactions and tunneling leading to coupling of the fluctuations that develop along each chain. This coupling results in a finite transition temperature T_{3D} below which the three-dimensional long-range order occurs. The region below T_c^{MF} is characterized by one-dimensional fluctuations which, at some temperature $T^* > T_{3D}$, cross over to fluctuations with two- or three-dimensional character. A number of experimental results [9, 11, 38] give evidence that such fluctuations play an important role for the electrodynamics of quasi-one-dimensional materials, and a lot have been discussed on the effects of these fluctuations [2, 45, 46]. To understand the importance of fluctuations of order parameters completely, we need to know the statistics of the order parameter field and develop a proper method to describe them. That is what we will discuss in the next chapter.

Chapter 2

Order Parameter Fluctuations

In Chapter 1, we showed that the order parameters satisfy the Ginzburg-Landau functional Eq. (1.53) and a mean-field solution to the FGM gives a qualitative explanation to the Peierls instability of quasi-one-dimensional systems. But as we argued in the last part of Chapter 1, in the low-dimensional system, the fluctuations play an important role, the existence of fluctuations of order parameters fails the validity of the mean-field description. Thus we need to take into account the fluctuations effect and to see what will happen to the electronic properties. Before we do so, we need to get a fully understanding of the statistics of the order parameter fluctuations in the whole temperature region and derive the generating function of the order parameter fluctuations, which can be put into later calculations.

For very large temperature which is greater than the mean-field critical temperature T_c^{MF}, we have $a(T) \gg b(T)$, thus we can just neglect the fourth order term. This is the so called harmonic approximation and in this case, the order parameters are Gaussian distributed. We refer to this region as the Gaussian region. As the temperature is lowered and approaches the mean-field critical temperature T_c^{MF}, the above harmonic approximation does not hold any more, and we need to take into account anharmonic corrections. The order parameter fluctuations become non-Gaussian, which is the most interesting and important case. When the temperature is much lower than the mean-field critical temperature, the amplitudes of the order parameters get frozen out, and only the phases of the order parameters fluctuate. Thus it is called the phase fluctuations only region.

Using the Monte Carlo simulation, a large configuration of the order parameters can be simulated in general according to the Ginzburg-Landau action. But it is not only time consuming but also very inconvenient for our later calculation. Here we will use a more sophisticated method which was proposed by H.Monien [24]. The new method is based on the transfer matrix method [47]. It in general can cover the whole temperature region which we are interested in. In the following part of this chapter, we first discuss two special cases, i.e. the Gaussian fluctuations at high temperature and the phase fluctuations only at relative low temperature. We show that using the Ornstein-Uhlenbeck process, we can generate Gaussian fluctuations with required correlation lengths. And in the phase fluctuations only case, the phase fluctuations can be described by a simple Wiener process. At last we will use the transfer matrix method to derive a general Langevin equation for generating order parameter fluctuations at any temperature. And we will show that for relative large and small temperature, this method will reproduce Gaussian fluctuations

and phase fluctuations only results separately.

2.1 Gaussian Fluctuations

When the temperature is much larger than the mean-filed critical temperature T_c^{MF}, the coefficient $a(T)$ becomes very large and the second order dominates the free energy functional. Neglecting the fourth order, Eq.(1.48) becomes

$$F\{\Delta,\Delta^*\} = \frac{L}{\pi v_F}\sum_q (a(T)+c(T)q^2)\Delta_q^*\Delta_q. \tag{2.1}$$

the correlation functions are

$$\langle\Delta_q\rangle = 0, \tag{2.2}$$
$$\langle\Delta_q\Delta_{q'}^*\rangle = \frac{k_BT}{\pi v_F}\frac{\delta_{q,q'}}{a(T)+c(T)q^2}. \tag{2.3}$$

here $\langle\cdots\rangle = \int\Pi_q\mathcal{D}\{\Delta_q,\Delta_q^*\}e^{-\beta F[\Delta,\Delta^*]}\cdots$ is the average over all different configurations. Using the Fourier transformation

$$\Delta(x) = \sum_q e^{iqx}\Delta_q, \tag{2.4}$$
$$\Delta_q = \frac{1}{L}\int_0^L dx e^{-iqx}\Delta(x), \tag{2.5}$$

we can get the correlation functions in real space

$$\langle\Delta(x)\rangle = 0, \tag{2.6}$$
$$\langle\Delta(x)\Delta^*(x')\rangle = \Delta_s^2(T)e^{-|x-x'|/\xi(T)}, \tag{2.7}$$

where

$$\Delta_s^2 = \frac{k_BT}{2\pi v_F\sqrt{a(T)c(T)}}, \tag{2.8}$$
$$\xi^{-1}(T) = \left(\frac{a(T)}{c(T)}\right)^{1/2}. \tag{2.9}$$

The fluctuating order parameters with standard deviation σ and correlation length ξ are characterized by the correlation functions given above, and all higher moments can be given by Wick's theorem.

2.1.1 Ornstein-Uhlenbeck Process

We use Ornstein-Uhlenbeck process to generate the fluctuating order parameters with finite correlation lengths. For real $\Delta(x)$, we consider the one-dimensional equation

$$\partial_x\Delta(x) = -a\Delta(x) + \sqrt{a}\sigma\eta, \tag{2.10}$$

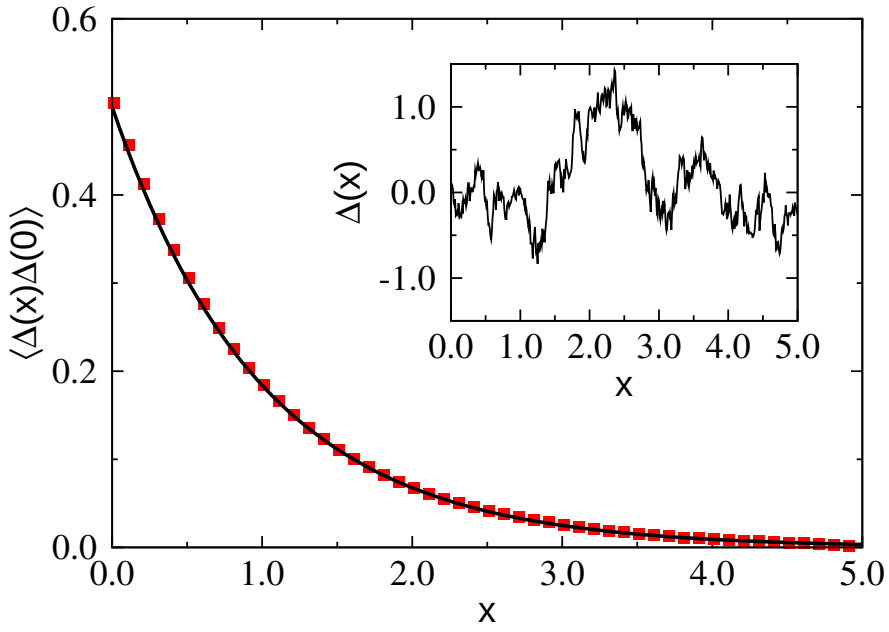

Figure 2.1: Correlation function of the 1-dimensional stochastic process with standard deviation $\sigma = 1$ and correlation length $\xi = 1$. The inset shows a typic realization of the order parameters

---

where η is the white Gaussian noise with $\langle\eta\rangle = 0$ and $\langle\eta(x)\eta(x')\rangle = \delta(x - x')$. The transition probability satisfies the Fokker-Planck equation

$$\partial_x p(\Delta, x|\Delta', x') = \left(-\frac{\partial}{\partial_\Delta}(a\Delta) + \frac{a\sigma^2}{2}\frac{\partial^2}{\partial\Delta^2}\right) p(\Delta, x|\Delta', x'). \tag{2.11}$$

By solving this equation we can get

$$p(\Delta, x|\Delta', x') = (2\pi)^{-\frac{1}{2}} \left(\frac{\sigma^2}{2}(1 - e^{-2a(x-x')})\right)^{-\frac{1}{2}} \exp\left(-\frac{(\Delta - \Delta' e^{-a(x-x')})^2}{\sigma^2(1 - e^{-2a(x-x')})}\right), \tag{2.12}$$

and the stationary density

$$p(\Delta) = \frac{1}{\sigma\sqrt{\pi}} e^{-\frac{\Delta^2}{\sigma^2}}. \tag{2.13}$$

Plugging both of them into the following equation

$$\langle\Delta(x)\Delta(x')\rangle = \int d\Delta' \int d\Delta\Delta p(\Delta, x|\Delta', x')\Delta' p(\Delta', x'), \tag{2.14}$$

we will get

$$\langle\Delta(x)\Delta(x')\rangle = \frac{1}{2}\sigma^2 e^{-a(x-x')}. \tag{2.15}$$

From this expression we can see that here a serves as the inverse of the correlation length ξ^{-1}.

A typical realization of the Gaussian order parameter fluctuations is shown in Fig. (2.1) which is generated using Eq. (2.10) with $\sigma = 1$ and $\xi = 1$. We also calculated the correlation function using the generated order parameter fluctuations. In this figure, we can see that the numerical result agrees with the exact result Eq. (2.15) very well.

For the complex order parameters, we define $\vec{\Delta}(x) = \Delta_1(x) + i\Delta_2(x)$ where $\Delta_1(x)$ and $\Delta_2(x)$ are both real and can be described by the stochastic process Eq. (2.10), which means

$$\langle \Delta_1(x)\Delta_1(x')\rangle = \frac{1}{2}\sigma^2 e^{-a(x-x')}, \langle \Delta_2(x)\Delta_2(x')\rangle = \frac{1}{2}\sigma^2 e^{-a(x-x')}, \tag{2.16}$$

and

$$\langle \Delta_1(x)\Delta_2(x')\rangle = 0. \tag{2.17}$$

Using these equations we can get

$$\begin{aligned} \langle \vec{\Delta}(x)\vec{\Delta}^*(x')\rangle &= \langle \Delta_1(x)\Delta_1(x')\rangle + \langle \Delta_2(x)\Delta_2(x')\rangle \\ &\quad +i\left(\langle \Delta_2(x)\Delta_1(x')\rangle - \langle \Delta_1(x)\Delta_2(x')\rangle\right) \\ &= \sigma^2 e^{-a|x-x'|} \end{aligned} \tag{2.18}$$

and

$$\langle \vec{\Delta}(x)\vec{\Delta}(x')\rangle = 0, \langle \vec{\Delta}^*(x)\vec{\Delta}^*(x')\rangle = 0. \tag{2.19}$$

2.2 Phase Fluctuations Only

For very small temperature, the amplitude fluctuations of the order parameters have been frozen out. We can write the order parameter as

$$\Delta(x) \approx \Delta_0 e^{i\vartheta(x)}. \tag{2.20}$$

Δ_0 is just the minimum of the free energy function, which can be determined by the usual BCS gap equation (1.60). In the commensurate case, where the fluctuating order parameters are real, the value of $\Delta(x)$ can be taken as $\pm\Delta_0$. On the other hand, in the incommensurate case, where the fluctuating order parameters are complex, the phase $\vartheta(x)$ is a continuous function of x. Using the generalized Ginzburg-Landau functional [42, 48] which is not restricted to small Δ and hence is valid at arbitrary temperature, we will have the free energy functional up to an irrelevant constant

$$\begin{aligned} F\{V(x)\} &= F\{\partial_x\vartheta(x)\} \\ &= \frac{1}{8}s\rho_0\frac{2\pi}{\beta}\sum_{\tilde{\omega}_n>0}\frac{\Delta_0^2(T)}{\left(\tilde{\omega}_n^2+\Delta_0^2(T)\right)^{\frac{3}{2}}}\int_0^L dx\left(\partial_x\vartheta(x)\right)^2 \\ &= \frac{1}{8}s\rho_s(T)\int_0^L dx V^2(x), \end{aligned} \tag{2.21}$$

where

$$V(x) \equiv \partial_x\vartheta(x), \tag{2.22}$$

and

$$\rho_s(T) = \rho_0\frac{2\pi}{\beta}\sum_{\tilde{\omega}_n>0}\frac{\Delta_0^2(T)}{\left(\tilde{\omega}_n^2+\Delta_0^2(T)\right)^{\frac{3}{2}}} \tag{2.23}$$

is the superfluid density. For $T = 0$, the sum turns into an integral which can be done analytically and gives

$$\rho_s(0) = \rho_0. \tag{2.24}$$

For any other temperature, we can calculate $\rho_s(T)$ using the $\Delta_0(T)$ calculated from the BCS gap equation. In these case, we have

$$\begin{aligned}
\left\langle \Delta(x)\Delta^*(x') \right\rangle &= \Delta_0^2 \left\langle \exp\left(i[\vartheta(x) - \vartheta(x')]\right) \right\rangle \\
&= \Delta_0^2 \left\langle \exp\left(i \int_x^{x'} dx'' V(x'') \right) \right\rangle \\
&= \Delta_0^2 \frac{\int \mathcal{D}\{V\} \exp\left(i \int_x^{x'} dx'' V(x'') - s\rho_s(T)/8k_BT \int_0^L dx'' V^2(x'') \right)}{\int \mathcal{D}\{V\} \exp\left(-s\rho_s(T)/8k_BT \int_0^L dx'' V^2(x'') \right)} \\
&= \Delta_0^2 \exp\left(-2k_BT/s\rho_s(T)|x - x'| \right) \\
&\equiv \Delta_0^2 \exp\left(-|x - x'|/\xi(T) \right),
\end{aligned} \tag{2.25}$$

where

$$\xi(T) = \frac{s\rho_s(T)}{2k_BT} \tag{2.26}$$

is the temperature-dependent correlation length. For very small temperature $\rho_s(T) \approx \rho_s(0) = 1/\pi$, so that $\xi(T) \propto 1/T$, which agrees with Grüner's result [49].

2.2.1 Wiener Process

Since the free energy functional Eq. (2.21) is Gaussian in $V(x)$, we then have

$$\langle V(x) \rangle = 0, \left\langle V(x)V(x') \right\rangle = \frac{2}{\xi(T)} \delta(x - x'). \tag{2.27}$$

The correlation function given above shows that $V(x)$ is Gaussian white noise with standard deviation $\sigma = \sqrt{2/\xi(T)}$, thus for the phase fluctuations $\vartheta(x)$ we have

$$\partial_x \vartheta(x) = \sqrt{\frac{2}{\xi(T)}} \eta. \tag{2.28}$$

2.3 Transfer Matrix Method

When the temperature is close to the mean-field critical temperature T_c^{MF}, we cannot apply above approximations anymore. To describe the order parameters fluctuations in this intermediate temperature region, we need a more general method. In the following, we will introduce the transfer matrix method, which was proposed by Scalapino, Sears and Ferrell in 1972 [47]. In this method, the partition function is expressed in terms of eigenvalues of a transfer Hamiltonian. By solving this transfer-matrix-eigenvalue problem, we can obtain the free energy of the original system which is just the ground state energy of the transfer Hamiltonian. Also the expectation value of the square of the order parameters and the correlation length of the order parameters can be calculated in the same manner.

Since the temperature is close to T_c^{MF}, we set $a(T)$ vary linearly with the temperature $a(T) = (T/T_c^{MF} - 1)$ and $b(T)$, $c(T)$ to be values at the mean-filed critical temperature, which are temperature independent. We also introduce the correlation length

$$\xi_0^2 = \left(\frac{v_F}{4\pi k_B T_c^{MF}}\right)^2 7\zeta(3), \tag{2.29}$$

with which we can rewrite the free energy functional as

$$F\{\Delta(x)\} = \int_0^L \frac{dx}{\xi_0}(a(T)|\Delta(x)|^2 + b|\Delta(x)|^4 + c|\partial_x\Delta(x)|^2). \tag{2.30}$$

Here

$$a(T) = \frac{\xi_0}{\pi v_F}\left(\frac{T - T_c^{MF}}{T_c^{MF}}\right), \tag{2.31}$$

$$b = \frac{b(T_c^{MF})\xi_0}{\pi v_F}, c = \frac{c(T_c^{MF})\xi_0}{\pi v_F}. \tag{2.32}$$

2.3.1 Partition Function

The partition function of the system with the free energy functional defined above can be expressed as a functional integral

$$Z = \int \delta\Delta e^{-\beta F\{\Delta\}}. \tag{2.33}$$

Dividing the whole system chain into N segments of length $\Delta x = L/N$, where L is the length of the chain and using the periodic boundary condition $\Delta_{N+1} = \Delta_1$, the partition function can be written as

$$\begin{aligned} Z &= \prod_i^N \int d\tilde{\Delta}_i \exp(-\beta_c(\Delta x/\xi_0) f(\Delta_{i+1}, \Delta_i)) \\ &= \int d\tilde{\Delta}_1 d\tilde{\Delta}_2 \cdots d\tilde{\Delta}_N \exp\left[-\beta_c\left(\Delta x/\xi_0\right) f(\Delta_1, \Delta_N)\right] \\ &\quad \exp\left[-\beta_c\left(\Delta x/\xi_0\right) f(\Delta_N, \Delta_{N-1})\right] \cdots \exp\left[-\beta_c\left(\Delta x/\xi_0\right) f(\Delta_2, \Delta_1)\right], \end{aligned} \tag{2.34}$$

where

$$f(\Delta_{i+1}, \Delta_i) = a|\Delta_{i+1}|^2 + b|\Delta_{i+1}|^4 + c\left|\frac{\Delta_{i+1} - \Delta_i}{\Delta x}\right|^2. \tag{2.35}$$

The integration elements are

$$d\tilde{\Delta}_i \equiv \left(\frac{\beta_c c}{\pi \Delta x \xi_0}\right)^{1/2} d\Delta_i \tag{2.36}$$

in the commensurate case and

$$d\tilde{\Delta}_i \equiv \left(\frac{\beta_c c}{\pi \Delta x \xi_0}\right)^{1/2} d(\mathrm{Re}\,\Delta_i) d(\mathrm{Im}\,\Delta_i) \tag{2.37}$$

in the incommensurate case. Since the temperature is close to the mean-filed critical temperature, We have set the parameter β to be $\beta_c = (kT_c^{MF})^{-1}$, then the significant temperature variation is contained just in the parameter a.

By introducing an additional variable $\tilde{\Delta}_1'$, we can rewrite Eq. (2.34) as follow

$$\begin{aligned} Z &= \int d\tilde{\Delta}_1' d\tilde{\Delta}_1 d\tilde{\Delta}_2 \cdots d\tilde{\Delta}_N \delta(\tilde{\Delta}_1' - \tilde{\Delta}_1) \exp\left[-\beta_c \left(\Delta x/\xi_0\right) f(\Delta_1', \Delta_N)\right] \\ &\quad \exp\left[-\beta_c \left(\Delta x/\xi_0\right) f(\Delta_N, \Delta_{N-1})\right] \cdots \exp\left[-\beta_c \left(\Delta x/\xi_0\right) f(\Delta_2, \Delta_1)\right]. \end{aligned} \tag{2.38}$$

Using a complete set of normalized eigenstates to expand the δ function

$$\delta(\tilde{\Delta}_1' - \tilde{\Delta}_1) = \sum_n \Psi_n^*(\tilde{\Delta}_1') \Psi_n(\tilde{\Delta}_1), \tag{2.39}$$

and making sure that eigenstates Ψ_n are eigenfunctions of the transfer operator

$$\int d\tilde{\Delta}_i \exp\left[-\beta_c(\Delta x/\xi_0) f(\Delta_{i+1}, \Delta_i)\right] \Psi_n(\tilde{\Delta}_i) = \exp\left[-\beta_c(\Delta x/\xi_0)\epsilon_n\right] \Psi_n(\tilde{\Delta}_{i+1}), \tag{2.40}$$

where ϵ_n are eigenvalues. Plugging them into Eq. (2.38) we can get that

$$Z = \sum_n e^{-\beta_c(L/\xi_0)\epsilon_n}. \tag{2.41}$$

For the thermodynamic limit, which is $L/\xi_0 \to \infty$, only the ground state contributes and the free energy per unit length is

$$f = (-kT_c/L) \ln Z = \epsilon_0/\xi_0. \tag{2.42}$$

The average value of the square of the order parameter is defined as:

$$\langle|\Delta|^2\rangle = \frac{\int d\tilde{\Delta}|\Delta|^2 e^{-\beta_c F\{\Delta\}}}{\int d\tilde{\Delta} e^{-\beta_c F\{\Delta\}}}, \tag{2.43}$$

and since $|\Delta|^2$ can be expressed as $\partial_a F(\Delta)$, then Eq. (2.43) can also be written in the form

$$\langle|\Delta|^2\rangle = \partial_a \ln Z. \tag{2.44}$$

Thus in the thermodynamic limit where only the ground state contributes, the average value of the square of the order parameter reads

$$\langle|\Delta|^2\rangle = \frac{\partial \epsilon_0}{\partial a}. \tag{2.45}$$

Following the same procedure, the correlation function can be expressed in terms of the Ψ_n eigenstates

$$C_1(x) = \sum_n |\langle\Psi_n|\Delta|\Psi_0\rangle|^2 \exp\left[-\beta_c(x/\xi_0)(\epsilon_n - \epsilon_0)\right]. \tag{2.46}$$

For distance $x \gg \xi_0$, the lowest excited state coupled by the matrix element determines the behavior of the correlation functions.

2.3.2 Transfer Matrix

In order to calculate the transfer-matrix-eigenvalue problem [Eq. (2.40)], we can further reduce it to a one-particle quantum mechanical problem by expanding $\Psi_n(\tilde{\Delta}_i)$ about $\Psi_n(\tilde{\Delta}_{i+1})$ and carrying out the $d\tilde{\Delta}_i$ integration.

$$\Psi_n(\tilde{\Delta}_i) = \Psi_n(\tilde{\Delta}_{i+1}) + (\tilde{\Delta}_i - \tilde{\Delta}_{i+1})\Psi_n'(\tilde{\Delta}_{i+1}) + \frac{1}{2}(\tilde{\Delta}_i - \tilde{\Delta}_{i+1})^2\Psi_n''(\tilde{\Delta}_{i+1}) + \cdots \tag{2.47}$$

Plugging the above expansion into Eq. (2.40), and integrating out $\tilde{\Delta}_i$, since $\tilde{\Delta}_i$ now is in Gaussian, only the even terms contribute and to leading order in Δx, we can get

$$\begin{aligned} &\int d\tilde{\Delta}_i \exp\left[-\beta_c\left(\Delta x/\xi_0\right) f(\Delta_{i+1}, \Delta_i)\right] \Psi_n(\tilde{\Delta}_i) \\ = \;& \exp\left[-\beta_c\left(\Delta x/\xi_0\right)\left(a|\Delta_{i+1}|^2 + b|\Delta_{i+1}|^4\right)\right]\left(1 + \frac{1}{4}\frac{\Delta x \xi_0}{\beta_c c}\frac{\partial^2}{\partial \Delta_{i+1}^2}\right)\Psi_n(\tilde{\Delta}_{i+1}) \end{aligned} \tag{2.48}$$

Further more we can exponentiate the derivative term and combine them together with the power terms to order Δx, so that the transfer-matrix-eigenvalue equation becomes

$$\exp\left[-\beta_c\left(\Delta x/\xi_0\right) H\right]\Psi_n = \exp\left[-\beta_c\left(\Delta x/\xi_0\right)\epsilon_n\right]\Psi_n. \tag{2.49}$$

The effective Hamiltonian of the transfer matrix for Eq. (2.30) is:

$$H = -\frac{1}{4}\frac{\xi_0^2}{\beta_c^2 c}\nabla^2 + a|\Delta|^2 + b|\Delta|^4. \tag{2.50}$$

2.3.3 Langevin Equation

Rewriting all the quantities in appropriate units, the length in units of ξ_0, the size of the order parameter in units of $\Delta_0 = \sqrt{a'/2b}$ and the reduced Ginzburg temperature $\Delta\tau = (a'^2/bk_BT_c^{MF})^{-2/3}$, the temperature in units of T_c^{MF}, $\tau = T/T_c^{MF} - 1$, the transfer matrix thus can be written in the following form:

$$\frac{\hat{H}}{k_BT_c} = \sqrt{\Delta\tau}\left[-\frac{1}{2}\nabla^2 + \frac{1}{2}\frac{\tau}{\Delta\tau}|\vec{\Delta}|^2 + \frac{1}{4}|\vec{\Delta}|^4\right]. \tag{2.51}$$

Here $\vec{\Delta} = (\Delta', \Delta'')$ are the complex order parameter fluctuations, and the Nabla operator is defined as $\nabla = (\partial_{\Delta'}, \partial_{\Delta''})$.

In the path integral approach, we can treat the evolution of the wave function in the imaginary time according to the Schrödinger equation

$$-\partial_x\psi(\vec{\Delta}, x) = \hat{H}\psi(\vec{\Delta}, x) \tag{2.52}$$

as a random walk procedure. For the transfer matrix Hamiltonian, the "imaginary time" corresponds to the spatial coordinate along the chain and the "spatial coordinate" is the order parameter fluctuation. Using the guided random walk method, defining $\Phi(\vec{\Delta}, x) = \psi(\vec{\Delta}, x)\psi_0(\vec{\Delta})$, where $\psi_0(\vec{\Delta})$ is the ground state wave function of the transfer matrix, we can show that $\Phi(\vec{\Delta}, x)$ is just the probability density of $\vec{\Delta}$ at point x [41]. Plugging $\psi(\vec{\Delta}, x)$ into Eq. (2.52), we can see that the distribution function $\Phi(\vec{\Delta}, x)$ obeys the equation:

$$\frac{\partial\Phi}{\partial x} = -\nabla\cdot\left(\frac{\nabla\psi_0}{\psi_0}\Phi\right) + \frac{1}{2}\nabla^2\Phi, \tag{2.53}$$

which is a typical Fokker-Planck equation.

Using the equivalence between the Fokker-Planck equation and the Langevin equation [50], we can see that the stochastic process described by this Fokker-Planck equation can also be generated by the corresponding Langevin equation

$$\frac{\partial \vec{\Delta}}{\partial x} = \frac{\nabla \psi_0}{\psi_0}(|\vec{\Delta}|) + \vec{\eta}, \tag{2.54}$$

which can be simulated very easily. Here $\vec{\eta} = (\eta', \eta'')$ is uncorrelated Gaussian noise in complex plane.

2.4 Anharmonic Oscillator

For the convenience of the further discussion, we just consider the reduced effective Hamiltonian

$$H = -\frac{1}{2}\nabla^2 + \frac{1}{2}\frac{\tau}{\Delta\tau}|\vec{\Delta}|^2 + \frac{1}{4}|\vec{\Delta}|^4 \tag{2.55}$$

In order to use the Langevin equation to generate the order parameter fluctuations, the first thing we need to know is the ground state wave function of the effective transfer Hamiltonian. The effective Hamiltonian describes a quantum-mechanical anharmonic oscillator. Before we solve it exactly, we will discuss the mean-field solution and the harmonic approximation first.

2.4.1 Mean Field Approximation

The anharmonic potential has been shown in Fig. (1.3) for different temperature. The ground state energy is dominated by the potential minimum. For $T \geq T_c^{MF}$, the minimum lies at the origin, while for $T < T_c^{MF}$, it occurs at $|\vec{\Delta}|^2 = -\frac{\tau}{\Delta\tau}$. Within the mean-field approximation, where the order parameters are spatially constant, the gradient term vanishes, and the free energy per unit length is just

$$f = -\frac{1}{4\xi_0}\left(\frac{\tau}{\Delta\tau}\right)^2, T \leq T_c^{MF} \tag{2.56}$$

and 0 otherwise.

2.4.2 Harmonic Approximation

Adding a small perturbation term to the mean-field value of the order parameter and expanding it, we can get the harmonic approximation. For the real order parameter we have

$$\Delta = \pm\left(-\frac{\tau}{\Delta\tau}\right)^{1/2} + \delta\Delta, \tag{2.57}$$

and for the complex order parameter

$$\vec{\Delta} = \left[\left(-\frac{\tau}{\Delta\tau}\right)^{1/2} + \delta\Delta\right] e^{i\phi} \tag{2.58}$$

at $T < T_c^{MF}$. Inserting these transformations into the reduced effective Hamiltonian and only keeping terms up to quadratic in $\delta\Delta$, we can get, for both real and complex order parameter Δ,

$$H = -\frac{1}{2}\frac{\partial^2}{\partial\delta\Delta^2} - \frac{\tau}{\Delta\tau}(\delta\Delta)^2 - \frac{1}{4}\left(\frac{\tau}{\Delta\tau}\right)^2, \tag{2.59}$$

which describes a harmonic oscillator with the eigenvalue $(n+\frac{1}{2})(2\frac{\tau}{\Delta\tau})^{1/2}, n = 0, 1, 2, \ldots$. So the ground state energy for the harmonic approximation is

$$\epsilon_0 = -\left(\frac{1}{2}\frac{\tau}{\Delta\tau}\right)^2 + \left(-\frac{1}{2}\frac{\tau}{\Delta\tau}\right)^{1/2}. \tag{2.60}$$

Above T_c, the mean field vanishes and the harmonic approximation gives for the real order parameter

$$\epsilon_0 = \frac{1}{2}\left(\frac{\tau}{\Delta\tau}\right)^{1/2}, \tag{2.61}$$

and for the complex order parameter, there is an extra factor of 2 which arises from the two-dimensional nature of the Hamiltonian.

2.4.3 Exact Solution

The anharmonic oscillator problem Eq. (2.55) can be solved by various approaches [51]. Here we have adopted the variational approximation technique [52] to solve the anharmonic oscillator exactly. We use a basis of n harmonic oscillator states to generate and truncate the matrix representation of the Hamiltonian. The matrix is then diagonalized numerically which gives eigenvalues and eigenvectors. As discussed before, the statistical mechanics is dominated by the ground state and first few excited states.

Matrix Elements

To simplify the notation, we will rewrite the Hamiltonian of the anharmonic oscillator. In the commensurate case,

$$H = \frac{p^2}{2} + \frac{\tau}{\Delta\tau}\frac{x^2}{2} + \frac{x^4}{4}, \tag{2.62}$$

where we have used p and x to replace $i\nabla$ and Δ respectively. To construct the matrix representation of the anharmonic oscillator, we use the basis functions of the harmonic oscillator

$$H_0 = \frac{p^2}{2} + \frac{\omega^2 x^2}{2} = \omega\left(a^\dagger a + \frac{1}{2}\right). \tag{2.63}$$

Thus

$$x = \left(\frac{1}{2\omega}\right)^{1/2}\left(a^\dagger + a\right), \tag{2.64}$$

$$p = i\left(\frac{\omega}{2}\right)^{1/2}\left(a^\dagger - a\right). \tag{2.65}$$

Where ω can be determined by minimizing the ground-state expectation value of H. Using the wavefunctions of eigenstates of the harmonic oscillator as the basis, the required matrix

elements are

$$\begin{aligned}
\left\langle n \left| \frac{p^2}{2} \right| n \right\rangle &= \frac{2\omega}{3}(2n+1), \\
\left\langle n \left| \frac{x^4}{4} \right| n \right\rangle &= \frac{1}{3\omega^2}(2n^2+2n+1), \\
\left\langle n-2 \left| \frac{p^2}{2} \right| n \right\rangle &= -\frac{2\omega}{3}\left[n(n-1)\right]^{1/2}, \\
\left\langle n-2 \left| \frac{x^4}{4} \right| n \right\rangle &= \frac{2}{9\omega^2}(2n-1)\left[n(n-1)\right]^{1/2}, \\
\left\langle n-4 \left| \frac{x^4}{4} \right| n \right\rangle &= \frac{1}{9\omega^2}\left[n(n-1)(n-2)(n-3)\right]^{1/2}. \qquad (2.66)
\end{aligned}$$

In the incommensurate case, we can use the same procedure, only this time, the Hamiltonian is a two dimensional anharmonic oscillator. The matrix elements of the Hamiltonian are

$$\left\langle m,n \left| \frac{p_x^2}{2} \right| m,n \right\rangle = \frac{\omega}{4}(2m+1), \left\langle m,n \left| \frac{p_y^2}{2} \right| m,n \right\rangle = \frac{\omega}{4}(2n+1),$$

$$\left\langle m,n \left| \frac{x^2}{2} \right| m,n \right\rangle = \frac{1}{4\omega}(2m+1), \left\langle m,n \left| \frac{y^2}{2} \right| m,n \right\rangle = \frac{1}{4\omega}(2n+1),$$

$$\left\langle m,n \left| \frac{x^4}{4} \right| m,n \right\rangle = \frac{3}{16\omega^2}(2m^2+2m+1), \left\langle m,n \left| \frac{y^4}{4} \right| m,n \right\rangle = \frac{3}{16\omega^2}(2n^2+2n+1),$$

$$\begin{aligned}
\left\langle m,n \left| \frac{x^2y^2}{2} \right| m,n \right\rangle &= \frac{1}{8\omega^2}(2m+1)(2n+1), \\
\left\langle m-2,n+2 \left| \frac{x^2y^2}{2} \right| m,n \right\rangle &= \frac{1}{8\omega^2}\left[m(m-1)(n+1)(n+2)\right]^{1/2}, \\
\left\langle m+2,n-2 \left| \frac{x^2y^2}{2} \right| m,n \right\rangle &= \frac{1}{8\omega^2}\left[(m+1)(m+2)n(n-1)\right]^{1/2},
\end{aligned}$$

$$\left\langle m-2,n \left| \frac{p_x^2}{2} \right| m,n \right\rangle = -\frac{\omega}{4}\left[m(m-1)\right]^{1/2}, \left\langle m,n-2 \left| \frac{p_y^2}{2} \right| m,n \right\rangle = -\frac{\omega}{4}\left[n(n-1)\right]^{1/2},$$

$$\left\langle m-2,n \left| \frac{x^2}{2} \right| m,n \right\rangle = \frac{1}{4\omega}\left[m(m-1)\right]^{1/2}, \left\langle m,n-2 \left| \frac{y^2}{2} \right| m,n \right\rangle = \frac{1}{4\omega}\left[n(n-1)\right]^{1/2},$$

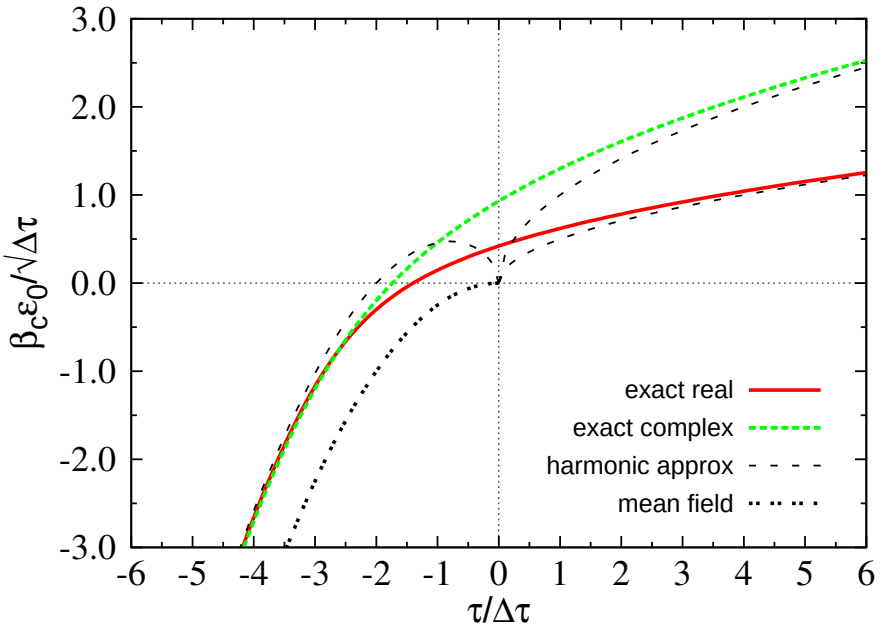

Figure 2.2: The ground state energy for different temperature. The red and green dashed lines show the exact results for real and complex order parameter fields separately. The dashed line shows the harmonic approximations and the dotted line shows the mean field result.

$$
\begin{aligned}
\left\langle m-2,n\left|\frac{x^4}{4}\right|m,n\right\rangle &= \frac{1}{8\omega^2}(2m-1)\left[m(m-1)\right]^{1/2}, \\
\left\langle m,n-2\left|\frac{y^4}{4}\right|m,n\right\rangle &= \frac{1}{8\omega^2}(2n-1)\left[n(n-1)\right]^{1/2}, \\
\left\langle m-2,n\left|\frac{x^2y^2}{2}\right|m,n\right\rangle &= \frac{1}{8\omega^2}(2*n+1)\left[m(m-1)\right]^{1/2}, \\
\left\langle m,n-2\left|\frac{x^2y^2}{2}\right|m,n\right\rangle &= \frac{1}{8\omega^2}(2*m+1)\left[n(n-1)\right]^{1/2}, \\
\left\langle m-2,n-2\left|\frac{x^2y^2}{2}\right|m,n\right\rangle &= \frac{1}{8\omega^2}\left[m(m-1)n(n-1)\right]^{1/2}, \\
\left\langle m-4,n\left|\frac{x^4}{4}\right|m,n\right\rangle &= \frac{1}{16\omega^2}\left[m(m-1)(m-2)(m-3)\right]^{1/2}, \\
\left\langle m,n-4\left|\frac{y^4}{4}\right|m,n\right\rangle &= \frac{1}{16\omega^2}\left[n(n-1)(n-2)(n-3)\right]^{1/2}. \qquad (2.67)
\end{aligned}
$$

Ground State Energy

By diagonalizing the above matrix, we can get the ground state energy of the Hamiltonian. The ground state energy ϵ_0 is plotted in Fig. (2.2) for both real and complex order parameter. The red line shows the exact result for the real order parameter and the blue line is for the complex order parameter. As a comparison, we also present here the

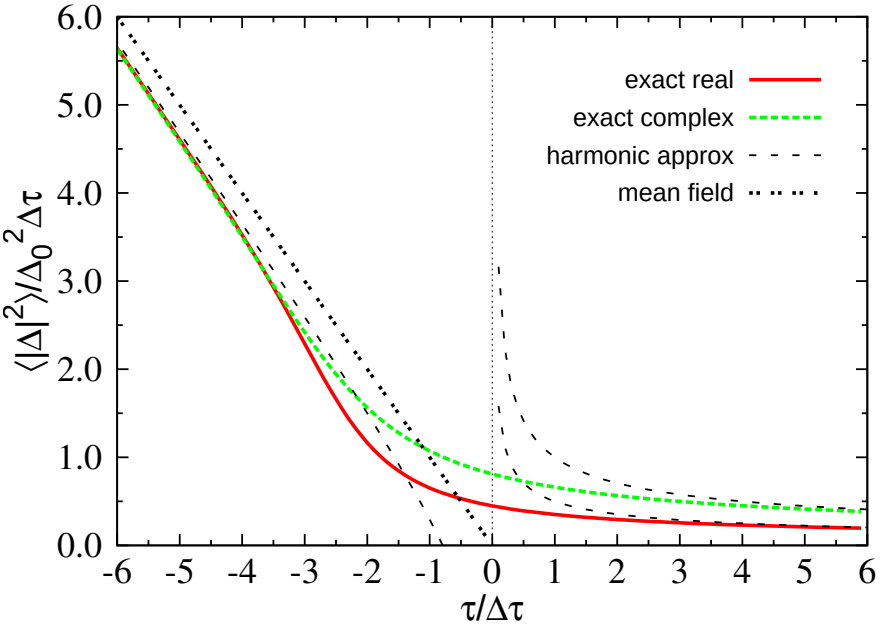

Figure 2.3: The expectation value of the square of the order parameters. The solid lines shows the exact results obtained from differentiating the ground state energy with respect to $\tau/\Delta\tau$. The red line is for the real order parameter and the green dashed line is for the complex order parameter. Dashed lines and dotted line are the harmonic approximation and mean field results respectively.

harmonic approximation results, which represented by the dashed lines. We can see that when the temperature is far away from the mean-field critical temperature, both the exact results for the real and complex order parameter approach the harmonic approximation results. While in between, we can see that the exact results vary smoothly and catch the physics which can not be obtained from the harmonic approximation. In the whole temperature region, the mean-field results have large discrepancy with both exact results and harmonic approximation results.

Ground State Expectation Value of The Square of The Order Parameters

As discussed before, the ground state expectation value of the square of the order parameter can be obtained by differentiating ϵ_0 with respect to $\tau/\Delta\tau$,

$$\langle|\Delta|^2\rangle = 2\frac{\partial\epsilon_0}{\partial(\tau/\Delta\tau)}. \tag{2.68}$$

Using the harmonic approximation, this gives for $T < T_c^{MF}$

$$\langle|\Delta|^2\rangle = -\frac{\tau}{\Delta\tau} - \left(-2\frac{\tau}{\Delta\tau}\right)^{-1/2}. \tag{2.69}$$

Above T_c, for the real order parameter, one finds

$$\langle|\Delta|^2\rangle = \frac{1}{2}\left(\frac{\tau}{\Delta\tau}\right)^{-1/2}, \tag{2.70}$$

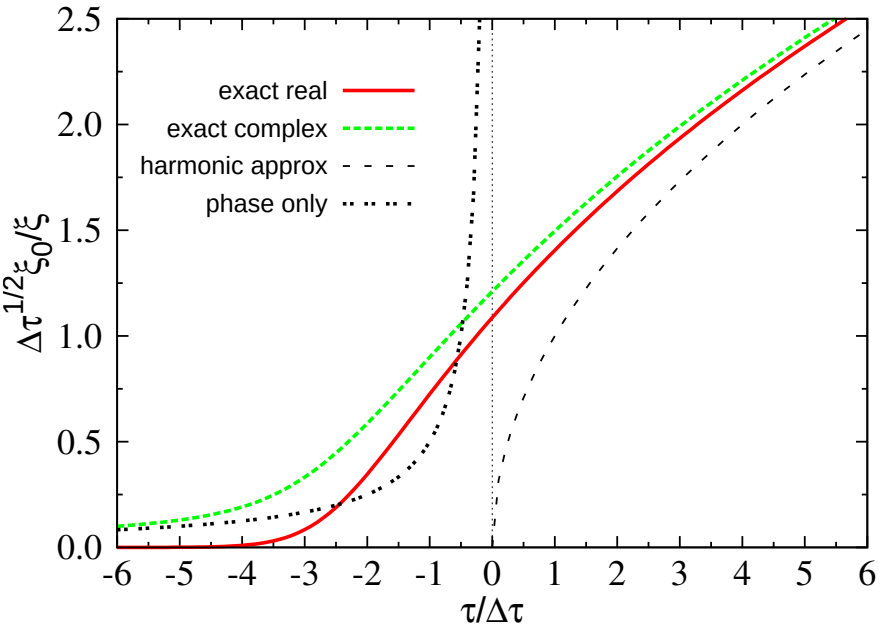

Figure 2.4: The inverse correlation length as a function of the temperature. The red line is for the real order parameter and the green dashed line is for the complex order parameter. Dashed lines and dotted line are the harmonic approximation and phase fluctuations only results respectively.

---

and as before, there is an extra factor of 2 for the complex order parameter. In the mean-field approximation, since the order parameters are spatially constant, then $\langle|\Delta|^2\rangle$ is just the minimum of the anharmonic potential, which is

$$\langle|\Delta|^2\rangle = -\frac{\tau}{\Delta\tau}. \tag{2.71}$$

We plot the results in Fig. (2.3), where the red and green lines are results obtained by solving the anharmonic oscillator for real and complex order parameter respectively. We can see that at large temperature, both results agree with the harmonic approximation. As the temperature is lowered, they also approaches harmonic approximation result from below, and always smaller than the mean-field result.

Correlation Length

As has been discussed before, the correlation function is given by Eq. (2.46), and for large distance $x \gg \xi_0$, the behavior of the correlation function is dominated by the lowest excited state coupled by the matrix element. Thus the correlation length is given by

$$\xi^{-1} = \xi_0^{-1}\beta(\epsilon_1 - \epsilon_0). \tag{2.72}$$

For the real order parameter, ϵ_1 is just the first excited state. For the complex order parameter, ϵ_1 is the lowest excited state having one unit of angular momentum. In Fig. (2.4) we plot the inverse correlation length as a function of the temperature. We can

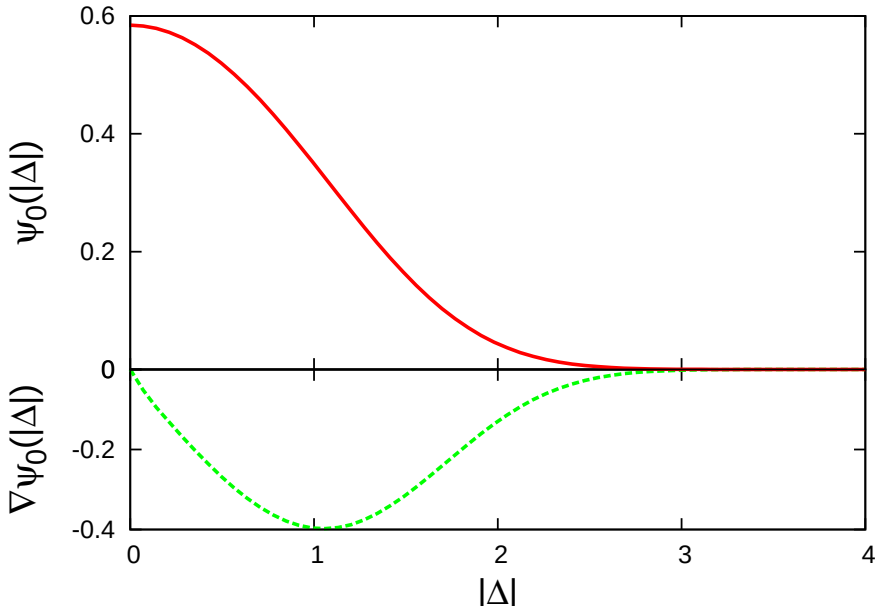

Figure 2.5: The ground-state wavefunction of the anharmonic oscillator and its gradient along the radial.

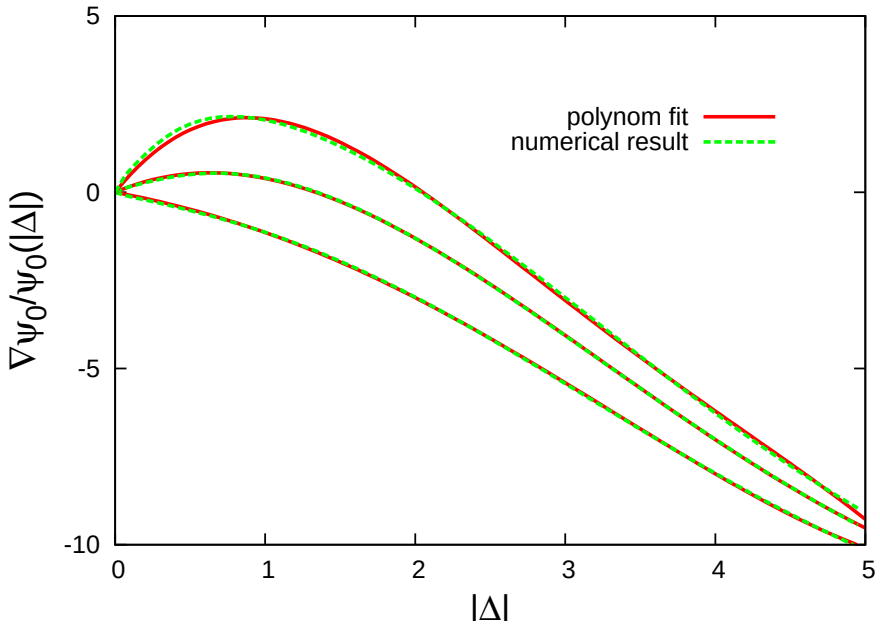

Figure 2.6: The drift term $\nabla\psi_0/\psi_0(|\vec{\Delta}|)$ as function of the amplitude of the order parameter $\vec{\Delta}$. The dashed lines are numerical results and solid lines are fitting results with fourth order polynomials. From top to bottom, $\Delta\tau/\tau = -1, -3, -5$.

see that for temperature below T_c^{MF}, the correlation length for the real order parameter approaches 0 very rapidly, and for the complex order parameter, it behaves as $1/(\tau/\Delta\tau)$, which we also derived in the phase fluctuations only case. The reason for that is as follows: since physically, the loss of order-parameter-order-parameter correlation involves changes in the sign of Δ, for the real order parameter, Δ can only be around either one of $\pm\Delta_0$, the finite energy associated with the hoping from one value to another provides a barrier which gives rise to the exponential growth of ξ_1. For the complex order parameter, however the change of the order parameters can be achieved simply by the phase fluctuations which by gradually changing θ involves arbitrarily small energies, and as the temperature decreases, the value varies as $1/T$, which is just the result we got from the phase fluctuations only case.

2.4.4 Ground State Wave Function and The Drift Term

The ground state wavefunction can also be constructed once we solved the matrix eigenvalue problem. The ground state wavefunction is just a superposition of different eigenfunctions of the harmonic oscillator. In Fig. (2.5) we show as an example the ground state wavefunction for $\tau = 0$ anharmonic oscillator. Since the ψ_0 is only a function of $|\Delta|$, so the drift term in the Langevin equation (2.54) can be written as $|\nabla\psi_0|/\psi_0(|\Delta|)e^{i\theta}$. For the later calculation, we approximate here the logarithmic derivative of the ground state wave function by a fourth order polynomial in $|\Delta|$, which can be seen in Fig. (2.6) is apparently a very good approximation.

For the harmonic oscillator, we have the ground state wavefunction

$$\psi_0(\Delta) = N_c e^{-\frac{1}{2}\frac{\tau}{\Delta\tau}|\Delta|^2}, \tag{2.73}$$

where N_c is the normalizing factor. The drift term is then

$$\frac{|\nabla\psi_0|}{\psi_0}(\Delta) = -\sqrt{\frac{\tau}{\Delta\tau}}|\Delta|. \tag{2.74}$$

Putting the result into the Langevin equation (2.54) we will have

$$\partial_x\Delta(\vec{x}) = -\sqrt{\frac{\tau}{\Delta\tau}}\vec{\Delta} + \vec{\eta}, \tag{2.75}$$

which is just the Ornstein-Uhlenbeck process Eq. (2.10) we have discussed before.

2.5 Numerical Simulation

Once we have the drift term, we can use the Langevin equation (2.54) to simulate different configurations of the order parameters, with which we can calculated the expectation value of the square of order parameters and the correlation length. As a comparison, we show numerical results simulated by the Langevin equation and exact results obtained by Scalapino et al. [47] in Fig. (2.7). The dots are the results calculated using the Langevin equation. It shows that even for a relative short chain, the calculated variance and correlation length are almost the same as the exact results. The difference is due to the numerical evaluation of the drift term, which we have approximated it by a fourth order

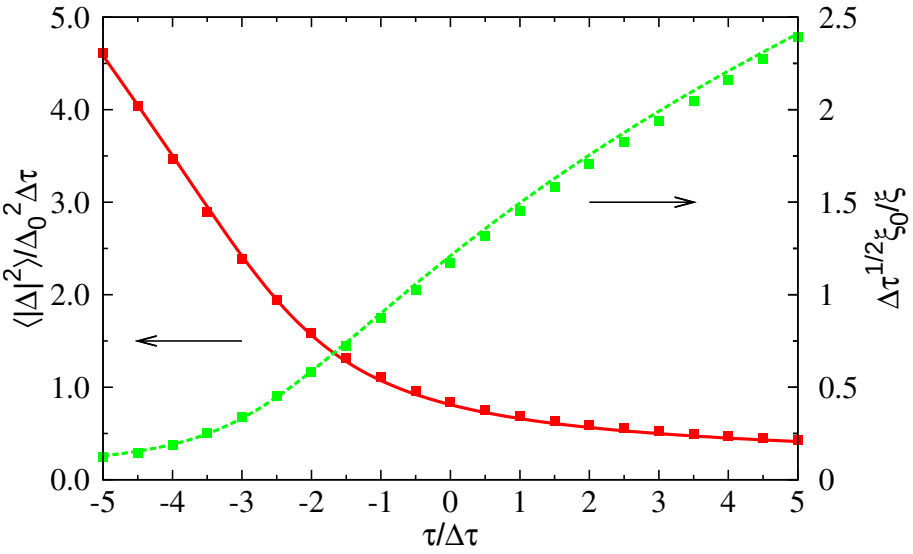

Figure 2.7: The variance and the inverse correlation length as functions of the temperature. The red lines are the exact results, the dots are numerical simulated results.

polynomial. We can see that both the simulated results using the Langevin equation agree very well with the exact results calculated from solving the anharmonic oscillator. Thus we can say that the order parameter fluctuations generated from the Langevin equation have precisely the statistics given by the action Eq. (1.53).

2.6 Polar Coordinate

From the above discussion, we have shown that the order parameters can be generated using the Langevin equation (2.54) in general. The drift term is a polynomial in the amplitude of the order parameter $|\Delta|$. In the Gaussian case, the drift term is proportional to $|\Delta|$ and in the non-Gaussian case, we have approximated the drift term by a fourth order polynomial. When the order parameters $\vec{\Delta}(x)$ are complex, we can also write it in the form $\vec{\Delta}(x) = \Delta(x)e^{i\theta(x)}$, where $\Delta(x)$ and $\theta(x)$ are amplitude and phase fluctuations of the complex order parameters. In both Gaussian and non-Gaussian cases, we can write the Langevin equations which generate the order parameters in the following form

$$\frac{\partial\vec{\Delta}(x)}{\partial x} = a(|\Delta|)\frac{\vec{\Delta}}{|\Delta|} + \vec{\eta}, \tag{2.76}$$

where $\vec{\eta} = \eta_1 + i\eta_2$, η_1 and η_2 are uncorrelated Gaussian noise. Plugging the form $\vec{\Delta}(x) = \Delta(x)e^{i\theta(x)}$ into Eq. (2.54) we get

$$\partial_x\Delta(x) = a(\Delta) + \cos\theta\eta_1 + \sin\theta\eta_2, \tag{2.77}$$

$$\partial_x\theta(x) = \frac{1}{\Delta}(-\sin\theta\eta_1 + \cos\theta\eta_2). \tag{2.78}$$

Now we will use the equivalence of the Fokker-Planck equation and the Langevin equation. In the multidimensional case with stratonovich interpretation, the stochastic

process is described by the Langevin equation

$$\dot{X}_i(t) = a_i(X_t, t) + b_{ij}(X_t, t)\eta_j(t), \tag{2.79}$$

and the probability distribution function of X_i satisfies the Fokker-Planck equation

$$\partial_t P(x,t) = \left[-\partial_i a_i(x,t) + \frac{1}{2}\partial_i b_{ik}(x,t)\partial_j b_{jk}(x,t)\right] P(x,t). \tag{2.80}$$

Here the differential operator ∂_i acts on all functions to its right. Applying this to our case, we have

$$\begin{aligned}\partial_x P(\Delta,\theta;x) \;=\; & \Big[-\partial_\Delta a(\Delta) + \frac{1}{2}\partial_\Delta \cos\theta\partial_\Delta \cos\theta + \frac{1}{2}\partial_\Delta \sin\theta\partial_\Delta \sin\theta \\ & -\frac{1}{2}\partial_\Delta \cos\theta\partial_\theta \frac{1}{\Delta}\sin\theta + \frac{1}{2}\partial_\Delta \sin\theta\partial_\theta \frac{1}{\Delta}\cos\theta \\ & -\frac{1}{2}\partial_\theta \frac{1}{\Delta}\sin\theta\partial_\Delta \cos\theta + \frac{1}{2}\partial_\theta \frac{1}{\Delta}\cos\theta\partial_\Delta \sin\theta \\ & +\frac{1}{2}\partial_\theta \frac{1}{\Delta}\sin\theta\partial_\theta \frac{1}{\Delta}\sin\theta + \frac{1}{2}\partial_\theta \frac{1}{\Delta}\cos\theta\partial_\theta \frac{1}{\Delta}\cos\theta\Big] P(\Delta,\theta;x).\end{aligned} \tag{2.81}$$

Simplifying the above equation, it becomes

$$\partial_x P(\Delta,\theta;x) = \left[-\partial_\Delta(a(\Delta) + \frac{1}{2\Delta}) + \frac{1}{2}\partial_\Delta^2 + \frac{1}{2\Delta^2}\partial_\theta^2\right] P(\Delta,\theta;x). \tag{2.82}$$

The Fokker-Planck equation we have derived above is equivalent to the Langevin equation

$$\partial_x \Delta(x) = a(\Delta) + \frac{1}{2\Delta} + \eta_\Delta, \tag{2.83}$$

$$\partial_x \theta(x) = \frac{1}{\Delta}\eta_\theta, \tag{2.84}$$

where η_Δ and η_θ are uncorrelated white Gaussian noise. From now on, we will use Eqs. (2.83) and (2.84) rather than Eq. (2.54) to describe the order parameters.

From the Langevin equation given above, we can see that the probability distribution function of Δ can be determined just by the function $a(\Delta)$

$$\partial_x P(\Delta;x) = \left[-\partial_\Delta\left(a(\Delta) + \frac{1}{2\Delta}\right) + \frac{1}{2}\partial_\Delta^2\right] P(\Delta;x). \tag{2.85}$$

Setting the left-hand side of the equation to be zero and solving the ordinary differential equation, we can get the stationary distribution function of Δ as

$$P(\Delta) = \frac{1}{C}\Delta \exp\left(\int_0^\infty 2a(\Delta)d\Delta\right), \tag{2.86}$$

where C is the normalization factor.

2.7 Langevin Equations for The Fluctuating Order Parameters

As a conclusion we will summerize all the Langevin equations for generating the order parameters in different cases. If the order parameters are Gaussian white noise, which means

$$\Delta(x) = \Delta_1\eta_1 + i\Delta_2\eta_2. \tag{2.87}$$

Here Δ_1, Δ_2 are two real constants, and η_1, η_2 are uncorrelated Gaussian white noise with $\langle\eta_i\eta_j\rangle = \delta_{ij}$. In the commensurate case, the order parameters are real, then we can set $\Delta_2 = 0$. In the incommensurate case, Δ_1 and Δ_2 are both non-zero.

If the order parameters are either Gaussian fluctuations with finite correlation lengths or non-Gaussian fluctuations, we have the following equations of motion for the order parameters:

$$\partial_x\Delta(x) = a(\Delta) + \eta \tag{2.88}$$

when the order parameters are real, and

$$\partial_x\Delta(x) = a(\Delta) + \eta_\Delta, \tag{2.89}$$

$$\partial_x\theta = \frac{1}{\Delta}\eta_\theta. \tag{2.90}$$

with η_Δ and η_θ two uncorrelated Gaussian white noise, when the order parameters are complex.

In the phase fluctuations only case, we have $\partial_x\theta(x) \equiv V(x)$. And from the Eq. (2.21) we see that $V(x)$ is Gaussian distributed, thus it ends up

$$\partial_x\theta(x) = \sqrt{\frac{2}{\xi(T)}}\eta, \tag{2.91}$$

where η is as usual the Gaussian white noise.

Chapter 3

Electronic Properties

In the previous chapter, we have discussed the statistics of the order parameter fluctuations. We derived the Langevin equations for generating the order parameter fluctuations according to the Ginzburg-Landau functional. Now we will come back to the electronic part of the system. As has been shown in chapter one, the low energy physics of the one-dimensional electron phonon system can be described by the so called Fluctuating Gap Model (FGM). For a given configuration of the order parameters, the Hamiltonian is given by Eq. (1.56). Here we write it in a different way

$$\hat{H}(x, -i\partial_x) = -iv_F\sigma_3\partial_x + \Delta(x)\sigma_+ + \Delta^*(x)\sigma_-. \tag{3.1}$$

As before, v_F is the Fermi velocity (hereforth we set $v_F = 1$) and $\Delta(x)$ is the order parameter which serves as a back scattering potential. $\sigma_i, i = 1, 2, 3$ are the usual Pauli matrices with $\sigma_\pm = (\sigma_1 \pm i\sigma_2)/2$. We have discussed the mean-field solution to this Hamiltonian in the first chapter. For a given spatially constant back scattering potential Δ, the calculated density of states shows that a gap opens right below $|\omega| < \Delta$. In this chapter, we will put the fluctuations of the order parameters into account and show how all electronic properties change. Since the charge density wave generally induces a zone that is incommensurate with the underlying lattice [36], in our later discussion we will mainly focus on the the complex order parameter fluctuations

First we will discuss the Gaussian order parameter fluctuations. The perturbation theory can be used to calculate the Green's function in principle. Based on that, we can calculate the density of states and the spectral function with further approximations. The suppression of the density of states at low energy indicates the opening of a pseudogap and the broadening of the quasi-particle peak with increasing correlation length suggests the break down of the Fermi liquid picture. Furthermore, we will show a method based on the phase formalism, which can be used to calculate the density of states and the spectral function exactly, but only with the Gaussian white order parameter fluctuations. In the last part of this chapter, we will use the Stochastic Method to solve the problem exactly and calculate the electronic properties with different statistics of order parameter fluctuations.

3.1 Perturbation Theory

The retarded Green's function $G^R(x,x';\omega)$ is of special interest because it can be related to several quantities which are in principle experimentally accessible. Using $\alpha = 1$ for right- and $\alpha = -1$ for left-moving fermions, the retarded Green's function is defined as

$$G^R_{\alpha\alpha'}(x,x';t,t') = -i\langle T[\Psi_\alpha(x,t)\Psi^*_{\alpha'}(x',t')]\rangle, \tag{3.2}$$

where $\Psi_\alpha(\Psi^*_\alpha)$ is the field operator. The Fourier transformation of the retarded Green's function satisfies the differential equation

$$[\omega + i0^+ - \hat{H}(x,-i\partial_x)]G^R(x,x';\omega) = \delta(x-x')\sigma_0. \tag{3.3}$$

3.1.1 Free Fermions

First we discuss the free fermions. Using Eq. (3.1) and setting $\Delta(x) = 0$, we can simplify the above equation to

$$[\omega + i0^+ + i\sigma_3\partial_x]G^R_0(x-x';\omega) = \delta(x-x')\sigma_0. \tag{3.4}$$

By using the Fourier transformation, we change this equation from real space to momentum space. It gives

$$[\omega + i0^+ - k\sigma_3]G^R_0(k;\omega) = \sigma_0. \tag{3.5}$$

After a simple matrix inversion, the matrix elements of $G^R_0(k,\omega)$ are given by

$$\left(G^R_0\right)_{\alpha\alpha'}(k;\omega) = \frac{\delta_{\alpha\alpha'}}{\omega - \alpha k + i0^+}. \tag{3.6}$$

The retarded Green's function in real space can be obtained by using the Fourier transformation again

$$G^R_0(x;\omega) = \int_{-\infty}^{+\infty} dk e^{ikx} G^R_0(k;\omega), \tag{3.7}$$

and the result reads

$$i\left(G^R_0\right)_{\alpha\alpha'}(x;\omega) = \delta_{\alpha\alpha'}\theta(\alpha x)e^{i\alpha\omega x}. \tag{3.8}$$

Here, $\theta(x)$ is the Heaviside step function. Eq. (3.8) indicates that fermions can only propagate in a single direction. As we will see later, the free fermion Green's function gives a starting point for the perturbative calculation.

3.1.2 Dyson Equation

With the presence of disordered back scattering potential, we can expand the Green's function in powers of the potential $\mathbf{\Delta}(x) = \Delta(x)\sigma_+ + \Delta^*(x)\sigma_-$, thus Eq. (3.3) can be written as

$$[i\sigma_3\partial_x + \omega + i0^+]G^R(x,x';\omega) = \delta(x-x')\sigma_0 + \mathbf{\Delta}(x)G^R(x,x';\omega). \tag{3.9}$$

Substituting x by x_1, multiplying the resulting equation from the left with the free Green's function $G^R_0(x,x_1;\omega)$ and then integrating over x_1 gives the Dyson equation

$$G^R(x,x';\omega) = G^R_0(x,x';\omega) + \int dx_1 G^R_0(x,x_1;\omega)\mathbf{\Delta}(x_1)G^R(x_1,x';\omega). \tag{3.10}$$

Iterating the above procedure, the exact Green's function can be expressed in terms of the free Green's function and the disorder potential.

$$G^R(x,x';\omega) = \sum_{n=0}^{\infty} G_n^R(x,x';\omega). \tag{3.11}$$

Where $G_0^R(x,x';\omega) = G_0^R(x-x';\omega)$ is the Green's function for free fermions. For $n \geq 1$ the functions $G_n^R(x,x';\omega)$ are given by

$$\begin{aligned} G_n^R(x,x';\omega) &= \int dx_1 \cdots \int dx_n G_0^R(x-x_n;\omega) \\ &\quad \mathbf{\Delta}(x_n) G_0^R(x_n - x_{n-1};\omega) \cdots \mathbf{\Delta}(x_1) G_0^R(x_1 - x';\omega). \end{aligned} \tag{3.12}$$

Now we consider the disorder-averaged Green's function. From Eq. (3.11) we can have

$$\left\langle G^R(x,x';\omega) \right\rangle = \sum_{n=0}^{\infty} \left\langle G_n^R(x,x';\omega) \right\rangle. \tag{3.13}$$

where $\langle \cdots \rangle$ represents averaging over configurations of the order parameters.

3.1.3 Lowest-Order Correction

The lowest-order correction $\left\langle G_2^R \right\rangle$ is a diagonal matrix. For example, for right-moving fermions, from Eq. (3.12)

$$\begin{aligned} \left\langle (G_2^R)_{11}(x,x';\omega) \right\rangle &= \left\langle \int dx_1 \int dx_2 (G_0^R)_{11}(x-x_2;\omega) \Delta(x_2) \right. \\ &\quad \left. \times (G_0^R)_{-1-1}(x_2-x_1;\omega) \Delta^*(x_1) (G_0^R)_{11}(x_1-x';\omega) \right\rangle \\ &= \int dx_1 \int dx_2 \left\langle \Delta(x_2)\Delta^*(x_1) \right\rangle (G_0^R)_{11}(x-x_2;\omega) \\ &\quad \times (G_0^R)_{-1-1}(x_2-x_1;\omega)(G_0^R)_{11}(x_1-x';\omega). \end{aligned} \tag{3.14}$$

Above the Peierls transition, the order parameter field $\Delta(x)$ has the Gaussian statistics, and the correlation function satisfies following equations:

$$\langle \Delta(x) \rangle = 0, \left\langle \Delta(x)\Delta^*(x') \right\rangle = \Delta_s^2 e^{-|x-x'|/\xi}. \tag{3.15}$$

All the higher moments of the order parameter field can be obtained by the Wick's theorem. Plugging this correlation function and also the explicit expression of the free fermion Green's function Eq. (3.8) into Eq. (3.14), we will have

$$\begin{aligned} \left\langle (G_2^R)_{11}(x,x';\omega) \right\rangle &= i\Delta_s^2 \int dx_1 \int dx_2 e^{-|x_2-x_1|/\xi} \theta(x-x_2) e^{i\omega(x-x_2)} \\ &\quad \times \theta(x_1-x_2) e^{i\omega(x_1-x_2)} \theta(x_1-x') e^{i\omega(x_1-x')}. \end{aligned} \tag{3.16}$$

With the presence of the step function, it is more convenient to integrate over path lengths l_1, l_2, l_3 than over intermediate coordinates x_1, x_2. We define

$$l_1 = |x_1 - x'|, l_2 = |x - x_2|, l_3 = |x_1 - x_2|, \tag{3.17}$$

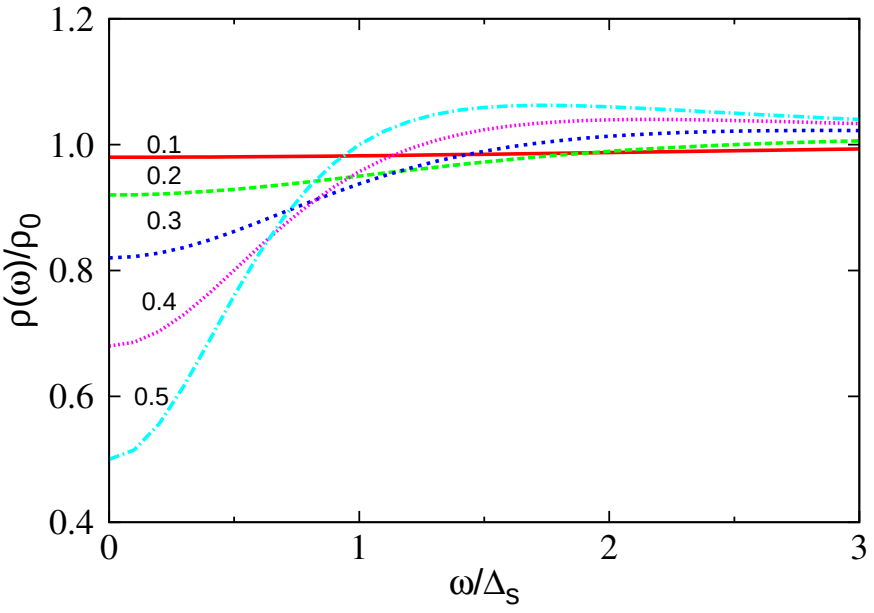

Figure 3.1: The density of states with the lowest correction term for different correlation lengths $\Delta_s\xi = 0.1, 0.2, 0.3, 0.4, 0.5$.

and they must fulfill the constraint

$$x - x' = l_1 + l_2 - l_3. \tag{3.18}$$

This constraint can be implemented by inserting

$$\delta(x - x' - l_1 - l_2 + l_3) = \int_{-\infty}^{+\infty} \frac{dk}{2\pi} e^{ik(x-x'-l_1-l_2+l_3)} \tag{3.19}$$

into the integrand.

In particular, we are interested in the local density of states, thus we just need to evaluate

$$\begin{aligned} \left\langle (G_2^R)_{11}(x,x;\omega) \right\rangle &= i\Delta_s^2 \int \frac{dk}{2\pi} \int_0^\infty dl_3 e^{i(\omega+k+i\xi^{-1})l_3} \\ &\quad \times \int_0^\infty dl_2 e^{i(\omega-k)l_2} \int_0^\infty dl_1 e^{i(\omega-k)l_1} \\ &= \Delta_s^2 \int \frac{dk}{2\pi} \frac{1}{\omega + k + i\xi^{-1}} \frac{1}{(\omega-k)^2}. \end{aligned} \tag{3.20}$$

Using the contour integration, we finally get

$$\left\langle (G_2^R)_{11}(x,x;\omega) \right\rangle = \frac{-i\Delta_s^2}{(2\omega + i\xi^{-1})^2}. \tag{3.21}$$

Since the local density of states is related to the Green's function by

$$\rho(\omega) = -\frac{1}{\pi} \operatorname{Im} \operatorname{Tr} \left[G^R(x,x;\omega) \right], \tag{3.22}$$

then the total density of states by considering just the second-order correction is

$$\rho(\omega) = \rho^{(0)}(\omega) + \rho^{(2)}(\omega) = \frac{1}{\pi}\left(1 + \mathrm{Re}\,\frac{2\Delta_s^2}{(2\omega + i\xi^{-1})^2}\right), \tag{3.23}$$

where the factor 2 comes from adding the contribution of left-moving fermions. We plot density of states for various correlation lengths in Fig. (3.1). The density of states is reduced in the range $|\omega| < \xi^{-1}/2$, that means a pseudogap opens up. But people should also notice that, this approximation is valid only when the fluctuations are fast enough, $\Delta_s\xi \ll 1/2$.

3.1.4 Higher-Order Correction

Next we take into account the higher-order correction terms, the 2n-th order correction is

$$\begin{aligned}\left\langle (G_{2n}^R)_{11}(x,x';\omega)\right\rangle &= \int dx_n dx_n' \ldots dx_1 dx_1' (G_0^R)_{11}(x-x_n;\omega)\ldots(G_0^R)_{-1-1}(x_1-x_1';\omega) \\ &\quad \times (G_0^R)_{11}(x_1'-x';\omega) D(x_n,x_n',\ldots,x_1,x_1'),\end{aligned} \tag{3.24}$$

where the 2n-point correlation function is

$$D(x_n,x_n',\ldots,x_1,x_1') = \left\langle \Delta(x_n)\Delta^*(x_n')\ldots\Delta(x_1)\Delta^*(x_1')\right\rangle. \tag{3.25}$$

In principle, it is rather difficult to determine the 2n-point correlation function for any given statistics. In the following, we will discuss some special cases, in which people can sum up a series of infinite number of terms in Eq. (3.12), or even all of the terms to calculate the retarded Green's function.

3.1.5 Second Order Born Approximation

We still keep the Gaussian statistics of the order parameters. The two-point correlation function is given by Eq. (3.15) and the 2n-point correlation function $D(x_n,x_n',\ldots,x_1,x_1')$ can be constructed using the Wick's theorem. For example, the four-point correlation function is then

$$D(x_2,x_2',x_1,x_1') = \Delta_s^4 e^{-|x_2-x_2'|/\xi} e^{-|x_1-x_1'|/\xi} + \Delta_s^4 e^{-|x_2-x_1'|/\xi} e^{-|x_1-x_2'|/\xi}. \tag{3.26}$$

In the diagrammatic representation of the averaged Green's function, an infinite number of diagrams can be summed up by introducing irreducible diagrams. The corresponding amputated diagram is obtained by eliminating all outer propagators. The sum of all amputated irreducible diagrams is known as the self-energy $\Sigma(k;\omega)$. In terms of the self-energy, the averaged Green's function can be expressed in momentum space as

$$\left(\left\langle G^R(k;\omega)\right\rangle\right)^{-1} = \left(G_0^R(k;\omega)\right)^{-1} - \Sigma(k;\omega). \tag{3.27}$$

The Self-Energy

If we only consider the contribution of the simplest irreducible diagram, we will come to the Born approximation. The self-energy in the second order Born approximation is given by

$$\Sigma_B(x-x';\omega) = \left\langle \mathbf{\Delta}(x) G_0^R(x-x';\omega)\mathbf{\Delta}(x')\right\rangle. \tag{3.28}$$

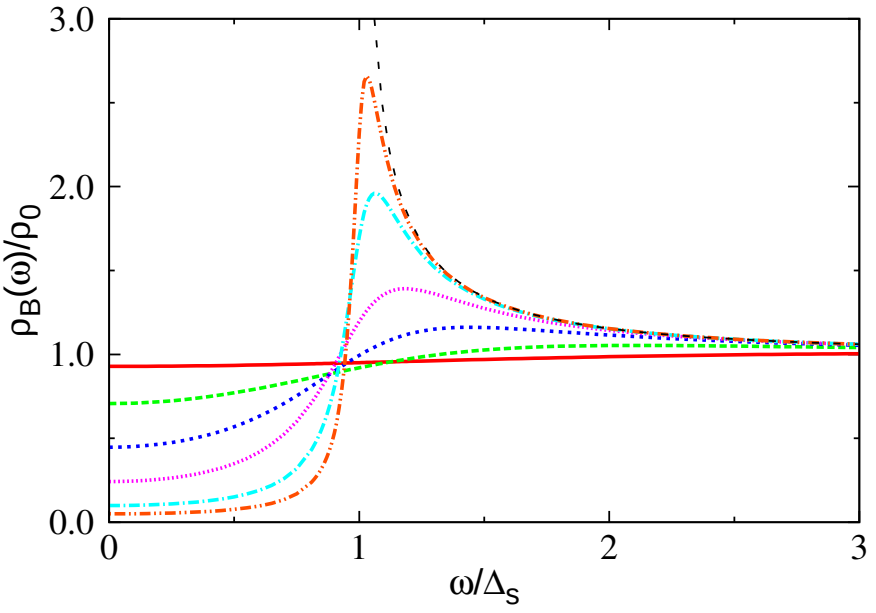

Figure 3.2: The density of states in second order Born approximation for different correlation lengths $\Delta_s\xi = 0.2, 0.5, 1.0, 2.0, 5.0, 10.0$. The black dashed line shows the mean-field result.

Inserting the retarded Green's function for the free fermions into the above equation, we can get

$$\begin{aligned}(\Sigma_B)_{\alpha\alpha'}(x-x';\omega) &= \delta_{\alpha,\alpha'}\Delta_s^2 e^{-|x-x'|/\xi}\left(G_0^R\right)_{\bar{\alpha},\bar{\alpha}}(x-x';\omega) \\ &= -i\delta_{\alpha,\alpha'}\Delta_s^2\theta(-\alpha(x-x'))e^{-i\alpha[\omega+i/\xi](x-x')}. \end{aligned} \tag{3.29}$$

Taking the Fourier transformation, we will get

$$\begin{aligned}(\Sigma_B)_{\alpha\alpha'}(k;\omega) &= \int_{-\infty}^{+\infty} dx e^{-ikx}(\Sigma_B)_{\alpha\alpha'}(x;\omega) \\ &= \delta_{\alpha,\alpha'}\frac{\Delta_s^2}{\omega+\alpha k+i/\xi}, \end{aligned} \tag{3.30}$$

and the averaged Green's function

$$\left(G_B^R\right)_{\alpha,\alpha'}(k,\omega) = \frac{\delta_{\alpha,\alpha'}}{\omega-\alpha k-\frac{\Delta_s^2}{\omega+\alpha k+i/\xi}}. \tag{3.31}$$

Density of States

Integrating Eq. (3.31) over k and taking the trace, we obtain

$$\mathrm{Tr}\, G_B^R(x,x;\omega) = -i\frac{\omega+i/2\xi}{\sqrt{(\omega+i/2\xi)^2-\Delta_s^2}}, \tag{3.32}$$

where $\sqrt{z}$ is defined as the principal part of the square root with the cut chosen along the negative real axis. The density of states is just the imaginary part of Eq. (3.32),

$$\rho_B(\omega) = \rho_0 \operatorname{Re} \frac{w + i/2\xi}{\sqrt{(\omega + i/2\xi)^2 - \Delta_s^2}}. \tag{3.33}$$

Spectral Function

The spectral function is defined as

$$A(\alpha k_F + k; \omega) = -\frac{1}{\pi} \operatorname{Im}(G^R(k;\omega))_{\alpha,\alpha}. \tag{3.34}$$

It directly follows from Eq. (3.31) that in the second order Born approximation the spectral function is given by

$$A(\alpha k_F + k; \omega) = \rho_0 \frac{\Delta_s^2 \xi}{\left(\Delta_s^2 - (\omega^2 - k^2)\right)^2 \xi^2 + (\omega - \alpha k)^2}. \tag{3.35}$$

In the second order Born approximation, we have summed up a series of infinite number of the diagrams, but it is still just a small part of all the diagrams we need to consider. In the following, we will discuss two cases where people can actually take into account all the diagrams.

3.1.6 Mean-Field

First we consider a rather trivial example, the mean-field approximation. In this approximation, we set $\Delta(x) = \Delta_s$, that means the order parameters are spatially constant. Thus

$$D(x_n, x_n', \ldots, x_1, x_1') = \Delta_s^{2n}. \tag{3.36}$$

Then the Fourier transformation of Eq. (3.12) gives

$$\begin{aligned} \left\langle G_{11}^R(k;\omega) \right\rangle &= \sum_{n=0}^{\infty} \left\langle (G_{2n}^R)_{11}(k;\omega) \right\rangle \\ &= \sum_{n=0}^{\infty} \frac{\Delta_s^{2n}}{(\omega - k)^{n+1}(\omega + k)^n} \\ &= \frac{\omega + k}{\omega^2 - k^2 - \Delta_s^2}. \end{aligned} \tag{3.37}$$

The spectral function now is

$$\begin{aligned} A(k;\omega) &= -\frac{1}{\pi} \operatorname{Im} G_{11}^R(k; \omega + i0^+) \\ &= \frac{E_k + k}{2E_k} \delta(\omega - E_k) + \frac{E_k - k}{2E_k} \delta(\omega + E_k), \end{aligned} \tag{3.38}$$

where

$$E_k = \sqrt{k^2 + \Delta_s^2}, \tag{3.39}$$

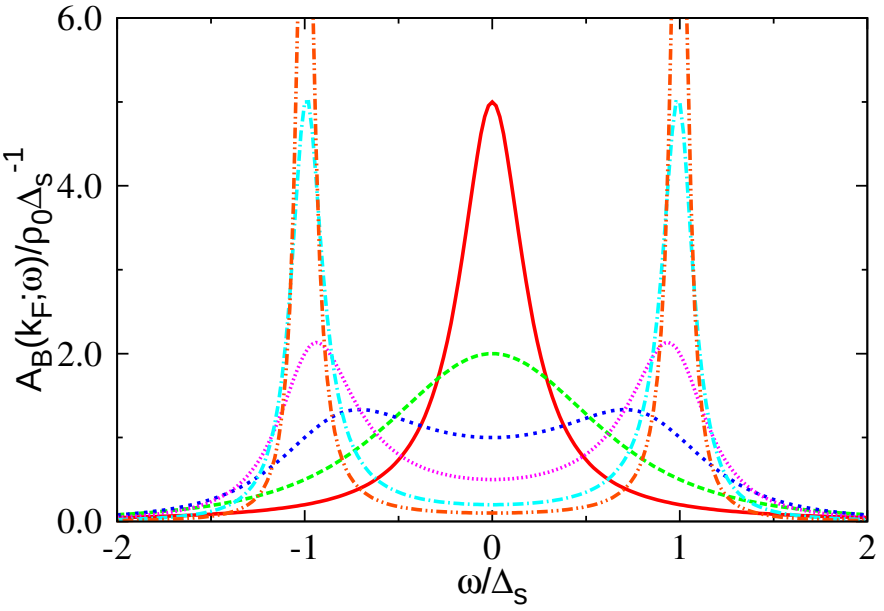

Figure 3.3: The spectral function $A_B(k_F + k; \omega)$ with $k = 0$ in second order Born approximation for different correlation lengths $\Delta_s\xi = 0.2, 0.5, 1.0, 2.0, 5.0, 10.0$.

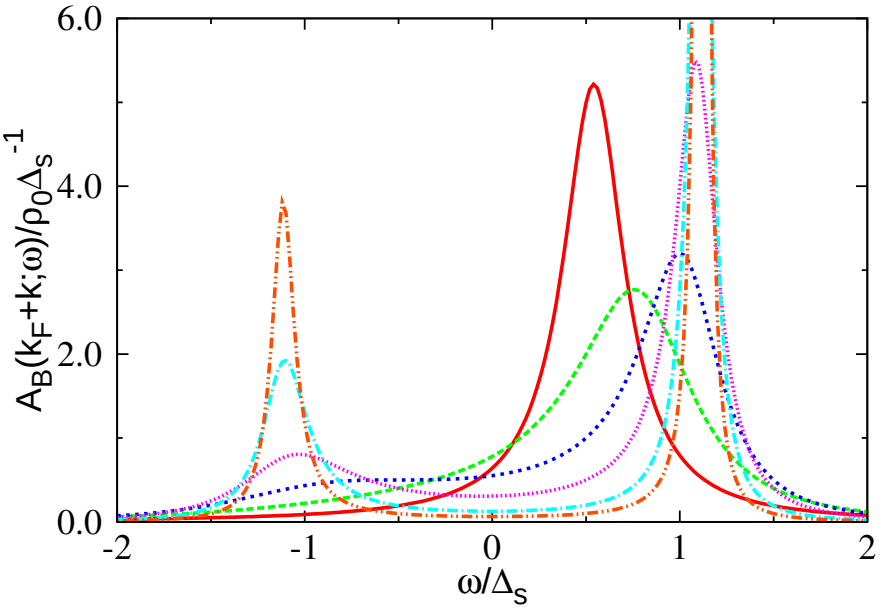

Figure 3.4: The spectral function $A_B(k_F + k; \omega)$ with $k = 0.5\Delta_s$ in second order Born approximation for different correlation lengths $\Delta_s\xi = 0.2, 0.5, 1.0, 2.0, 5.0, 10.0$.

which shows that the spectral function has two narrow peaks at $\pm E_k$. The density of states is

$$\rho(\omega) = \frac{1}{\pi}\frac{|\omega|}{\sqrt{\omega^2 - \Delta_s^2}}\theta(\omega^2 - \Delta_s^2). \tag{3.40}$$

We can see that the calculation reproduces all the results we have obtained in Chapter 1.

3.1.7 Infinite Correlation Length

Now we switch to the Gaussian fluctuations with infinite correlation length. In the limit of infinite correlation length, the correlation function (3.15) reduces to

$$\left\langle \Delta(x)\Delta^*(x')\right\rangle = \Delta_s^2, \tag{3.41}$$

and thus the 2n-point correlation function becomes

$$D(x_n, x_n', \ldots, x_1, x_1') = n!\Delta_s^{2n}. \tag{3.42}$$

We see that this is different from the 2n-correlation function in the mean-field case by a factor of $n!$. We then write the retarded Green's function in the form

$$\left\langle G_{11}^R(k;\omega)\right\rangle = \sum_{n=0}^{\infty} n!\frac{\Delta_s^{2n}}{(\omega - k)^{n+1}(\omega + k)^n}. \tag{3.43}$$

We can use the Stiltjes integral to evaluate the sum

$$\sum_{n=0}^{\infty} n!x^n = \int_0^{\infty} dt\frac{e^{-t}}{1 - xt}. \tag{3.44}$$

The integral on the right-hand side is perfectly finite for any x away from the positive real axis. If x approaches the real axis from the complex plane, $x \pm i0$, the integral has a nonzero imaginary part, which we cannot get from the sum of positive numbers on the left-hand side. Applying the above identity, we get the retarded Green's function

$$\left\langle G_{11}^R(k;\omega)\right\rangle = \int_0^{\infty} dte^{-t}\frac{\omega + k}{\omega^2 - k^2 - t\Delta_s^2}. \tag{3.45}$$

We can see that the integrand $(\omega + k)/(\omega^2 - k^2 - t\Delta_s^2)$ is just the mean-field retarded Green's function Eq. (3.37) with the field $\sqrt{t}\Delta_s$. By adding an infinitesimal small imaginary number to the energy and taking the Imaginary part of the retarded Green's function, we end up with the spectral function for the right-moving fermion

$$\begin{aligned} A(k;\omega) &= -\int_0^{\infty} dte^{-t}(\omega + k)\delta(\omega^2 - k^2 - t\Delta_s^2) \\ &= \frac{1}{\Delta_s^2}\theta(\omega^2 - k^2)(\omega + k)e^{-(\omega^2 - k^2)/\Delta_s^2}. \end{aligned} \tag{3.46}$$

The density of states can be obtained by integrating the spectral function $A(k,\omega)$ over k,

$$\begin{aligned} \rho(\omega) &= 2\int_{-\infty}^{+\infty}\frac{dk}{2\pi}A(k,\omega) \\ &= \frac{2\omega}{\pi\Delta_s^2}e^{-\omega^2/\Delta_s^2}\int_0^{\omega} dke^{k^2/\Delta_s^2} \\ &= \frac{2}{\pi}\frac{\omega}{\Delta_s}e^{-\omega^2/\Delta_s^2}\,\mathrm{Erfi}\left(\frac{\omega}{\Delta_s}\right). \end{aligned} \tag{3.47}$$

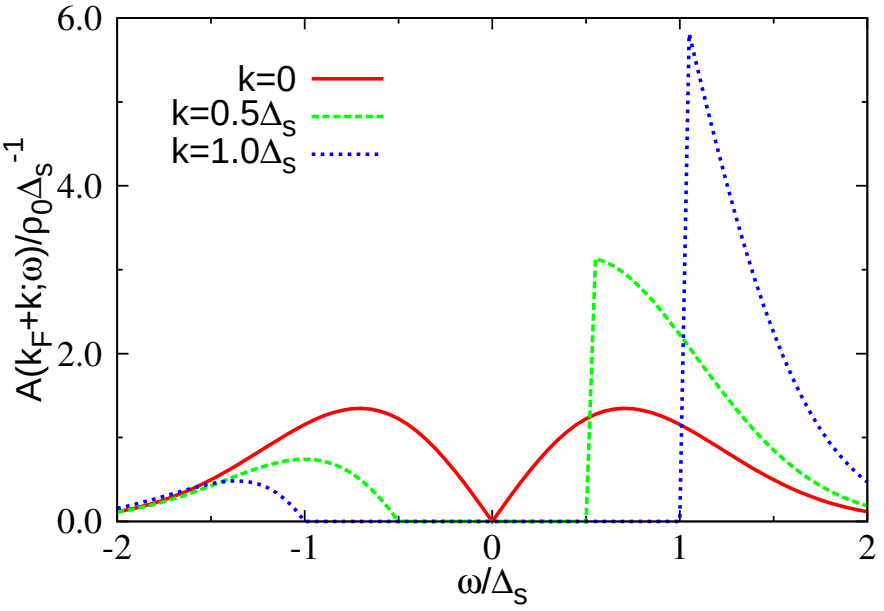

Figure 3.5: The spectral function $A(k_F + k; \omega)$ with $k = 0, 0.5\Delta_s, 1.0\Delta_s$ for infinite correlation length. The sudden jump at $\omega = \pm k$ are due to the presence of a step function

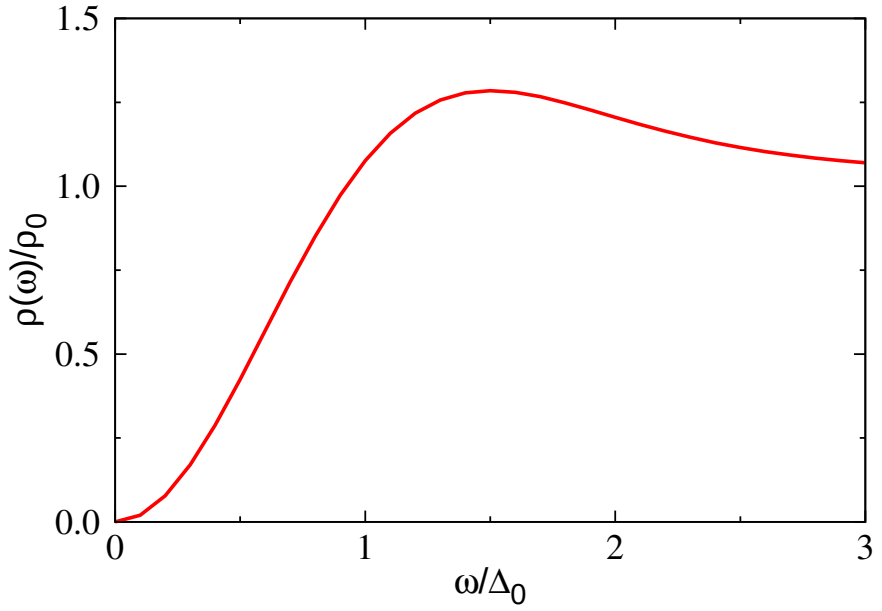

Figure 3.6: The density of states for infinite correlation length. An pseudogap opens up at low energy region and there is never a real gap.

Here

$$\mathrm{Erfi}(x) = \int_o^x e^{t^2} dt \tag{3.48}$$

is the error function with an imaginary argument.

It is also possible to go back to the original assumption about the Gaussian statistics. In the limit of $\xi \to \infty$, instead of a random order parameter $\Delta(x)$, we have a single random variable Δ describing the value of the gap field everywhere on the chain. Its Gaussian character is realized by considering an ensemble of chains, each with a different but fixed Δ, with the distribution function

$$p(\Delta) = \frac{e^{-|\Delta|^2/\Delta_s^2}}{\pi \Delta_s^2}. \tag{3.49}$$

So the 2n-point correlation function now is given by

$$\begin{aligned} D(x_n, x_n', \ldots, x_1, x_1') &= \left\langle |\Delta|^{2n} \right\rangle \\ &= \int |\Delta|^{2n} p(\Delta) d^2\Delta = n! \Delta_s^{2n}. \end{aligned} \tag{3.50}$$

On every chain, there is a perfect gap with size $|\Delta|$, and it varies from chain to chain. The density of states and the spectral function now can be calculated by taking the ensemble average of the result for a single gap.

3.2 Non-Perturbative Method

Although the calculation presented above can qualitative explain the pseudogap phenomenon, it is all based on the perturbation theory. As we know that for the correlated one-dimensional electronic system, interface effects due to perfect nesting between two Fermi points invalidate a perturbative calculation near the Fermi level. Thus we need a more solid or even exact solution.

Considering the wave function

$$\Psi(x) = \begin{pmatrix} \psi_1(x) \\ \psi_2(x) \end{pmatrix}, \tag{3.51}$$

in the segment $(0, L)$, where $\psi_1(x)$, $\psi_2(x)$ represent right-moving and left-moving part of the wave function respectively. Then the wave function is the eigenfunction of the eigenvalue problem

$$\begin{pmatrix} -i\partial_x & \Delta_0 + \Delta(x) \\ \Delta_0 + \Delta^*(x) & i\partial_x \end{pmatrix} \begin{pmatrix} \psi_1(x) \\ \psi_2(x) \end{pmatrix} = \omega \begin{pmatrix} \psi_1(x) \\ \psi_2(x) \end{pmatrix}. \tag{3.52}$$

Here Δ_0 is a static gap potential and $\Delta(x) = \Delta_1(x) + i\Delta_2(x)$ with $\Delta_1(x)$ and $\Delta_2(x)$ are both Gaussian white noise. We choose the boundary conditions

$$\psi_1(0) = \psi_2(0) = 1, \psi_1(L)/\psi_2(L) = 1 \tag{3.53}$$

to ensure the Hermiticity of the Hamiltonian. Using Eq. (3.52) and the boundary conditions we chose above, it shows that there exists a symmetry relation between $\psi_1(x)$ and $\psi_2(x)$, i.e.

$$\psi_1(x) = \psi_2^*(x). \tag{3.54}$$

By using Eikonal ansatz, we can write $\psi_1(x)$ as follows:

$$\psi_1(x) = e^{\zeta(x)} i e^{i\varphi(x)/2}. \tag{3.55}$$

Putting the ansatz into Eq. (3.52), we can get the equations of motion for $\varphi(x)$ and $\zeta(x)$

$$\begin{aligned} \partial_x \varphi(x) &= 2\omega + 2(\Delta_0 + \Delta_1(x)) \cos\varphi(x) + 2\Delta_2(x) \sin\varphi(x), & (3.56)\\ \partial_x \zeta(x) &= 2\Delta_1(x) \cos\varphi(x) - 2\Delta_2(x) \sin\varphi(x). & (3.57) \end{aligned}$$

and the boundary conditions are

$$\varphi(0) = 0, \varphi(L) = 2n\pi, \zeta(0) = 0. \tag{3.58}$$

Also we introduce another linearly independent solution $\tilde{\psi} = e^{\tilde{\zeta}(x)} i e^{-i\tilde{\varphi}(x)/2}$, where $\tilde{\varphi}(x)$ and $\tilde{\zeta}(x)$ also satisfy Eqs. (3.56) and (3.57), and the boundary condition for $\tilde{\varphi}(x)$ and $\tilde{\zeta}(x)$ are

$$\tilde{\varphi}(L) = 0, \tilde{\varphi}(0) = 2n\pi, \tilde{\zeta}(L) = 0. \tag{3.59}$$

Since both ψ and $\tilde{\psi}$ are eigenfunctions of the same energy ω, from Eq. (3.52) we get that $\psi_1\tilde{\psi}_2 - \psi_2\tilde{\psi}_1$ is a constant independent of x. With the help of all these we can write the Green's function in the following form:

$$G(x, x'; \omega) = \frac{i}{\psi_1\tilde{\psi}_2 - \psi_2\tilde{\psi}_1} \begin{pmatrix} \tilde{\psi}_1(x)\psi_2(x') & \tilde{\psi}_1(x)\psi_1(x') \\ \tilde{\psi}_2(x)\psi_2(x') & \tilde{\psi}_2(x)\psi_1(x') \end{pmatrix}, \tag{3.60}$$

for $x > x'$.

We can obtain the retarded (advanced) Green's function $G^R(x, x')$ ($G^A(x, x')$) by solving for wave function with an infinitesimally small imaginary adding to the energy ω. For $\mathrm{Im}\,\omega > 0$ we have

$$\frac{\psi_1\tilde{\psi}_2}{\psi_2\tilde{\psi}_1} = \exp\left[-i\left(\varphi(x) - \tilde{\varphi}(x)\right)\right] < 1, \tag{3.61}$$

thus we can Taylor expand the denominator and write the retarded Green's function as

$$G^R(x, x'; \omega) = -i \sum_{n=0}^{\infty} \begin{pmatrix} \hat{C}_n(x, x')\hat{y}_n(x) & \hat{D}_n(x, x')\hat{y}_n(x) \\ \hat{C}_n(x, x')\hat{y}_{n+1}(x) & \hat{D}_n(x, x')\hat{y}_{n+1}(x) \end{pmatrix}, \tag{3.62}$$

where

$$\begin{aligned} \hat{y}_n(x) &= \left[\frac{\tilde{\psi}_2(x)}{\tilde{\psi}_1(x)}\right]^n, & (3.63)\\ \hat{C}_n(x, x') &= \left[\frac{\psi_1(x)}{\psi_2(x)}\right]^n \frac{\psi_2(x')}{\psi_1(x)}, & (3.64)\\ \hat{D}_n(x, x') &= \left[\frac{\psi_1(x)}{\psi_2(x)}\right]^n \frac{\psi_1(x')}{\psi_2(x)}. & (3.65) \end{aligned}$$

Now we take the $L \to \infty$ limit, and since ψ and $\tilde{\psi}$ are statistically independent, we can write the averaged retarded Green's function as the product of averages of $\hat{C}(\hat{D})$ and $\hat{y}$. The averaged quantities $C_n \equiv \left\langle \hat{C}_n(x, x') \right\rangle$ and $D_n \equiv \left\langle \hat{D}_n(x, x') \right\rangle$ are functions of $x - x'$ and $y_n \equiv \langle \hat{y}_n(x) \rangle$ is independent of x.

From the definition Eq. (3.63), we see that $\hat{y}_n(x) = (-1)^n e^{in\tilde{\varphi}(x)}$. Combined with the equation of motion of $\tilde{\varphi}(x)$, we have for the averaged quantity $\left\langle e^{in\tilde{\varphi}} \right\rangle$ the following equation:

$$\begin{aligned}\partial_x \left\langle e^{in\tilde{\varphi}(x)} \right\rangle &= in \Big(2\omega \left\langle e^{in\tilde{\varphi}(x)} \right\rangle + \Delta_0 \left\langle e^{i(n+1)\tilde{\varphi}(x)} \right\rangle + \Delta_0 \left\langle e^{i(n-1)\tilde{\varphi}(x)} \right\rangle \\ &\quad + \left\langle \Delta_1(x) e^{i(n+1)\tilde{\varphi}(x)} \right\rangle + \left\langle \Delta_1(x) e^{i(n-1)\tilde{\varphi}(x)} \right\rangle \\ &\quad - i \left\langle \Delta_2(x) e^{i(n+1)\tilde{\varphi}(x)} \right\rangle + i \left\langle \Delta_2(x) e^{i(n-1)\tilde{\varphi}(x)} \right\rangle \Big). \end{aligned} \tag{3.66}$$

Since both $\Delta_1(x)$ and $\Delta_2(x)$ are Gaussian white noise, we can decouple the averages of the form $\langle \Delta(x)_i f\{\Delta_i(x)\} \rangle$ $(i = 1, 2)$ using the Novikov's formula

$$\langle \Delta_i(x) f\{\Delta_i(x)\} \rangle = \int dx' \left\langle \Delta_i(x)\Delta_i(x') \right\rangle \left\langle \frac{\delta f\{\Delta_i(x)\}}{\delta \Delta_i(x')} \right\rangle. \tag{3.67}$$

Taking into account the correlation function $\langle \Delta_i(x)\Delta_i(x') \rangle = \Delta_s^2/2\delta(x - x')$, we transform the above equation to

$$\langle \Delta_i(x) f\{\Delta_i(x)\} \rangle = \frac{\Delta_s^2}{2} \left\langle \frac{\delta f\{\Delta_i(x)\}}{\delta \Delta_i(x - 0)} \right\rangle. \tag{3.68}$$

When we apply this to the quantity $\left\langle \Delta_i(x) e^{i(n\pm1)\tilde{\varphi}(x)} \right\rangle$, we need to be very careful about the functional derivative

$$\frac{\delta \tilde{\psi}(x)}{\delta \Delta_1(x')} = 2 \cos \tilde{\varphi}(x) \theta(x - x'). \tag{3.69}$$

Since in our case $x = x'$, we define here $\theta(0) = \lim_{x\to 0} \left[\theta(x) + \theta(-x)\right]/2 = 1/2$. As a result we get

$$\left\langle \Delta_1(x) e^{i(n+1)\tilde{\varphi}(x)} \right\rangle = \frac{i(n+1)}{4} \Delta_s^2 \left(\left\langle e^{i(n+2)\tilde{\varphi}(x)} \right\rangle + \left\langle e^{in\tilde{\varphi}(x)} \right\rangle \right), \tag{3.70}$$

$$\left\langle \Delta_1(x) e^{i(n-1)\tilde{\varphi}(x)} \right\rangle = \frac{i(n-1)}{4} \Delta_s^2 \left(\left\langle e^{in\tilde{\varphi}(x)} \right\rangle + \left\langle e^{i(n-2)\tilde{\varphi}(x)} \right\rangle \right), \tag{3.71}$$

$$\left\langle \Delta_2(x) e^{i(n+1)\tilde{\varphi}(x)} \right\rangle = \frac{(n+1)}{4} \Delta_s^2 \left(\left\langle e^{i(n+2)\tilde{\varphi}(x)} \right\rangle - \left\langle e^{in\tilde{\varphi}(x)} \right\rangle \right), \tag{3.72}$$

$$\left\langle \Delta_2(x) e^{i(n-1)\tilde{\varphi}(x)} \right\rangle = \frac{(n-1)}{4} \Delta_s^2 \left(\left\langle e^{in\tilde{\varphi}(x)} \right\rangle - \left\langle e^{i(n-2)\tilde{\varphi}(x)} \right\rangle \right). \tag{3.73}$$

Plugging all the quantities listed above into Eq. (3.66), multiplying both sides with the prefactor $(-1)^n$ and setting the left-hand side of the equation to be zero, we can get the recursion relation for y_n,

$$\left(2\omega + in\Delta_s^2\right) y_n - \Delta_0 y_{n+1} - \Delta_0 y_{n-1} = 0. \tag{3.74}$$

with the initial value $y_0 = 1$.

Using the same procedure, we can derive the equation for $C_n(x - x')$,

$$\begin{aligned}\frac{dC_n}{d(x - x')} &= i(2n+1)\omega C_n - i(n+1)\Delta_0 C_{n+1} \\ &\quad - in\Delta_0 C_{n-1} - (n^2 + n + \frac{1}{2})\Delta_s^2 C_n. \end{aligned} \tag{3.75}$$

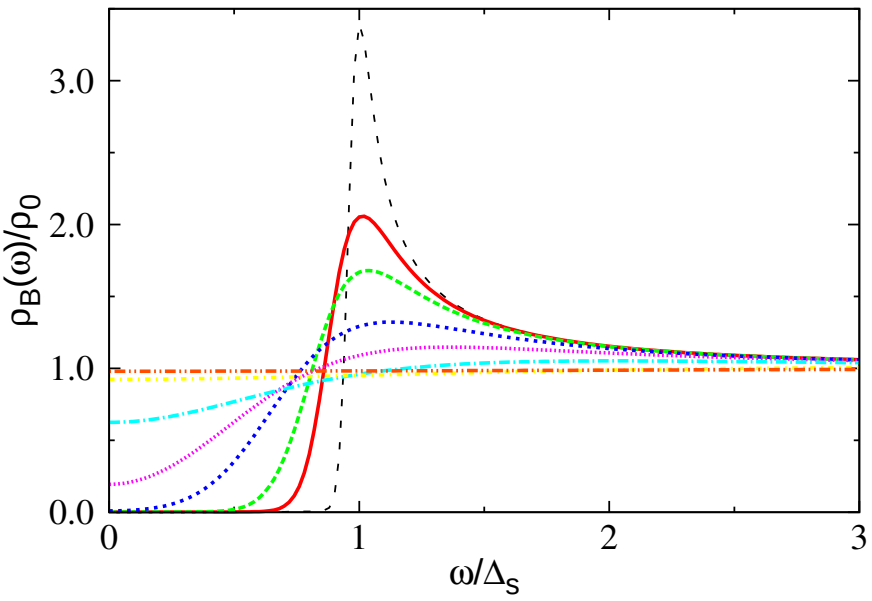

Figure 3.7: The density of states for $\Delta_s^2/\Delta_0 = 0.1, 0.2, 0.5, 1.0, 2.0, 5.0, 10.0, 50.0$.

Since we have $\left\langle (\tilde{\psi}_2/\tilde{\psi}_1)^n \right\rangle = \langle (\psi_1/\psi_2)^n \rangle$ [53], we have the initial condition $C_n(0) = y_n$. D_n satisfies the same equations as C_n with the initial condition $D_n = y_{n+1}$.

Now we solve Eqs. (3.74) and (3.75). Luckily y_n, C_n and D_n decay exponentially as a function of n. Thus we can set $y_n = 0$ for $n > N$, a relative large number, to truncate the number of equations we need to solve. Once we have all the y_n, C_n and D_n, we can construct the retarded Green's function using Eq. (3.62). And again, the density of states and spectral function can be obtained via the resulted retarded Green's function.

The density of states can be calculated by setting $x = x'$ and taking the imaginary part of the trace of the retarded Green's function. We show in Fig. (3.7) the density of states for different Δ_s^2/Δ_0. The density of states at low energy is suppressed from the free fermions results. And as the strength of the fluctuations increases, i.e. Δ_s becomes larger, the suppression is also stronger. As we can see, at $\Delta_s^2/\Delta_0 = 50$, the suppression is so strong that a nearly full gap shows up.

We also present the results of the spectral function in both symmetric and asymmetric cases in Figs. (3.8) and (3.9). It shows two peaks at around $\omega/\Delta_0 = \pm 1$. As Δ_s^2/Δ_0 increases, the height of the peaks decrease. For very small Δ_s^2/Δ_0, the peaks become narrower and higher, which for $\Delta_s^2/\Delta_0 = 0$ recovers the mean-field result. And for larger Δ_s^2/Δ_0, the fluctuations effect dominates, and the spectral function become very flat and delocalized, the electrons in this situation behave like free fermions.

We can also use this method to calculate the optical conductivity. The real part of the frequency-dependent optical conductivity for small temperature is [53, 54]:

$$\sigma(\omega) = \frac{e^2}{A}\frac{2}{\pi\omega}\int_{-\omega}^{\infty} d\epsilon \int_{x'}^{\infty} dx \,\mathrm{Re}\left[j^{+-}(x-x';\epsilon+\omega,\epsilon) - j^{++}(x-x';\epsilon+\omega,\epsilon)\right], \quad (3.76)$$

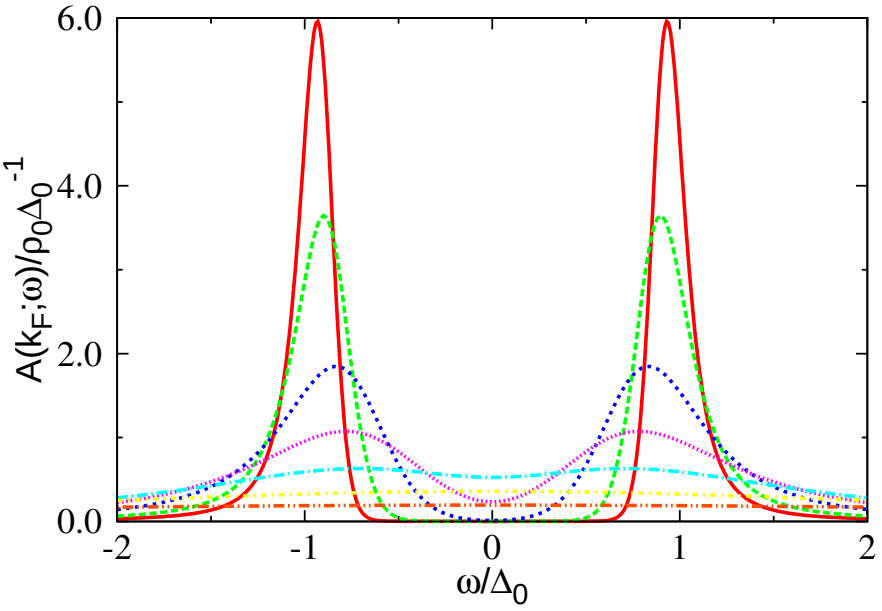

Figure 3.8: The spectral function $A(k_F + k; \omega)$ with $k = 0$ for Gaussian white noise and $\Delta_s^2/\Delta_0 = 0.1, 0.2, 0.5, 1.0, 2.0, 5.0, 10.0$.

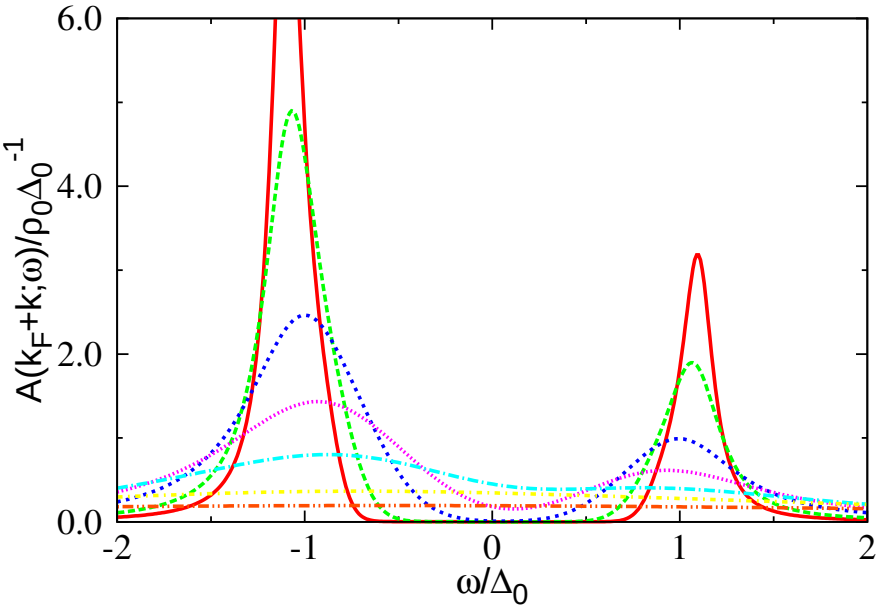

Figure 3.9: The spectral function $A(k_F + k; \omega)$ with $k = 0.5\Delta_0$ for Gaussian white noise and $\Delta_s^2/\Delta_0 = 0.1, 0.2, 0.5, 1.0, 2.0, 5.0, 10.0$.

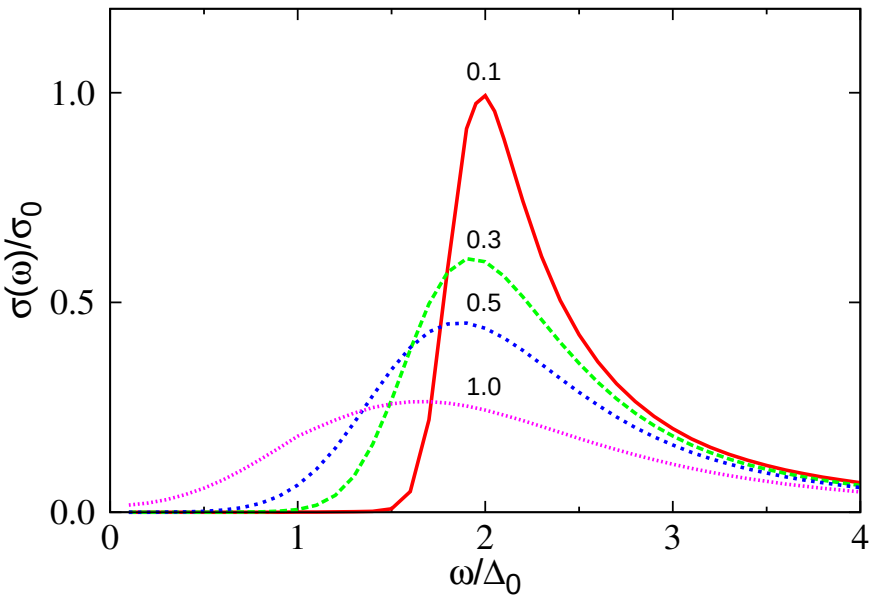

Figure 3.10: The optical conductivity for Gaussian white noise and $\Delta_s^2/\Delta_0 = 0.1, 0.3, 0.5, 1.0$.

where A is the cross-sectional area of a chain and

$$j^{\pm\pm}(x-x';\epsilon,\epsilon') = \left\langle \mathrm{Tr}\left[\sigma_3 G^{\pm}(x',x;\epsilon)\sigma_3 G^{\pm}(x,x';\epsilon')\right]\right\rangle \tag{3.77}$$

is the averaged correlator of the current. Here we have used G^+ (G^-) to denote the retarded (advanced) Green's function, and σ_3 is just the usual Pauli matrix. In the following we will use the approximation $\langle GG\rangle \approx \langle G\rangle\langle G\rangle$ to calculate $j^{\pm\pm}$, which we expect to be valid for $\omega \gg \Delta_s$.

Since we need to have the retarded and advanced Green's functions for both $x > x'$ and $x < x'$ in our calculation, we can use the above method to calculate them separately. But fortunately. with the help of the symmetry properties of the Green's functions, we can reduce large amount of work. From the symmetry condition $\psi_1(x) = \psi_2^*(x)$ the matrix elements of the Green's functions have the following relation:

$$\left[G_{11}^{\pm}(x,x';\epsilon)\right]^* = G_{11}^{\mp}(x',x;\epsilon) = G_{22}^{\mp}(x,x';\epsilon), \tag{3.78}$$
$$\left[G_{12}^{\pm}(x,x';\epsilon)\right]^* = G_{21}^{\mp}(x',x;\epsilon) = G_{21}^{\mp}(x,x';\epsilon), \tag{3.79}$$

and

$$G_{11}^{\pm}(x,x';-\epsilon) = -G_{22}^{\mp}(x,x';\epsilon), \tag{3.80}$$
$$G_{12}^{\pm}(x,x';-\epsilon) = G_{21}^{\mp}(x,x';\epsilon). \tag{3.81}$$

We show in Fig. (3.10) the calculated optical conductivity. As Δ_s^2/Δ_0 increases , the spectrum broadens rapidly, and the peak moves towards the low energy region.

3.3 Stochastic Method

Up to now, all the methods we have discussed can only be applied to some special cases. The second-order Born approximation, sums up an infinite number of diagrams, considers still just a small fraction of all the diagrams. Although some exact results can be obtained, they are only valid either for Gaussian fluctuations with the infinite correlation length or for the Gaussian white noise. For the Gaussian fluctuations with finite correlation lengths or more importantly for the non-Gaussian fluctuations, it is impossible to apply any of the above methods. In the following, based on the stochastic technique [25], we will develop a method, which can be used to calculate the electronic quantities for nearly all kinds of statistics of the order parameters fluctuations, and the results are formally exact.

3.3.1 Eigenstates and Eigenfunctions

Once we know all the eigenvalue and eigenstates of the Hamiltonian (3.1), we solve the problem completely. Recalling that the eigenvalue problem is

$$\begin{pmatrix} -i\partial_x & \Delta(x) \\ \Delta^*(x) & i\partial_x \end{pmatrix} \begin{pmatrix} \psi(x) \\ \psi^*(x) \end{pmatrix} = \omega \begin{pmatrix} \psi(x) \\ \psi^*(x) \end{pmatrix}, \tag{3.82}$$

here ω is the eigenenergy and $\psi(x)$ is the wave function we want to calculate. We will use the Eikonal ansatz for the wave function, $\psi(x) = e^{\zeta(x)} i e^{i\varphi(x)/2}$. By plugging the definition of $\psi(x)$ into Eq. (3.82), it is easy to get the equations of motion for both $\varphi(x)$ and $\zeta(x)$. The specific form of equations depends on the statistics of the order parameters we want to discuss. Not all functions satisfy equations of motion are the eigenfunctions of the original problem, unless they obey the right boundary condition. Since all physical quantities should be independent of the boundary conditions in the thermodynamic limit, we can choose the boundary condition to make our calculation as easy as possible. Here we will impose the boundary condition as follow

$$\varphi(0) = 0, \varphi(L) = \varphi_L. \tag{3.83}$$

In the following, using the generating function of the order parameter fluctuations along with the boundary conditions Eq. (3.83) we will derive the equations which will be used to calculate the density of states, the spectral function and the optical conductivity. Since for different statistics of order parameters, we have different equations, we need to discuss them separately.

3.3.2 Gaussian White Noise

First we will calculate the electronic properties when order parameter fluctuations are Gaussian white noise. We write the fluctuations in the form

$$\vec{\Delta}(x) = \Delta_0 + \Delta_1 \eta_1 + i\Delta_2 \eta_2, \tag{3.84}$$

where Δ_0 is a static gap potential, Δ_1 and Δ_2 are both real constants to denote the strength of the fluctuations, η_1 and η_2 are uncorrelated Gaussian white noise. Generally both Δ_1 and Δ_2 are nonzero, then $\vec{\Delta}(x)$ is complex which refers to the incommensurate case. To simplify the later calculation, we usually set $\Delta_1 = \Delta_2 = \Delta_s$. If we set $\Delta_2 = 0$,

then the fluctuating order parameters $\Delta(x)$ become real, which is just the commensurate case.

Putting both the ansatz for the wave function and order parameter fluctuations Eq. (3.84) into the Eq. (3.82), we then get the equations of motion for both $\varphi(x)$ and $\zeta(x)$,

$$\begin{aligned} \partial_x\varphi(x) &= 2\omega + 2\Delta_0\cos\varphi(x) + 2\Delta_1\cos\varphi(x)\eta_1 + 2\Delta_2\sin\varphi(x)\eta_2, && (3.85)\\ \partial_x\zeta(x) &= \Delta_0\sin\varphi(x) + \Delta_1\sin\varphi(x)\eta_1 - \Delta_2\cos\varphi(x)\eta_2. && (3.86) \end{aligned}$$

Density of States

The density of states is defined as:

$$\rho(\omega) = \frac{1}{L}\left\langle \sum_n \delta(\omega - \omega_n) \right\rangle, \tag{3.87}$$

here $\langle\cdots\rangle$ represents averaging over different configurations of the order parameters, ω_n is the energy of the nth eigenstate, which is nth ω satisfies the boundary condition $\varphi(L,\omega) = \varphi_L$. Using the identity

$$\delta[f(x)] = \sum_i \frac{\delta(x - x_i)}{|f'(x_i)|}, \tag{3.88}$$

where x_i are zeros of the function $f(x)$, we have

$$\sum_i \delta(\omega - \omega_i) = \delta[\varphi_L - \varphi(L,\omega)]|\partial\varphi(L,\omega)/\partial\omega|. \tag{3.89}$$

We define the function $U_1(x)$ by

$$U_1(x) = \frac{\partial\varphi(x,\omega)}{\partial\omega}. \tag{3.90}$$

Using Eq. (3.85) and changing the order of the differential operators ∂_x and ∂_ω, we can get the equation of motion for $U_1(x)$

$$\partial_x U_1(x) = 2 - 2U_1(x)\left[\Delta_0\sin\varphi(x) - \Delta_1\sin\varphi(x)\eta_1 + \Delta_2\cos\varphi(x)\eta_2\right]. \tag{3.91}$$

Then the density of states Eq. (3.87) can be written as

$$\rho(\omega) = \frac{1}{L}\left\langle |U_1(x)|\delta[\varphi_L - \varphi(L,\omega)]\right\rangle. \tag{3.92}$$

Later we will show that $U_1(x)$ is always non-negative, thus we can just replace $|U_1(x)|$ in Eq. (3.92) by $U_1(x)$.

We further define the joint probability distribution function $P(\varphi, U_1; x)$ by

$$P(\varphi, U_1; x) = \left\langle \delta(\varphi - \varphi(x))\delta(U_1 - U_1(x))\right\rangle. \tag{3.93}$$

Then the density of states becomes

$$\rho = \frac{1}{L}\int_{-\infty}^{+\infty} U_1 P(\varphi_L, U_1; L) dU_1. \tag{3.94}$$

Using the equivalence of the Fokker-Planck equation and the Langevin equation in the multidimensional multiplicative noise case, we can write down the equation of motion for $P(\varphi, U_1; x)$:

$$\begin{aligned}\partial_x P(\varphi, U_1; x) &= \big[2\Delta_1^2\partial_\varphi \cos\varphi\partial_\varphi \cos\varphi + 2\Delta_2^2\partial_\varphi \sin\varphi\partial_\varphi \sin\varphi \\ &\quad -2\Delta_1^2\partial_\varphi \cos\varphi\partial_{U_1} \sin\varphi U_1 + 2\Delta_2^2\partial_\varphi \sin\varphi\partial_{U_1} \cos\varphi U_1 \\ &\quad -2\Delta_1^2\partial_{U_1} \sin\varphi U_1\partial_\varphi \cos\varphi + 2\Delta_2^2\partial_{U_1} \cos\varphi U_1\partial_\varphi \sin\varphi \\ &\quad +2\Delta_1^2\partial_{U_1} \sin\varphi U_1\partial_{U_1} \sin\varphi U_1 + 2\Delta_2^2\partial_{U_1} \cos\varphi U_1\partial_{U_1} \cos\varphi U_1 \\ &\quad -\partial_\varphi(2\omega + 2\Delta_0 \cos\varphi) - \partial_{U_1}(2 - 2U_1\Delta_0 \sin\varphi)\big] P(\varphi, U_1; x). \quad (3.95)\end{aligned}$$

In the following, if not mentioned specifically, the differential operator ∂_i acts on all functions to its right. If we just consider the symmetric case, where we set $\Delta_1 = \Delta_2 = \Delta_s$, we can simplify the above equation for $P(\varphi, U_1; x)$ to

$$\begin{aligned}\partial_x P(\varphi, U_1; x) &= [-\partial_\varphi(2\omega + 2\Delta_0 \cos\varphi) - \partial_{U_1}(2 - 2\Delta_0 \sin\varphi U_1) \\ &\quad +2\Delta_s^2\partial_\varphi^2 + 2\Delta_s^2\partial_{U_1}U_1 + 2\Delta_s^2(\partial_{U_1}U_1)^2\big] P(\varphi, U_1; x). \quad (3.96)\end{aligned}$$

Since $P(\varphi, U_1; x)$ is a probability distribution function of φ and U_1, it satisfies the following boundary condition

$$\lim_{U_1\to\pm\infty} U_1^s P(\varphi, U_1; x) = 0, s = 0, 1. \quad (3.97)$$

It is very difficult to solve for $P(\varphi, U_1; x)$ directly, thus we define two functions $P_s(\varphi, x), s = 0, 1$ by

$$P_s(\varphi; x) = \int_{-\infty}^{+\infty} dU_1 U_1^s P(\varphi, U_1; x), \quad (3.98)$$

and $P_s(\varphi; x)$ satisfy the equations of motion

$$\partial_x P_0(\varphi; x) = \big[-\partial_\varphi(2\omega + 2\Delta_0 \cos\varphi) + 2\Delta_s^2\partial_\varphi^2\big] P_0, \quad (3.99)$$

$$\partial_x P_1(\varphi; x) = \big[-(2\omega + 2\Delta_0 \cos\varphi)\partial_\varphi + 2\Delta_s^2\partial_\varphi^2\big] P_1 + 2P_0. \quad (3.100)$$

It is clear that, by using the above defined function, the density of states can be given by

$$\rho(\omega) = \frac{1}{L} P_1(\varphi; L). \quad (3.101)$$

In the asymmetric case, the equations become much more complicated. Here we will just give the results for $\Delta_2 = 0$, which is just the commensurate case. The whole procedure we used above can also be applied. Setting $\Delta_1 = \Delta_s$, and the equations of motion for both $P(\varphi, U; x)$ and $P_s(\varphi; x)$ are

$$\begin{aligned}\partial_x P(\varphi, U_1; x) &= \big[-\partial_\varphi(2\omega + 2\Delta_0 \cos\varphi + \Delta_s^2 \sin 2\varphi) + 2\Delta_s^2\partial_\varphi \cos^2\varphi\partial_\varphi \\ &\quad -2\Delta_s^2(1 - 3\sin^2\varphi)\partial_{U_1}U_1 + 2\Delta_s^2 \sin^2\varphi(\partial_{U_1}U_1)^2 \\ &\quad -2\Delta_s^2 \sin 2\varphi\partial_\varphi\partial_{U_1}U_1 - \partial_{U_1}(2 - 2\Delta_0 \sin\varphi U_1)\big] P(\varphi, U_1; x) \quad (3.102)\end{aligned}$$

and

$$\partial_x P_0(\varphi; x) = \big[-\partial_\varphi(2\omega + 2\Delta_0 \cos\varphi + \Delta_s^2 \sin 2\varphi) + 2\Delta_s^2\partial_\varphi \cos^2\varphi\partial_\varphi\big] P_0 \quad (3.103)$$

$$\partial_x P_1(\varphi; x) = \big[-(2\omega + 2\Delta_0 \cos\varphi - \Delta_s^2 \sin 2\varphi)\partial_\varphi + 2\Delta_s^2\partial_\varphi \cos^2\varphi\partial_\varphi\big] P_1 + 2P_0. \quad (3.104)$$

Since we are interested in the macroscopic systems, we only need to find the density of states in the limit $L \to \infty$. As can be shown that [25], for large x, the P_s have asymptotic forms

$$P_0(\varphi; x) \sim p_0(\varphi) \tag{3.105}$$
$$P_1(\varphi; x) \sim Cx + f(\varphi). \tag{3.106}$$

where p_0, f and constant C are independent of x, the density of states is given for large L, by

$$\rho(\omega) = C. \tag{3.107}$$

It is independent of the length L and independent of the boundary conditions. Setting the left-hand side of equation (3.99) to be zero, the function p_0 satisfies equation

$$\left[-\partial_\varphi(2\omega + \Delta_0 \cos\varphi) + 2\Delta_s^2 \partial_\varphi^2\right] p_0 = 0, \tag{3.108}$$

and in the commensurate case

$$\left[-\partial_\varphi(2\omega + 2\Delta_0 \cos\varphi + \Delta_s^2 \sin 2\varphi) + 2\Delta_s^2 \partial_\varphi \cos^2\varphi \partial_\varphi\right] p_0 = 0. \tag{3.109}$$

In both cases p_0 obeys normalization condition

$$\int_0^{2\pi} p_0(\varphi) d\varphi = 1, \tag{3.110}$$

which is imposed by the fact $P_0(\varphi, x)$ is a probability distribution function. Substituting Eqs. (3.105) and (3.106) in Eq. (3.100), multiplying both sides of equation by $p_0(-\varphi)$, and integrating with respect to φ, we end up with

$$\rho(\omega) = 2\int_o^{2\pi} p_0(-\varphi) p_0(\varphi) d\varphi. \tag{3.111}$$

Spectral Function

The spectral function is defined by

$$\begin{aligned} A^\alpha(k;\omega) &= A(\alpha(k_F + k); \omega) \\ &= \frac{1}{L}\left\langle \frac{|\int_0^L e^{ikx}\psi_n(x)dx|^2}{2\int_0^L |\psi_n(x)|^2 dx} \delta(\omega - \omega_n) \right\rangle, \end{aligned} \tag{3.112}$$

where $\psi_n(x)$ are wave functions of the nth eigenstates of the Hamiltonian. Since $\psi_n(x)$ usually are not properly normalized, here we divide them by the normalization factor $\int |\Psi_n(x)|^2 dx = 2\int |\psi_n(x)|^2 dx$. As what we did in calculating the density of states, we define two functions

$$W_1(x) = \frac{\int_0^x e^{ikx'}\psi(x')dx'}{e^{ikx}\psi(x)}, \tag{3.113}$$
$$U_2(x) = \frac{\int_0^x |\psi(x')|^2 dx'}{|\psi(x)|^2}. \tag{3.114}$$

Along with the equations of motion for $\varphi(x)$ and $\zeta(x)$, we can write down the equations of motion for $W_1(x)$ and $U_2(x)$:

$$\partial_x W_1(x) = 1 - iW_1(x)\left[\omega + k + \Delta_0 e^{-i\varphi(x)} + \Delta_1 e^{-i\varphi(x)}\eta_1 + i\Delta_2 e^{-i\varphi(x)}\eta_2\right] \quad (3.115)$$

$$\partial_x U_2(x) = 1 - 2U_2(x)\left[\Delta_0 \sin\varphi(x) - \Delta_1 \sin\varphi(x)\eta_1 + \Delta_2 \cos\varphi(x)\eta_2\right]. \quad (3.116)$$

From the definition of $U_1(x)$ and $U_2(x)$ we see that, at $x = 0$ the initial conditions are $U_1 = U_2 = 0$. The comparison of Eqs. (3.91) and (3.116) establishes that, for all x, $U_1(x) = 2U_2(x)$. And from the definition of $U_2(x)$, we have $U_2(x) > 0$ for $x > 0$, thus we have $U_1(x)$ is greater than or equal to zero at any x.

The spectral function then can be expressed as

$$\begin{aligned} A(k,\omega) &= \frac{1}{L}\left\langle \frac{|\int_0^L e^{ikx}\psi(x)dx|^2}{2\int_0^L |\psi(x)|^2 dx}\delta(\omega-\omega_n)\right\rangle \\ &= \frac{1}{L}\left\langle \frac{|W_1(L;\omega)|^2}{2U_2(L;\omega)}|U_1(L;\omega)|\delta(\varphi-\varphi(L;\omega))\right\rangle \\ &= L^{-1}\left\langle |W_1(L;\omega)|^2\delta(\varphi-\varphi(L;\omega))\right\rangle. \end{aligned} \quad (3.117)$$

Defining the probability distribution function $P(W_1, \varphi; x)$ by

$$P(W_1,\varphi;x) = \langle \delta(W_1 - W_1(x))\delta(\varphi-\varphi(x))\rangle, \quad (3.118)$$

together with Eq. (3.85) and Eq. (3.115), we can write down the equation for $P(W_1, \varphi; x)$

$$\begin{aligned} \partial_x P(W_1,\varphi;x) = &\left[-\partial_{W_1}[1 - iW_1(k+\omega+\Delta_0 e^{-i\varphi} - i\Delta_s^2)]\right. \\ &\left. -2i\Delta_s^2\partial_\varphi\partial_{W_1}W_1 - \partial_\varphi(2\omega + 2\Delta_0\cos\varphi) + 2\Delta_s^2\partial_\varphi^2\right] P. \end{aligned} \quad (3.119)$$

Then two functions $P_s(\varphi; x), s = 0, 1$

$$P_s(\varphi;x) = \int dW_1 W_1^s P(W_1,\varphi;x) \quad (3.120)$$

satisfy equations

$$\partial_x P_0(\varphi;x) = \left[-\partial_\varphi(2\omega + 2\Delta_0\cos\varphi) + 2\Delta_s^2\partial_\varphi^2\right] P_0, \quad (3.121)$$

$$\begin{aligned} \partial_x P_1(\varphi;x) = &\left[-(2\omega + 2\Delta_0\cos\varphi - 2i\Delta_s^2)\partial_\varphi + 2\Delta_s^2\partial_\varphi^2\right. \\ &\left. -i(k+\omega+\Delta_0 e^{i\varphi}) - \Delta_s^2\right] P_1 + P_0. \end{aligned} \quad (3.122)$$

In Eq. (3.117), it shows that the spectral function is related to the function $|W_1(x)|^2$. We thus need to define another function $W_2(x) = |W_1(x)|^2$, where

$$\begin{aligned} \partial_x W_2(x) &= W_1^*(x)\partial_x W_1(x) + W_1(x)\partial_x W_1^*(x) \\ &= 2\,\mathrm{Re}\, W_1(x) - 2W_2(x)\left[\Delta_0\sin\varphi + \Delta_1\sin\varphi - \Delta_2\cos\varphi\right]. \end{aligned} \quad (3.123)$$

With the help of the probability distribution function $P(W_2, W_1, \varphi; x)$, we can define the function $P_2(\varphi; x)$ by

$$P_2(\varphi;x) = \int dW_2 W_2 \int dW_1 P(W_2, W_1, \varphi; x), \quad (3.124)$$

and it satisfies equation

$$\partial_x P_2(\varphi;x) = \left[-(2\omega + 2\Delta_0\cos\varphi)\partial_\varphi + 2\Delta_s^2\partial_\varphi^2\right] P_2 + 2\,\mathrm{Re}\,P_1. \tag{3.125}$$

In terms of $P_2(\varphi;x)$ the spectral function can be expressed as

$$A(k;\omega) = L^{-1}P_2(\varphi_L;L). \tag{3.126}$$

At the limit $x\to\infty$, functions P_s also have the following asymptotic behavior [25]

$$P_0(\varphi;x) \sim p_0(\varphi), \tag{3.127}$$
$$P_1(\varphi;x) \sim p_1(\varphi), \tag{3.128}$$
$$P_2(\varphi;x) \sim Cx + f(\varphi). \tag{3.129}$$

Where both p_0, p_1, f and C are independent of x. Thus in the limit $L\to\infty$, we have $A(k;\omega) = C$. Putting the asymptotic behavior of $P_s(\varphi;x)$ into Eq. (3.125), multiplying both side by $p_0(-\varphi)$ and integrating out φ, we finally arrive at

$$A(k;\omega) = 2\int_0^{2\pi} \mathrm{Re}\,p_1(\varphi)p_0(-\varphi)d\varphi. \tag{3.130}$$

3.3.3 Finite Correlation and Non-Gaussian

When the order parameter fluctuations are Gaussian with finite correlation lengths or non-Gaussian, we can still use the above procedure to get the equations. We only need to do some modification. In order to simplify the calculation, in the following, we will focus on the incommensurate case. In this case. we write the fluctuating order parameters as $\vec{\Delta}(x) = \Delta(x)e^{i\theta(x)}$, where $\Delta(x)$ and $\theta(x)$ are both real functions and are described by Langevin equations

$$\partial_x\Delta(x) = a(\Delta) + \eta_\Delta, \tag{3.131}$$
$$\partial_x\theta(x) = \frac{1}{\Delta}\eta_\theta. \tag{3.132}$$

Different from Eq. (2.89), here we have absorbed the term $1/(2\Delta)$ into $a(\Delta)$. Then the equations of motion for $\varphi(x)$ and $\zeta(x)$ are

$$\partial_x\varphi(x) = 2\omega + 2\Delta(x)\cos\left[\varphi(x) - \theta(x)\right], \tag{3.133}$$
$$\partial_x\zeta(x) = \Delta(x)\sin\left[\varphi(x) - \theta(x)\right]. \tag{3.134}$$

Using the gauge transformation $\varphi(x)\to\varphi(x)+\theta(x)$, we can obtain the equations of motion

$$\partial_x\varphi(x) = 2\omega + 2\Delta(x)\cos\varphi(x) - \partial_x\theta(x), \tag{3.135}$$
$$\partial_x\zeta(x) = \Delta(x)\sin\varphi(x). \tag{3.136}$$

Density of States

As what we did in the Gaussian white fluctuations case, we also define the function $U_1(x) = \partial\varphi(x;\omega)/\partial\omega$, then we have

$$\begin{aligned} \partial_x \Delta(x) &= a(\Delta) + \eta_\Delta, & (3.137)\\ \partial_x \varphi(x) &= 2\omega + 2\Delta\cos\varphi + \frac{1}{\Delta}\eta_\theta, & (3.138)\\ \partial_x U_1(x) &= 2 - 2\Delta\sin\varphi. & (3.139) \end{aligned}$$

In this case we need to introduce an extra variable Δ in our probability distribution function and will integrate it out in the last step. So now $P(\Delta, \varphi, U_1; x)$ is defined by

$$P(\Delta, \varphi, U_1; x) = \langle \delta(\Delta - \Delta(x)\delta(\varphi - \varphi(x;\omega))\delta(U_1 - U_1(x;\omega)))\rangle\,, \tag{3.140}$$

and

$$\begin{aligned} \partial_x P(\Delta, \varphi, U_1; x) &= \left[-\partial_\Delta a(\Delta) + \frac{1}{2}\partial_\Delta^2 - \partial_{U_1}(2 - 2\Delta\sin\varphi U_1)\right.\\ &\quad \left. -\partial_\varphi(2\omega + 2\Delta\cos\varphi) + \frac{1}{2\Delta^2}\partial_\varphi^2\right] P(\Delta, \varphi, U_1; x). \quad (3.141) \end{aligned}$$

Similarly the functions $P_s(\Delta, \varphi; x), s = 0, 1$

$$\begin{aligned} P_s(\Delta, \varphi; x) &= \langle U_1^s \delta(\Delta - \Delta(x))\delta(\varphi - \varphi(x;\omega))\rangle & (3.142)\\ &= \int_{-\infty}^{+\infty} dU_1 U_1^s P(\Delta, \varphi, U_1; x) & (3.143) \end{aligned}$$

obey the equations of motion

$$\begin{aligned} \partial_x P_0 &= \left[-\partial_\Delta a(\Delta) + \frac{1}{2}\partial_\Delta^2 - \partial_\varphi(2\omega + 2\Delta\cos\varphi) + \frac{1}{2\Delta^2}\partial_\varphi^2\right] P_0, & (3.144)\\ \partial_x P_1 &= \left[-\partial_\Delta a(\Delta) + \frac{1}{2}\partial_\Delta^2 - (2\omega + 2\Delta + \cos\varphi)\,\partial_\varphi + \frac{1}{2\Delta^2}\partial_\varphi^2\right] P_1 + 2P_0. & (3.145) \end{aligned}$$

The density of states is now given by

$$\rho(\omega) = \frac{1}{L}\int_0^{+\infty} d\Delta P_1(\Delta, \varphi, L). \tag{3.146}$$

As what we have discussed before, we only need consider the large x limit, where we have the asymptotic forms for the functions P_s

$$\begin{aligned} P_0(\Delta, \varphi; x) &\sim p_0(\Delta, \varphi), & (3.147)\\ P_1(\Delta, \varphi; x) &\sim C(\Delta)x + p_1(\Delta, \varphi), & (3.148) \end{aligned}$$

Where both $p_0(\Delta, \varphi)$ and $p_1(\Delta, \varphi)$ are functions that independent of x, and $C(\Delta)$ is just a function of Δ. Then the density of states is given by

$$\rho(\omega) = \int_0^{+\infty} d\Delta C(\Delta). \tag{3.149}$$

For p_0, we just set the left-hand side of the equation (3.144) equal to zero,

$$\left[-\partial_\Delta a(\Delta) + \frac{1}{2}\partial_\Delta^2 - \partial_\varphi(2\omega + 2\Delta\cos\varphi)\right] p_0 = 0 \tag{3.150}$$

For p_1 we plug Eq. (3.148) into Eq. (3.145), which results

$$C(\Delta) = \left[-\partial_\Delta a(\Delta) + \frac{1}{2}\partial_\Delta^2 - (2\omega + 2\Delta\cos\varphi)\,\partial_\varphi\right] p_1 + 2p_0. \tag{3.151}$$

Multiplying both sides of Eq.(3.151) by $p_0(\Delta, -\varphi)$ and integrating out φ, we will get

$$P(\Delta)C(\Delta) = 2\int_0^{2\pi} d\varphi p_0(\Delta, -\varphi)p_0(\Delta, \varphi), \tag{3.152}$$

where $P(\Delta) = \int_0^{2\pi} d\varphi p_0(\Delta, -\varphi)$ is just the probability distribution function of Δ. Inserting $C(\Delta)$ obtained from Eq.(3.152) into Eq.(3.149), finally for the density of states we have

$$\rho = 2\int_0^{+\infty} d\Delta \int_0^{2\pi} d\varphi \frac{p_0(\Delta, -\varphi)p_0(\Delta, \varphi)}{P(\Delta)}. \tag{3.153}$$

Spectral Function

In this case we have

$$\partial_x W_1(x) = 1 - iW_1(x)\left[k + \omega + \Delta e^{-i\varphi(x)}\right], \tag{3.154}$$

$$\partial_x U_2(x) = 1 - 2\Delta\sin\varphi U_2(x). \tag{3.155}$$

where $W_1(x)$ and $U_2(x)$ are functions defined as before. And as in the Gaussian white case, we also have $U_1(x) = 2U_2(x)$ for all x. The probability distribution $P(W_1, \Delta, \varphi; x)$ satisfies equation

$$\begin{aligned}\partial_x P(W_1, \Delta, \varphi; x) = &\left[-\partial_{W_1}[1 - iW_1(k + \omega + \Delta e^{-i\varphi})] - \partial_\Delta a(\Delta) + \frac{1}{2}\partial_\Delta^2\right.\\ &\left.-\partial_\varphi(2\omega + 2\Delta\cos\varphi) + \frac{1}{2\Delta^2}\partial_\varphi^2\right] P(W_1, \Delta, \varphi; x),\end{aligned} \tag{3.156}$$

and functions $P_s(\Delta, \varphi; x), s = 0, 1$

$$\begin{aligned}P_s(\Delta, \varphi; x) &= \langle W_1(x)^s \delta(\Delta - \Delta(x))\delta(\varphi - \varphi(x))\rangle\\ &= \int dW_1 W_1^s P(W_1, \Delta, \varphi; x)\end{aligned} \tag{3.157}$$

satisfy equations of motion

$$\partial_x P_0(\Delta, \varphi; x) = \left[-\partial_\Delta a(\Delta) + \frac{1}{2}\partial_\Delta^2 - \partial_\varphi(2\omega + 2\Delta\cos\varphi) + \frac{1}{2\Delta^2}\partial_\varphi^2\right] P_0, \tag{3.158}$$

$$\begin{aligned}\partial_x P_1(\Delta, \varphi; x) = &\left[-\partial_\Delta a(\Delta) + \frac{1}{2}\partial_\Delta^2 - i(k + \omega + \Delta e^{i\varphi})\right.\\ &\left.-(2\omega + 2\Delta\cos\varphi)\partial_\varphi + \frac{1}{2\Delta^2}\partial_\varphi^2\right] P_1 + P_0.\end{aligned} \tag{3.159}$$

Defining $W_2(x) = |W_1(x)|^2$, then the probability distribution function $P(W_2, W_1, \Delta, \varphi; x)$ obeys equation

$$\begin{aligned}\partial_x P(W_2, W_1, \Delta, \varphi; x) &= \left[-\partial_{W_1}[1 - iW_1(k + \omega + \Delta e^{-i\varphi})] - \partial_{W_2}(2 - 2\Delta \sin\varphi W_1)\right. \\ &\left. \partial_\Delta a(\Delta) + \frac{1}{2}\partial_\Delta^2 - \partial_\varphi(2\omega + 2\Delta\cos\varphi) + \frac{1}{2\Delta^2}\partial_\varphi^2\right] P. \quad (3.160)\end{aligned}$$

Thus

$$\begin{aligned}P_2(\Delta, \varphi; x) &= \langle W_2(x)\delta(\Delta - \Delta(x))\delta(\varphi - \varphi(x))\rangle \\ &= \int dW_1 \int dW_2 W_2 P(W_1, W_2, \Delta, \varphi; x) \quad (3.161)\end{aligned}$$

satisfies

$$\partial_x P_2(\Delta, \varphi; x) = \left[-\partial_\Delta a(\Delta) + \frac{1}{2}\partial_\Delta^2 - (2\omega + 2\Delta\cos\varphi)\partial_\varphi + \frac{1}{2\Delta^2}\partial_\varphi^2\right] P_2 + 2\,\mathrm{Re}\, P_1. \quad (3.162)$$

For large x, the asymptotics of $P_s(\Delta, \varphi; x)$ are

$$\begin{aligned}P_0(\Delta, \varphi; x) &\sim p_0(\Delta, \varphi), \quad (3.163)\\ P_1(\Delta, \varphi; x) &\sim p_1(\Delta, \varphi), \quad (3.164)\\ P_2(\Delta, \varphi; x) &\sim C(\Delta)x + p_2(\Delta, \varphi). \quad (3.165)\end{aligned}$$

And the spectral function $A(k; \omega)$ is now

$$\begin{aligned}A(k; \omega) &= \lim_{L\to+\infty} \frac{1}{L}\int d\Delta P_2(\Delta, \varphi; L) \\ &= \int_0^{+\infty} d\Delta C(\Delta), \quad (3.166)\end{aligned}$$

with

$$C(\Delta) = 2\int_0^{2\pi} d\varphi \frac{\mathrm{Re}\, p_1(\Delta, \varphi) p_0(\Delta, -\varphi)}{P(\Delta)}. \quad (3.167)$$

Optical Conductivity

At finite temperature, the optical conductivity has the form

$$\sigma_1(\omega) = \pi\omega_P^2 \int_{-\infty}^{+\infty} d\epsilon \frac{f(\epsilon) - f(\epsilon + \omega)}{\omega} F(\epsilon, \epsilon + \omega), \quad (3.168)$$

where $\omega_p^2 = 4\pi n e^2/m^*$ is the square of the plasma frequency, n is the density of electrons, $-e$ and m^* is the charge and effective mass of an electron. $f(\epsilon) = (\exp(\epsilon/k_B T) + 1)^{-1}$ is the Fermi distribution function and

$$F(\epsilon, \epsilon') = \frac{1}{L}\left\langle \sum_{n,m} |J_{nm}|^2 \delta(\epsilon - \epsilon_n)\delta(\epsilon - \epsilon_m)\right\rangle \quad (3.169)$$

with

$$J_{nm} = \int dx \Psi_n^\dagger(x)\sigma_3\Psi_m(x) \quad (3.170)$$

is the current matrix element.

Just following the same procedure for calculating the density of states and the spectral function, we define

$$W_1(x;\epsilon,\epsilon') = \frac{\int_0^x \psi^*(x';\epsilon)\psi(x';\epsilon')dx'}{\psi^*(x;\epsilon)\psi(x;\epsilon')}, \tag{3.171}$$

and it obeys the following equation of motion,

$$\partial_x W_1(x;\epsilon,\epsilon') = 1 - i(\epsilon' - \epsilon + \Delta(x)e^{-i\varphi(x;\epsilon')} - \Delta(x)e^{i\varphi(x;\epsilon)})W_1(x;\epsilon,\epsilon'). \tag{3.172}$$

With the functions defined above, the F function can be written in the form

$$\begin{aligned} F(\epsilon,\epsilon') &= \frac{1}{L}\left\langle \frac{|\int_0^L \psi^*(x;\epsilon)\psi(x;\epsilon')dx|^2}{(2\int_0^L |\psi(x;\epsilon)|^2dx)(2\int_0^L |\psi(x;\epsilon')|dx)} \sum_{n,m}\delta(\epsilon-\epsilon_n)\delta(\epsilon'-\epsilon_m)\right\rangle \\ &= \frac{1}{L}\left\langle \frac{|W_1(L;\epsilon,\epsilon')|^2}{2U_1(L;\epsilon)2U_1(L;\epsilon')}|U_2(L;\epsilon)||U_2(L;\epsilon')|\delta(\varphi-\varphi(L;\epsilon))\delta(\varphi'-\varphi(L;\epsilon'))\right\rangle \\ &= \frac{1}{L}\left\langle |W_1(L;\epsilon,\epsilon')|^2\delta(\varphi-\varphi(L;\epsilon))\delta(\varphi'-\varphi(L;\epsilon'))\right\rangle . \end{aligned} \tag{3.173}$$

The probability distribution function is defined by

$$P(W_1,\Delta,\varphi,\varphi';x) = \left\langle \delta[W_1 - W_1(x;\epsilon,\epsilon')]\delta[\Delta-\Delta(x)]\delta[\varphi-\varphi(x;\epsilon)]\delta[\varphi'-\varphi(x;\epsilon')]\right\rangle . \tag{3.174}$$

The equation of motion for this distribution function reads

$$\begin{aligned} \partial_x P &= \Big[-\partial_{W_1}[1 - i(\epsilon'-\epsilon+\Delta e^{-i\varphi'} - \Delta e^{i\varphi})W_1] - \partial_\Delta a(\Delta) + \frac{\partial_\Delta^2}{2} \\ &\quad -\partial_\varphi(2\epsilon + 2\Delta\cos\varphi) - \partial_{\varphi'}(2\epsilon' + 2\Delta\cos\varphi') + \frac{(\partial_\varphi+\partial_{\varphi'})^2}{2\Delta^2}\Big]P. \end{aligned} \tag{3.175}$$

And functions $P_s(\Delta,\varphi,\varphi';x)$ are defined by

$$\begin{aligned} P_s(\Delta,\varphi,\varphi';x) &= \left\langle W_1(x;\epsilon,\epsilon')^s\delta[\Delta-\Delta(x;\epsilon)]\delta[\varphi-\varphi(x;\epsilon)]\delta[\varphi'-\varphi(x;\epsilon')]\right\rangle \\ &= \int dW_1 W_1^s P(W_1,\Delta,\varphi,\varphi';L) \end{aligned} \tag{3.176}$$

$(s = 0, 1)$, then $P_s(\Delta,\varphi,\varphi';x)$ satisfy the following coupled three-dimensional Fokker-Planck equations

$$\partial_x P_0 = \left[\frac{(\partial_\varphi+\partial_{\varphi'})^2}{2\Delta^2} - 2\partial_\varphi(\epsilon+\Delta\cos\varphi) - 2\partial_{\varphi'}(\epsilon'+\Delta\cos\varphi') + \frac{\partial_\Delta^2}{2} - \partial_\Delta a\right]P_0, \tag{3.177}$$

$$\begin{aligned} \partial_x P_1 = \Big[&\frac{(\partial_\varphi+\partial_{\varphi'})^2}{2\Delta^2} - 2(\epsilon+\Delta\cos\varphi)\partial_\varphi - 2(\epsilon'+\Delta\cos\varphi')\partial_{\varphi'} \\ &-i(\epsilon'-\epsilon+\Delta e^{i\varphi'} - \Delta e^{-i\varphi}) + \frac{\partial_\Delta^2}{2} - \partial_\Delta a\Big]P_1 + P_0. \end{aligned} \tag{3.178}$$

Since $F(\epsilon,\epsilon')$ is related to quantity $|W_1(L;\epsilon,\epsilon')|^2$, we also have to define another function $W_2(x;\epsilon,\epsilon') = |W_1(x;\epsilon,\epsilon')|^2$ which satisfies the equation of motion

$$\begin{aligned} \partial_x W_2(x;\epsilon,\epsilon') &= W_1(x;\epsilon,\epsilon')\partial_x W_1^*(x;\epsilon,\epsilon') + W_1^*(x;\epsilon,\epsilon')\partial_x W_1(x;\epsilon,\epsilon') \\ &= 2\,\mathrm{Re}\,W_1(x;\epsilon,\epsilon') - 2\Delta[\sin\varphi(x;\epsilon) + \sin\varphi(x;\epsilon')]W_2(x;\epsilon,\epsilon'). \end{aligned} \tag{3.179}$$

With the help of the probability distribution function

$$P'(W_2,W_1,\Delta,\varphi,\varphi';x) = \left\langle \delta[W_2-W_2(x;\epsilon,\epsilon')]\delta[W_1-W_1(x;\epsilon,\epsilon')] \right. \\ \left. \delta[\Delta-\Delta(x)]\delta[\varphi-\varphi(x;\epsilon)]\delta[\varphi'-\varphi(x;\epsilon')]\right\rangle, \quad (3.180)$$

we can get the function $P_2(\Delta,\varphi,\varphi';x)$

$$\begin{aligned} P_2(\Delta,\varphi,\varphi';x) &= \left\langle W_2(x;\epsilon,\epsilon')\delta[\Delta-\Delta(x;\epsilon)]\delta[\varphi-\varphi(x;\epsilon)]\delta[\varphi'-\varphi(x;\epsilon')]\right\rangle \\ &= \int dW_1 \int dW_2 W_2 P'(W_2,W_1,\Delta,\varphi,\varphi';x). \end{aligned} \quad (3.181)$$

The equation of motion reads

$$\partial_x P_2 = \left[\frac{(\partial_\varphi+\partial_{\varphi'})^2}{2\Delta^2} - 2(\epsilon+\Delta\cos\varphi)\partial_\varphi - 2(\epsilon'+\Delta\cos\varphi')\partial_{\varphi'} + \frac{\partial_\Delta^2}{2} - \partial_\Delta a\right] P_2 + 2\,\mathrm{Re}\,P_1. \quad (3.182)$$

As $L\to\infty$ the asymptotic behavior are

$$P_0(\Delta,\varphi,\varphi';x) \sim p_0(\Delta,\varphi,\varphi'), \quad (3.183)$$
$$P_1(\Delta,\varphi,\varphi';x) \sim p_1(\Delta,\varphi,\varphi'), \quad (3.184)$$
$$P_2(\Delta,\varphi,\varphi';x) \sim C(\Delta)x + f(\Delta,\varphi,\varphi'), \quad (3.185)$$

where p_0, p_1, f, and the constant C are independent of x. Plugging Eq.(3.185) into Eq.(3.182) and multiplying both side by $p_0(\Delta,-\varphi,-\varphi')$ and integrating with respect to φ and φ' we can get

$$C(\Delta) = 2\int_0^{2\pi} d\varphi \int_0^{2\pi} d\varphi' \frac{\mathrm{Re}\,p_1(\Delta,\varphi,\varphi')p_0(\Delta,-\varphi,-\varphi')}{P(\Delta)}, \quad (3.186)$$

with $P(\Delta) = \int_0^{2\pi} d\varphi \int_0^{2\pi} d\varphi' p_0(\Delta,-\varphi,-\varphi')$ the distribution function of Δ. Integrating out the auxiliary variable Δ, we can finally get

$$F(\epsilon,\epsilon') = 2\int_0^{+\infty} d\Delta \int_0^{2\pi} d\varphi \int_0^{2\pi} d\varphi' \frac{\mathrm{Re}\,p_1(\Delta,\varphi,\varphi')p_0(\Delta,-\varphi,-\varphi')}{P(\Delta)}. \quad (3.187)$$

3.4 Summary

We have derived the equations for calculating the density of states, the spectral function and the optical conductivity. As a summary, we will list all those equations in the following.

Gaussian White

Density of states:

$$\rho(\omega) = 2\int_0^{2\pi} p_0(\varphi)p_0(-\varphi)d\varphi. \quad (3.188)$$

Spectral function:

$$A(k;\omega) = 2\int_0^{2\pi} \mathrm{Re}\,p_1(\varphi)p_0(-\varphi)d\varphi. \quad (3.189)$$

$p_0(\varphi)$ and $p_1(\varphi)$ are stationary solution to the Fokker-Planck equations

$$\begin{aligned}\partial_x P_0(\varphi;x) &= \left[-\partial_\varphi(2\omega+2\Delta_0\cos\varphi)+2\Delta_s^2\partial_\varphi^2\right]P_0, &(3.190)\\ \partial_x P_1(\varphi;x) &= \left[-(2\omega+2\Delta_0\cos\varphi-2i\Delta_s^2)\partial_\varphi+2\Delta_s^2\partial_\varphi^2\right.\\ &\qquad \left.-i(k+\omega+\Delta_0 e^{i\varphi})-\Delta_s^2\right]P_1+P_0. &(3.191)\end{aligned}$$

Finite Correlation Lengths and Non-Gaussian

Density of states:

$$\rho(\omega)=2\int_0^{+\infty}d\Delta\int_0^{2\pi}d\varphi\frac{p_0(\Delta,\varphi)p_0(\Delta,-\varphi)}{P(\Delta)}. \tag{3.192}$$

Spectral function:

$$A(k;\omega)=2\int_0^{+\infty}d\Delta\int_0^{2\pi}d\varphi\frac{\mathrm{Re}\,p_1(\Delta,\varphi)p_0(\Delta,-\varphi)}{P(\Delta)}. \tag{3.193}$$

$p_0(\Delta,\varphi)$ and $p_1(\Delta,\varphi)$ are stationary solution to the Fokker-Planck equations

$$\begin{aligned}\partial_x P_0(\Delta,\varphi;x) &= \left[-\partial_\Delta a(\Delta)+\frac{1}{2}\partial_\Delta^2-\partial_\varphi(2\omega+2\Delta\cos\varphi)+\frac{1}{2\Delta^2}\partial_\varphi^2\right]P_0, &(3.194)\\ \partial_x P_1(\Delta,\varphi;x) &= \left[-\partial_\Delta a(\Delta)+\frac{1}{2}\partial_\Delta^2-i(k+\omega+\Delta e^{i\varphi})\right.\\ &\qquad \left.-(2\omega+2\Delta\cos\varphi)\partial_\varphi+\frac{1}{2\Delta^2}\partial_\varphi^2\right]P_1+P_0. &(3.195)\end{aligned}$$

Optical conductivity:

$$\sigma_1(\omega)=\pi\omega_P^2\int_{-\infty}^{+\infty}d\epsilon\frac{f(\epsilon)-f(\epsilon+\omega)}{\omega}F(\epsilon,\epsilon+\omega), \tag{3.196}$$

where

$$F(\epsilon,\epsilon')=2\int_0^{+\infty}d\Delta\int_0^{2\pi}d\varphi\int_0^{2\pi}d\varphi'\frac{\mathrm{Re}\,p_1(\Delta,\varphi,\varphi')p_0(\Delta,-\varphi,-\varphi')}{P(\Delta)} \tag{3.197}$$

with $p_0(\Delta,\varphi,\varphi')$ and $p_1(\Delta,\varphi,\varphi')$ are stationary solutions to Fokker-Planck equations

$$\partial_x P_0=\left[\frac{(\partial_\varphi+\partial_{\varphi'})^2}{2\Delta^2}-2\partial_\varphi(\epsilon+\Delta\cos\varphi)-2\partial_{\varphi'}(\epsilon'+\Delta\cos\varphi')+\frac{\partial_\Delta^2}{2}-\partial_\Delta a\right]P_0, \tag{3.198}$$

$$\begin{aligned}\partial_x P_1=\left[\frac{(\partial_\varphi+\partial_{\varphi'})^2}{2\Delta^2}\right.&-2(\epsilon+\Delta\cos\varphi)\partial_\varphi-2(\epsilon'+\Delta\cos\varphi')\partial_{\varphi'}\\ &\left.-i(\epsilon'-\epsilon+\Delta e^{i\varphi'}-\Delta e^{-i\varphi})+\frac{\partial_\Delta^2}{2}-\partial_\Delta a\right]P_1+P_0. &(3.199)\end{aligned}$$

Chapter 4

Numerical Method and Results

In Chapter 3, we have discussed several methods which can be used to calculate the electronic properties. As we have seen, all methods have some limitations, either it just gives approximated results or it is restricted to some special statistics of the order parameter fluctuations. In order to overcome all these shortages, we have developed a general method which is applicable to different statistics of the order parameter fluctuations. In that method, the original problem is converted into solving several coupled Fokker-Planck equations, and the electronic properties which we are interested in can then be obtained by simple quadrature of the stationary solutions to the Fokker-Planck equations. We have listed all equations for calculating various electronic properties for different statistics of the order parameter fluctuations in the last part of chapter 3. In this chapter, we will give the numerical method to solve the Fokker-Planck equations, and further, get the results of the density of states, the spectral function and the optical conductivity of the fluctuating gap model with both Gaussian and non-Gaussian order parameter fluctuations. We will confirm the existence of the Dyson singularity in the density of states at low energy when the order parameters are real and the static gap potential is small. In the incommensurate case, there is no Dyson singularity. When the order parameter fluctuations are Gaussian with finite correlation length, we show that the density of states at zero frequency $\rho(0)$ decreases with increasing correlation length, and it has a power law behavior which agrees with the second-order Born approximation calculation. Meanwhile in the phase fluctuations only case, $\rho(0)$ vanishes exponentially as a function of the correlation length ξ, which agrees with our calculation for the non-Gaussian fluctuations. In the calculation of the spectral function, we will show again that the Fermi liquid theory breaks down in the one-dimensional system as the correlation length increases. Our calculated results with non-Gaussian order parameter fluctuations actually can be used to describe the experimental ARPES data and shows qualitative agreement. Finally, our results of the optical conductivity reassure that in the one-dimensional system the dc conductivity is zero and the previous results obtained by Shannon [30] is just an artifact of the perturbation theory which they have used in their calculation.

4.1 Solution to The Fokker-Planck Equations

The problem now is to solve the multidimensional Fokker-Planck equation. We will use the finite element method as our choice. Since only the stationary solution is needed, we can

either simulate the process until it relaxes to the stationary distribution or we can just set the left hand side of the equation to be zero and solve it directly. In both ways, we should get the same result. For p_0, there is a more convenient way of getting the result. As can be shown from the definition, p_0 is just the probability distribution function of the underlying variables. Based on the physical meaning of the probability distribution function, we can simulate a large number of different chains using the corresponding Langevin equation. By collecting all the variables, we will be able to get the distribution function at different position. As has been proved in the work of Lifshits [55], all specific physical quantities are self-averaged, we thus just need to simulate one chain, and when the simulation is long enough, we will get the stationary distribution function p_0, which we can view as the correct probability distribution function and can be used to check the solution to the Fokker-Planck equation solved by the finite element method.

4.2 Results

Once we solved all the Fokker-Planck equations and obtained the stationary distribution functions p_0 and p_1, the electronic properties can be obtained by simple quadrature. In the following, we will present our calculation of the density of states, the spectral function and the optical conductivity for different statistics of the order parameter fluctuations

4.2.1 Density of States

First, we check the density of states. For Gaussian white noise $\Delta(x) = \Delta_0 + \Delta_1\eta_1 + i\Delta_2\eta_2$, the density of states is given by

$$\rho(\omega) = 2\int_0^{2\pi} d\varphi p_0(\varphi)p_0(-\varphi), \tag{4.1}$$

where $p_0(\varphi)$ is the stationary solution to the Fokker-Planck equation

$$\partial_x P_0(\varphi; x) = \left[-\partial_\varphi(2\omega + 2\Delta_0\cos\varphi) + 2\Delta_s^2\partial_\varphi^2\right] P_0, \tag{4.2}$$

when the order parameters are complex and $\Delta_1 = \Delta_2 = \Delta_s$. In corresponding, the Fokker-Planck equation for P_0 in the commensurate case is

$$\partial_x P_0(\varphi; x) = \left[-\partial_\varphi(2\omega + 2\Delta_0\cos\varphi + \Delta_s^2\sin 2\varphi) + 2\Delta_s^2\partial_\varphi\cos^2\varphi\partial_\varphi\right] P_0, \tag{4.3}$$

and here we set $\Delta_1 = \Delta_s$ and $\Delta_2 = 0$.

For other statistics of the order parameter fluctuations, we have for the density of states

$$\rho(\omega) = 2\int_0^{+\infty} d\Delta \int_0^{2\pi} d\varphi \frac{p_0(\Delta,\varphi)p_0(\Delta,-\varphi)}{P(\Delta)}, \tag{4.4}$$

with $P_0(\Delta, \varphi; x)$ satisfies the following equation of motion

$$\partial_x P_0(\Delta,\varphi; x) = \left[-\partial_\Delta a(\Delta) + \frac{1}{2}\partial_\Delta^2 - \partial_\varphi(2\omega + 2\Delta\cos\varphi) + \frac{1}{2\Delta^2}\partial_\varphi^2\right] P_0. \tag{4.5}$$

and $P(\Delta)$ is the probability distribution function of Δ.

Gaussian White

In this case, the fluctuations at different space points are uncorrelated, thus there exists an exact solution for the density of states. Ovchinnikov and Erikhman [13] first solved the commensurate case. They showed in the case where the back scattering potential is purely Gaussian white noise, i.e. $\langle\Delta(x)\rangle = 0$, the density of states has a Dyson singularity which was found by Dyson in a different model [56]. In the case of $\langle\Delta(x)\rangle \neq 0$, the density of states either exhibits a singularity or a pseudogap near the Fermi energy depending on the ratio of the fluctuation and the static gap. Later, using the technique of S-matrix summation, Golub and Chumakov [57] were able to solve the incommensurate case, where there is no such kind of singularity and the fluctuations can only lead to a filling up of the pseudogap.

In the commensurate case, the integrated density of states has the expression

$$N(\omega) = \frac{2\Delta_s^2}{\pi^2\left[J_\nu^2(\frac{\omega}{\Delta_s^2}) + N_\nu^2(\frac{\omega}{\Delta_s^2})\right]}, \tag{4.6}$$

here $\nu = \Delta_0/\Delta_s^2$, $J_\nu(x)$ and $N_\nu(x)$ are Bessel functions of the first and second kind respectively. Differentiating it with respect to ω, we can easily get the density of states. When $\Delta_0 = 0$, which implies $\nu = 0$, we have the asymptotic behavior of the integrated density of states near $\omega = 0$

$$N(\omega) \sim \frac{\Delta_s^2}{2\ln^2(\omega/\Delta_2^2)}, \tag{4.7}$$

with which we have the asymptotics of the density of states

$$\rho(\omega) \sim -\frac{1}{(\omega/\Delta_s^2)\ln^3(\omega/\Delta_s^2)}. \tag{4.8}$$

As ω approaches zero, the density of states diverges. This is the so called Dyson singularity.

In Fig. (4.1) we plot our calculated result in comparison with the result obtained from Eq. (4.6). Our result agrees with the exact solution very well, which verifies the validity of our numerical calculation. We confirm that there is a singularity at $\omega = 0$, and outside the singularity, the density of states is almost equal to the density of states for free fermions.

When $\Delta_0 > 0$, the asymptotical behavior of the integrated density of states at small ω can also be obtained. If $\nu > 0$ and $x \to 0$, the Bessel function $J_\nu(x)$ stays finite and $N_\nu \sim -(1/\pi)\Gamma(\nu)(x/2)^{-\nu}$, which gives

$$N(\omega) \sim \frac{2\Delta_s^2}{\Gamma^2(\nu)}\left(\frac{\omega}{2\Delta_s^2}\right)^{2\nu}, \tag{4.9}$$

so that

$$\rho(\omega) \sim \frac{2\nu}{\Gamma^2(\nu)}\left(\frac{\omega}{2\Delta_s^2}\right)^{2\nu-1}. \tag{4.10}$$

We can see that for $\nu < 1/2$ the exponent of the ω is negative, which implies divergence as ω approaches zero. For $\nu > 1/2$, the exponent is positive and the density of states vanishes algebraically. For $\nu = 1/2$, the Bessel functions are of half odd integer order and can be expressed in terms of $\sin x$ and $\cos x$ and powers of x, it is easy to find that $N(\omega) = \omega/\pi$, thus $\rho(\omega) = \rho_0 = 1/\pi$. The effects of the fluctuations are exactly

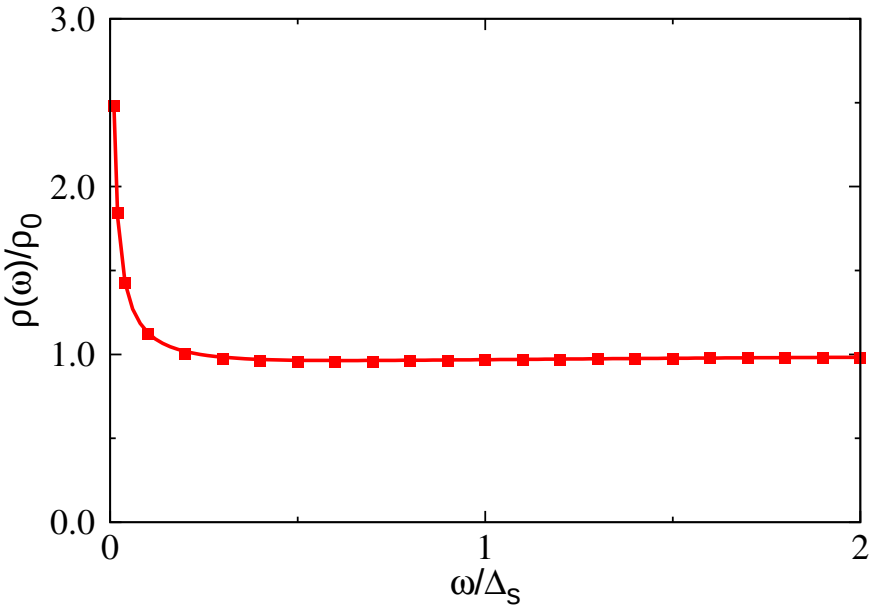

Figure 4.1: The density of states for the commensurate case with white Gaussian fluctuations for $\Delta_0 = 0$. The solid line shows the exact result and the dots are results calculated using our method.

canceled by those of the static gap. For very large ν, the fluctuations become irrelevant, $N(\omega) = \rho_0\theta(\omega^2 - \Delta_0^2)\left(\omega^2 - \Delta_0^2\right)^{1/2}$, and the density of states reduces to the mean-field result

$$\rho(\omega) = \rho_0\theta(\omega^2 - \Delta_0^2)\frac{\omega}{\sqrt{\omega^2 - \Delta_0^2}}. \tag{4.11}$$

In the commensurate case, we have the integrated density of states as

$$N(\omega) = \frac{\Delta_s^2}{\pi}\sinh\left(\frac{\pi\omega}{\Delta_s^2}\right)\frac{\rho_0}{\pi^2\left|I_{i\omega/\Delta_s^2}(\nu)\right|^2}, \tag{4.12}$$

here $I_\nu(x)$ is the modified (hyperbolic) Bessel function. We also define $\nu = \Delta_0/\Delta_s^2$, then the density of states at zero frequency $\rho(0)$ is always finite, and vanishes with increasing ν as $\rho(0) = \rho_0/\left[I_0(\nu)\right]^2$. So in the incommensurate case there is no Dyson singularity. In the absence of static gap Δ_0, the fluctuations have no effects on the density of states, so that $\rho(\omega) = 1/\pi$. For Δ_0 is not zero, the disorder leads to a filling of the static gap. As in the commensurate case, in the limit $\Delta_s \to 0$, i.e. $\nu \to \infty$, the density of states reduces to the mean-field result.

Our results for $\langle\Delta(x)\rangle \neq 0$ case are given in Fig. (4.2), the red dots are results for the real and the green ones are for the complex order parameters with $\Delta_0/\Delta_s^2 = 1.0$. They both have almost the same values as the exact results. We plot the density of states with different value of ν in both commensurate case in Fig. (4.3) and incommensurate case in Fig. (4.4). In the commensurate case, we see the singularity only appears for $\nu > 0.5$, for $\nu = 0.5$, the density of states is just constant and for $\nu < 0.5$ the effects of the static gap

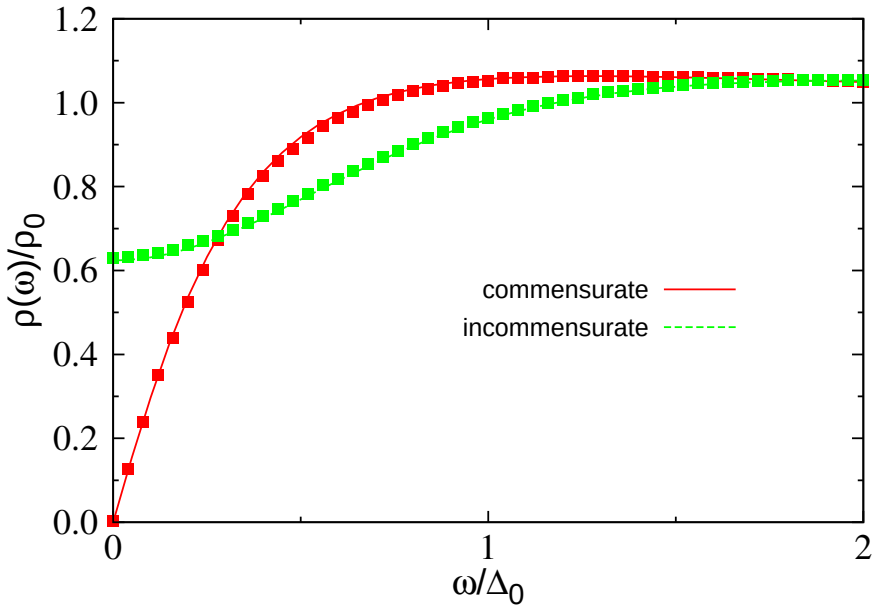

Figure 4.2: The calculated density of states in both commensurate and incommensurate cases with $\Delta_0/\Delta_s^2 = 1.0$. The dots are our calculated results, lines are results from Eqs. (4.6) and (4.12). Both results agree very well.

dominate, and a pseudogap emerges. In the incommensurate case, the density of states is always finite, and the static gap is filled up by the increasing of the strength of the fluctuations.

Finite Correlation Lengths

In the case of finite correlation lengths, there is no exact solution. We present our calculated results in Fig. (4.5) for different correlation lengths ξ in the incommensurate case. As can be seen, there is no singularity as $\omega \to 0$. $\rho(0)$ is always finite and decreases when the correlation length increases. For a more quantitative comparison, we plot in Fig. (4.6) the density of states $\rho(0)$ at the Fermi energy as a function of the correlation length $\Delta_s\xi$. A fit to a power law gives

$$\rho(0)/\rho_0 = C\,(\Delta_s\xi)^{-\mu} \tag{4.13}$$

with

$$C = 0.612 \pm 0.027, \mu = 0.673 \pm 0.018, \tag{4.14}$$

which can be compared with Sadovskii's approximated result of $C = 0.541 \pm 0.013$ and $\mu = 1/2$ [15].

For very large correlation length, the density of states approaches the result for infinite correlation length which we have obtained in the last chapter:

$$\rho(\omega) = 2\rho_0 \frac{\omega}{\Delta_s} e^{-(\omega^2/\Delta_s^2)}\,\mathrm{Erfi}\left(\frac{\omega}{\Delta_s}\right). \tag{4.15}$$

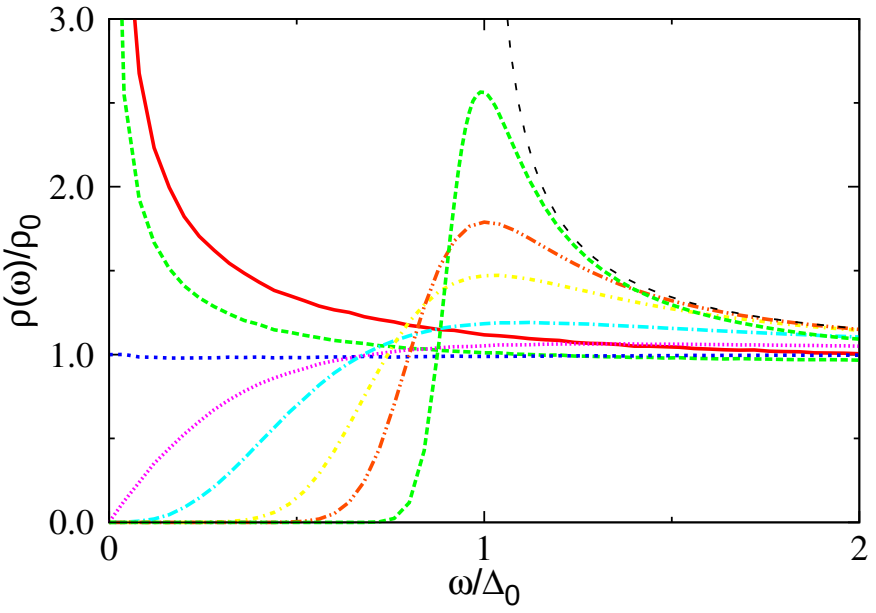

Figure 4.3: The density of states in the commensurate case with white Gaussian fluctuations and $\Delta_0/\Delta_s^2 = 0.1, 0.2, 0.5, 1.0, 2.0, 5.0, 10.0$. The black dashed line shows the mean-field result.

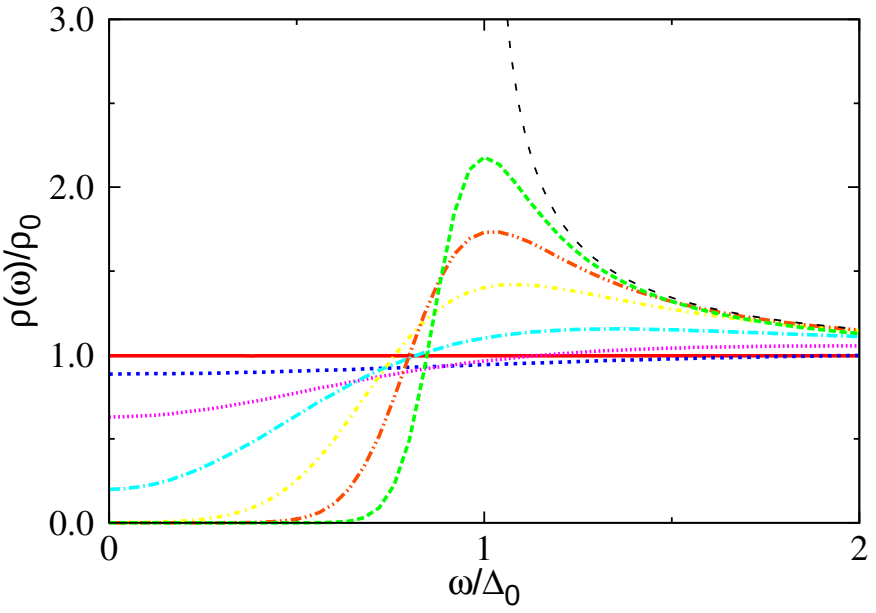

Figure 4.4: The density of states in the incommensurate case with white Gaussian fluctuations and $\Delta_0/\Delta_s^2 = 0.1, 0.5, 1.0, 2.0, 5.0, 10.0, 20.0$. The black dashed line shows the mean-field result.

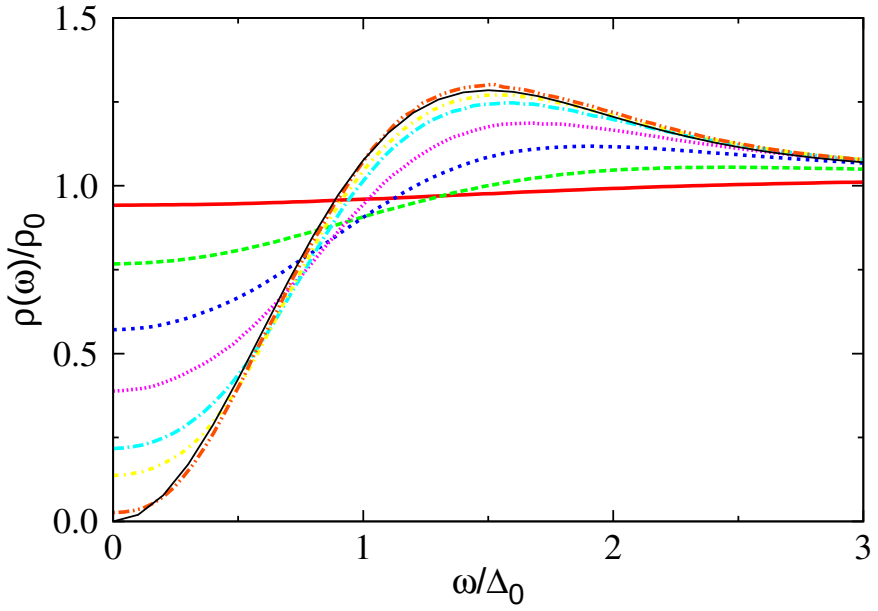

Figure 4.5: The density of states for the incommensurate case with finite correlation $\Delta_s\xi = 0.2, 0.5, 1.0, 2.0, 5.0, 10.0, 100.0$. The black dashed line shows the exact result for infinite correlation length.

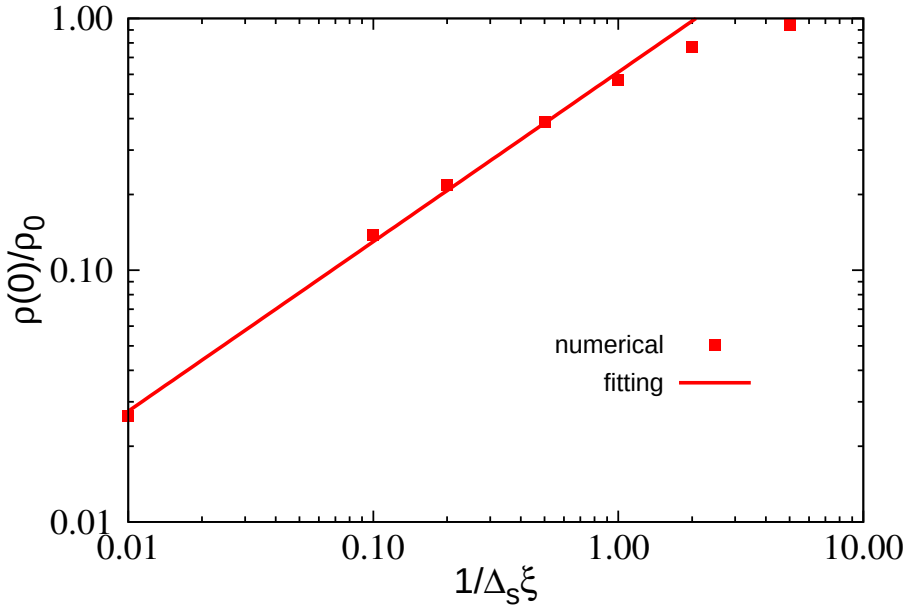

Figure 4.6: Double-logarithmic plot of the density of states at zero point $\rho(0)/\rho_0$ as a function of $1/\Delta_s\xi$.

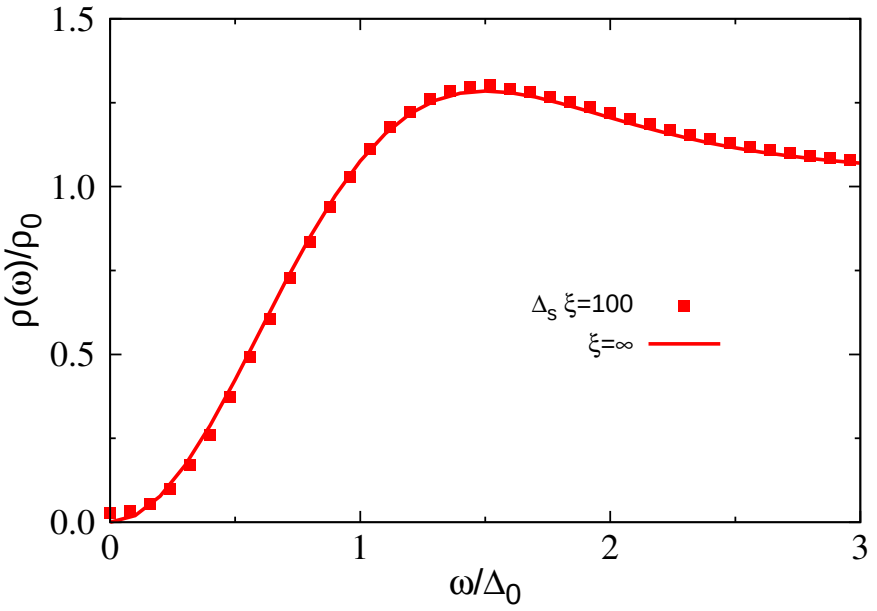

Figure 4.7: The calculated density of states for $\Delta_s\xi = 100.0$. The green dashed line shows the exact result for infinite correlation length. We can see that, for $\Delta_s\xi = 100.0$, the density of states is almost indistinguishable from the result for the infinite correlation length

We show both results in Fig. (4.7), as one can see, for $\Delta_s\xi = 100.0$, the result is almost the same as the result for the infinite correlation length.

Phase Fluctuations Only

In the phase fluctuations only case, the amplitudes of the order parameter fluctuations get frozen out, only the phase fluctuations remain. We can write the order parameter as $\Delta(x) = \Delta_s e^{i\vartheta(x)}$, where the amplitude is close to $T = 0$ value

$$\Delta_s \equiv \Delta_0(0) = 1.76 k_B T_c^{MF}. \tag{4.16}$$

In this case, the correlation functions are

$$\langle \Delta(x) \rangle = 0, \langle \Delta(x)\Delta(x') \rangle = 0, \tag{4.17}$$

$$\langle \Delta(x)\Delta^*(x') \rangle = \Delta_s^2 \exp(-|x - x'|/\xi(T)), \tag{4.18}$$

with

$$\xi(T) = \frac{s\rho_s(T)}{2T}. \tag{4.19}$$

Well below the mean-field critical temperature T_c^{MF}, $\rho_s(T) \approx \rho_0 = \pi^{-1}$, thus we can get

$$\Delta_s\xi(T) = 1.76 s T_c^{MF}/2\pi T. \tag{4.20}$$

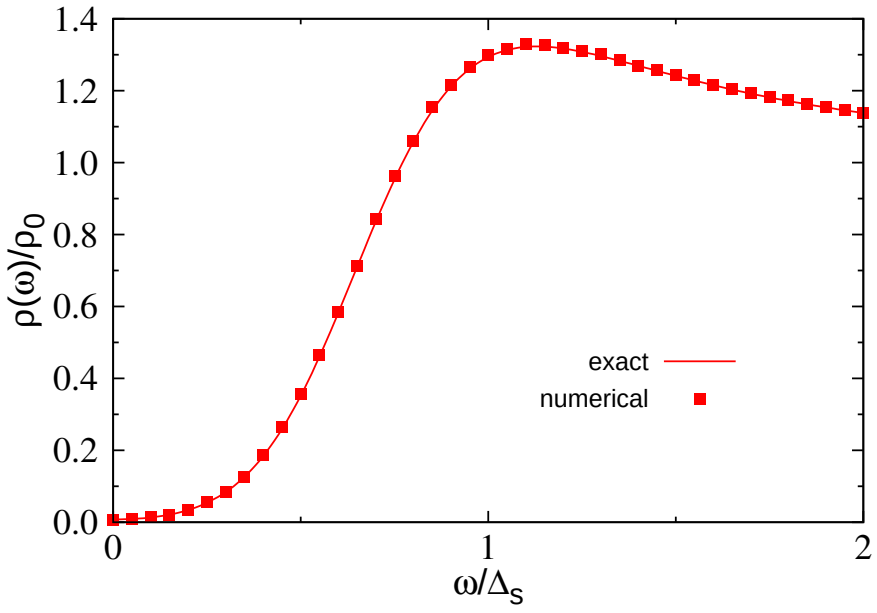

Figure 4.8: The density of states for the phase fluctuations only with correlation length $\Delta_s\xi = 2.0$. The solid line is the exact result given by the Eq. (4.21), and the dots are numerical results obtained using our method.

Using the gauge transformation, the phase fluctuations of the order parameter can be mapped onto the effective forward scattering potential $V(x) \equiv \partial_x\vartheta(x)$. Thus the integrated density of states is given by

$$N(\omega) = \rho_0 \frac{\sinh(2\pi\omega\xi)}{2\pi\xi} \frac{1}{|I_{i2\omega\xi}(2\Delta_s\xi)|^2}. \tag{4.21}$$

At the Fermi energy, the density of states simplifies to

$$\rho(0) = \frac{\rho_0}{|I_0(2\Delta_s\xi)|^2}. \tag{4.22}$$

As the temperature is lowered, the correlation length grows, the density of states vanishes exponentially,

$$\rho(0) \sim 4\pi\rho_0\Delta_s\xi \exp(-4\Delta_s\xi), 2\Delta_s\xi \gg 1. \tag{4.23}$$

This result is in contrast to the power-law behavior of the density of states in Gaussian statistics.

We plot our calculation in Fig. (4.9) for different correlation lengths, along with a comparison between our result and the exact result given by the Eq. (4.21) for $\Delta_s\xi = 2.0$. Also a plot of the density of states at the Fermi energy is shown in Fig. (4.10) as a function of $1/\Delta_s\xi$. For a comparison, we also plot $\rho(0)$ calculated using our method and the second-order Born approximation for Gaussian statistics with finite correlation lengths. As can be seen, for small correlation length, which corresponds to relative large temperature, all the results agree with each other. In contrast, at low temperature, where the correlation length becomes very large, the results for the phase fluctuations only decreases much faster. At

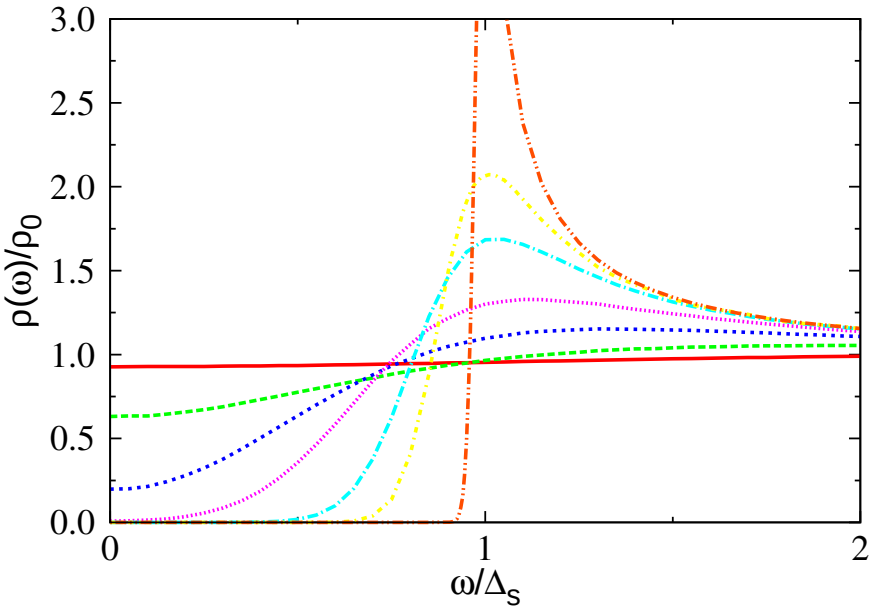

Figure 4.9: The density of states for the phase fluctuations only with finite correlation lengths $\Delta_s\xi = 0.2, 0.5, 1.0, 2.0, 5.0, 10.0, 100.0$.

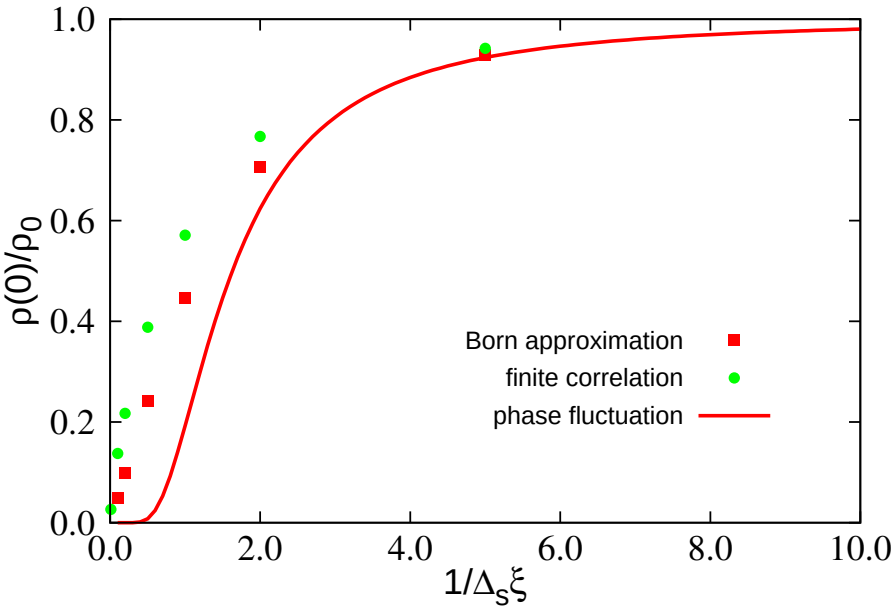

Figure 4.10: The density of states at the Fermi energy as a function of the inverse of the correlation length $1/\Delta_s\xi$. The green dots are results found in the second order Born approximation and red dots are results for Gaussian statistics with finite correlation length. The solid line gives the density of states for phase fluctuations only.

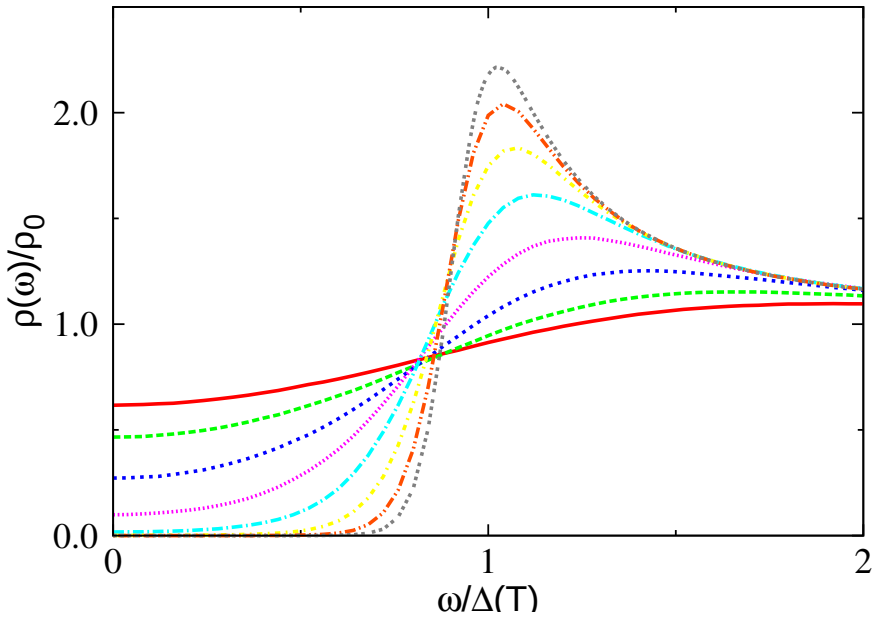

Figure 4.11: The density of states for the incommensurate case with non-Gaussian order parameter fluctuations. The temperature various from $\tau/\Delta\tau = -7 \ldots 0$ in step of one.

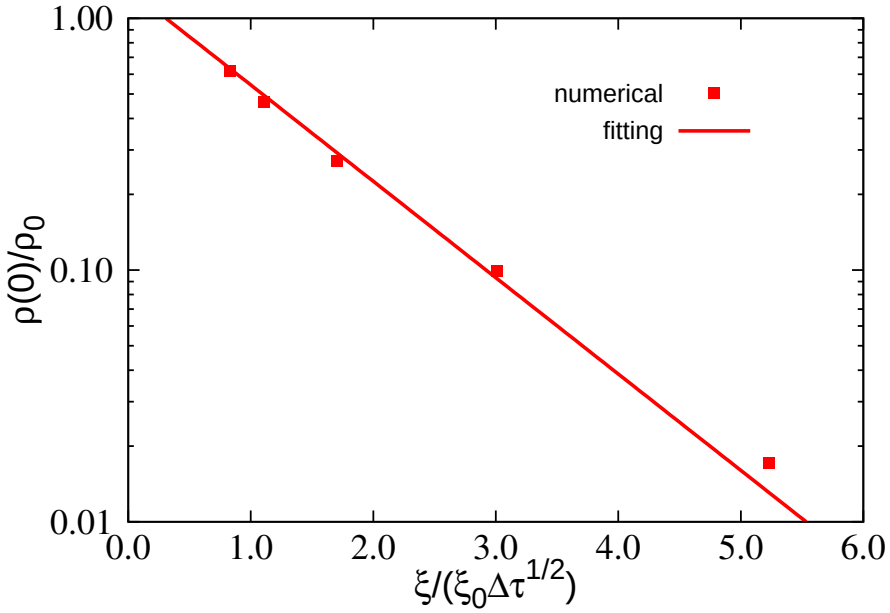

Figure 4.12: The logarithmic density of states at Fermi energy as a function of the correlation length. Notice that the y-axis is in logarithmic scale, which implies the density of states decreases exponentially as the correlation length grows.

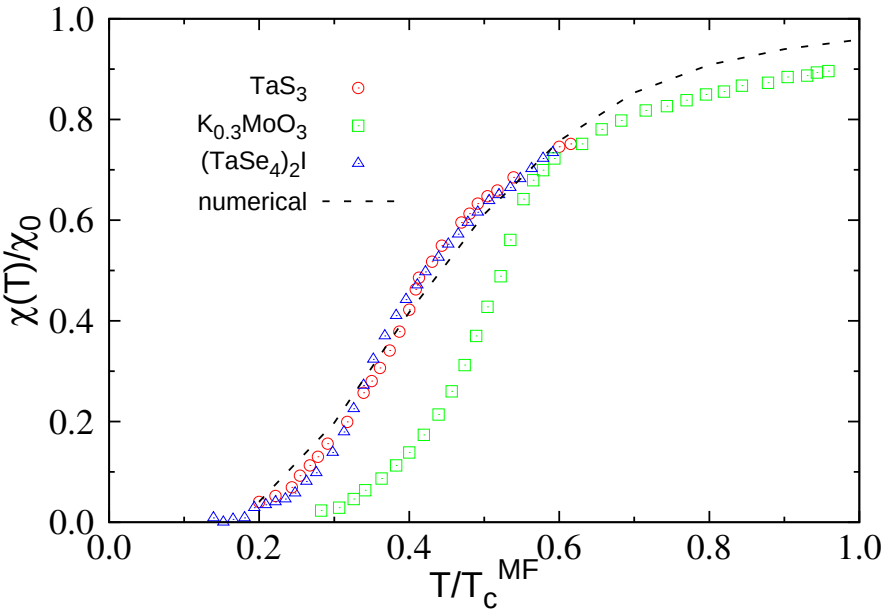

Figure 4.13: Static spin susceptibility $\chi(T)$ for various materials from [58] and numerical simulated result using the calculated density of states. The parameters are $\Delta_0 = 1.2T_c^{MF}$, $\Delta\tau = 0.1$.

$\Delta_s\xi \approx 2.0$, we find that the density of states $\rho(0)$ is significantly smaller than the results given by the Gaussian statistics, which corresponds to the temperature $T \approx T_c^{MF}/4$.

Non-Gaussian

At last, we give the results for the non-Gaussian order parameter fluctuations in Fig. (4.11) for different $\tau/\Delta\tau$. The density of states is suppressed very strongly even for relative high temperature. For low temperature, the density of states at low energy decreases exponentially as a function of the corresponding correlation length, this is just the characteristics of the phase only fluctuations. We use the correlation length calculated in Chapter 2 and plot the density of states at Fermi energy in Fig. (4.12) as a function of the corresponding correlation length ξ. We see that the density of states at the Fermi energy can be approximated by

$$\frac{\rho(0)}{\rho_0} = C \exp\left(-a\frac{\xi}{\xi_0\Delta\tau^{1/2}}\right), \tag{4.24}$$

the fitting parameters are

$$C = 1.31 \pm 0.15, a = 0.881 \pm 0.028. \tag{4.25}$$

4.2.2 Static Spin Susceptibility

The static spin susceptibility is defined as $\chi(T) \equiv dM(T)/dH$, where $M(T)$ is the magnetization density caused by a magnetic field H. An elementary calculation of the spin

susceptibility which can be found in the text book by Ashcroft and Mermin [59] shows that

$$\chi(T) = \mu_B^2 \int_{-\infty}^{\infty} d\omega 2\rho'(\omega) f(\omega), \tag{4.26}$$

where μ_B is the Bohr magneton and $f(\omega) = 1/(\exp(\omega/T)+1)$ is the Fermi function, $\rho'(\omega)$ is the derivative of the density of states with respect to frequency. The factor 2 comes from two spin directions. Integrating by parts we can get

$$\chi(T) = \mu_B^2 \int_{-\infty}^{\infty} d\omega 2\rho(\omega) \left(-\frac{df(\omega)}{d\omega}\right). \tag{4.27}$$

At zero temperature, we have $-df(\omega)/d\omega = \delta(\omega)$, then

$$\chi(T=0) = 2\mu_B^2 \rho(0). \tag{4.28}$$

For temperature not equal to zero, we can have

$$\frac{\chi(T)}{\chi_0} = \int_0^{\infty} \frac{d\omega}{2T} \frac{\rho(\omega)}{\rho_0} \frac{1}{\cosh(\omega/2T)^2}. \tag{4.29}$$

here $\chi_0 = 2\mu_B^2\rho_0$, and ρ_0 is the density of states for free fermions. Using the density of states we have calculated above, it is easy to calculate the spin susceptibility by just numerical integration. We plot our result in Fig. (4.13), along with experimental data for some materials. A good agreement can be seen from the plot.

4.2.3 Spectral Function

Now we come to the spectral function. As we have discussed in previous chapter, the spectral function can be obtained using

$$A(k;\omega) = 2\int_0^{2\pi} d\varphi \,\mathrm{Re}\, p_1(\varphi) p_0(-\varphi), \tag{4.30}$$

where p_1 and p_0 are stationary solutions to equations

$$\partial_x P_0(\varphi;x) = \left[-\partial_\varphi(2\omega + 2\Delta_0\cos\varphi) + 2\Delta_s^2\partial_\varphi^2\right] P_0, \tag{4.31}$$

$$\partial_x P_1(\varphi;x) = \left[-(2\omega + 2\Delta_0\cos\varphi - 2i\Delta_s^2)\partial_\varphi + 2\Delta_s^2\partial_\varphi^2 - i(k+\omega+\Delta_0 e^{i\varphi}) - \Delta_s^2\right] P_1 + P_0. \tag{4.32}$$

for Gaussian white noise. In other cases, the spectral function is given by

$$A(k,\omega) = 2\int_0^{+\infty} d\Delta \int_0^{2\pi} d\varphi \frac{\mathrm{Re}\, p_1(\Delta,\varphi) p_0(\Delta,-\varphi)}{P(\Delta)}. \tag{4.33}$$

Now the Fokker-Planck equations for $p_1(\Delta,\varphi)$ and $p_0(\Delta,\varphi)$ are

$$\partial_x P_0(\Delta,\varphi;x) = \left[-\partial_\Delta a(\Delta) + \frac{1}{2}\partial_\Delta^2 - \partial_\varphi(2\omega + 2\Delta\cos\varphi) + \frac{1}{2\Delta^2}\partial_\varphi^2\right] P_0, \tag{4.34}$$

$$\partial_x P_1(\Delta,\varphi;x) = \left[-\partial_\Delta a(\Delta) + \frac{1}{2}\partial_\Delta^2 - i(k+\omega+\Delta e^{i\varphi}) - (2\omega + 2\Delta\cos\varphi)\partial_\varphi + \frac{1}{2\Delta^2}\partial_\varphi^2\right] P_1 + P_0. \tag{4.35}$$

and $P(\Delta)$ are the distribution function of Δ.

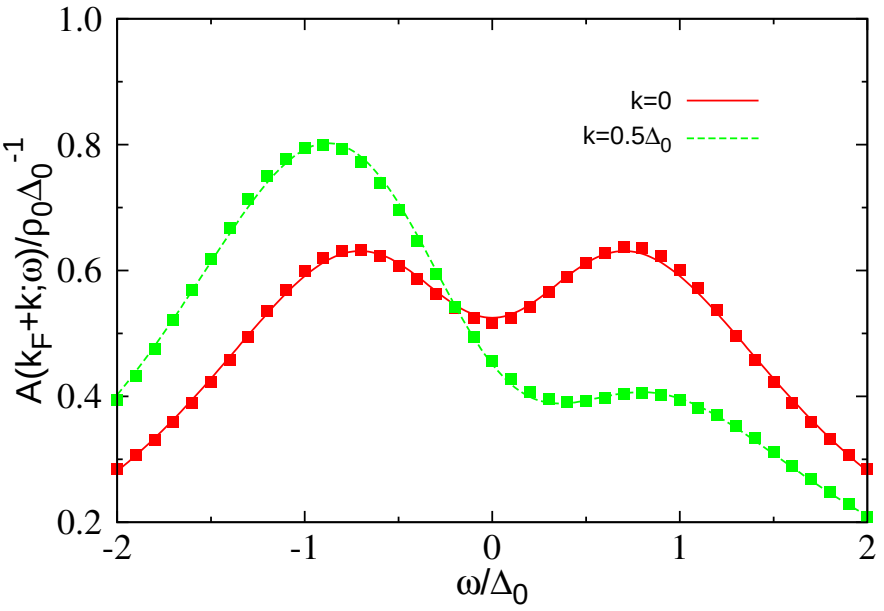

Figure 4.14: The calculated spectral function $A(k_F + k; \omega)$ for $k = 0$ and $k = 0.5\Delta_s$ with Gaussian white noise. The lines are results calculated using phase formalism, and dots represent our results. Both results show very good agreement.

Gaussian White

We compare our calculated results with those obtained using the phase formalism in Fig. (4.14). As we can see, two results are almost identical. Also we plot our calculation in Fig. (4.15) and (4.16) with $k = 0$ and $k = 0.5\Delta_s$ for different strength of the fluctuations. When Δ_0/Δ_s^2 is very large, the results approach the mean-field results,

$$A(k;\omega) = \frac{E_k + k}{2E_k}\delta(\omega - E_k) + \frac{E_k - k}{2E_k}\delta(\omega + E_k), \tag{4.36}$$

with

$$E_k = \sqrt{k^2 + \Delta_0^2}, \tag{4.37}$$

i.e. the spectral function contains two narrow peaks at $\omega = \pm E_k$. As Δ_0/Δ_s^2 decreases, the fluctuations become stronger and dominate. At the limit where there is no static gap, the pure Gaussian white noise should have no effect on spectral function in the incommensurate case, which means a quasi-particle peak should evolve at $\omega = k$, which in our plot, due to the rescale of the axis, is not very clear.

Finite Correlation lengths

We now present our results of the spectral function for Gaussian fluctuations with finite correlation length. In Fig. (4.17), we plot the spectral functions with the correlation length $\Delta_s\xi = 100.0$ in both symmetric $k = 0$ and asymmetric $k = 0.5\Delta_s$ cases. As we can

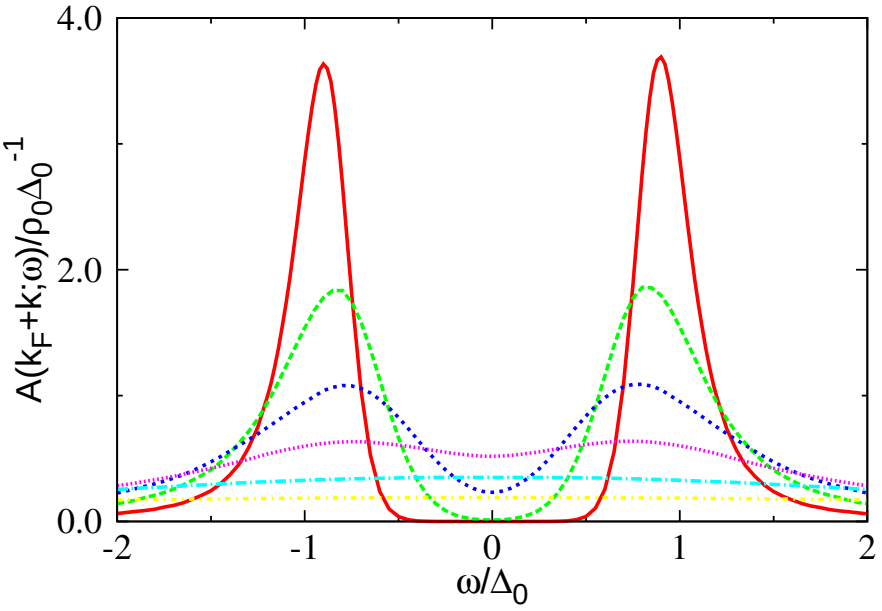

Figure 4.15: The spectral function $A(k_F + k; \omega)$ with $k = 0$ for Gaussian white noise and $\Delta_0/\Delta_s = 0.2, 0.5, 1.0, 2.0, 5.0, 10.0$.

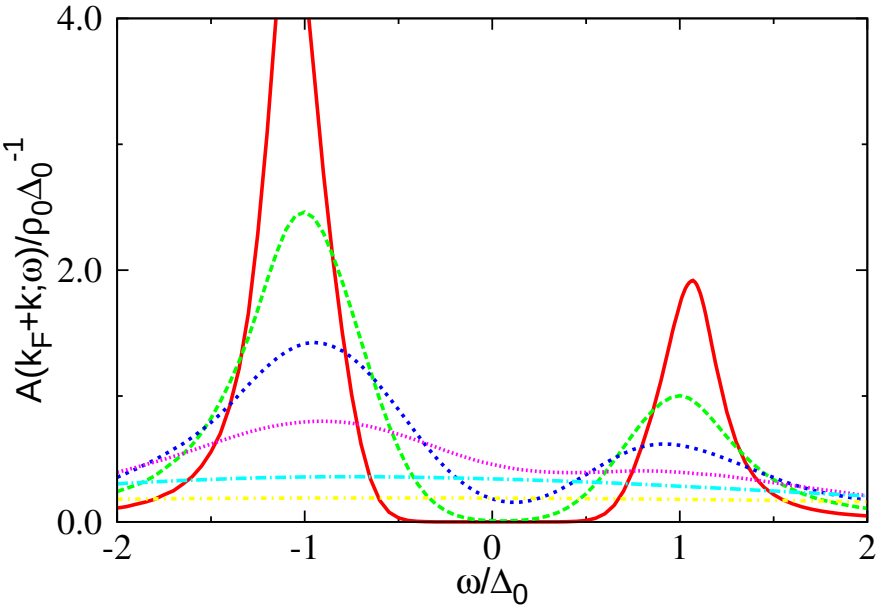

Figure 4.16: The spectral function $A(k_F + k; \omega)$ with $k = 0.5\Delta_s$ for Gaussian white noise and $\Delta_0/\Delta_s = 0.2, 0.5, 1.0, 2.0, 5.0, 10.0$.

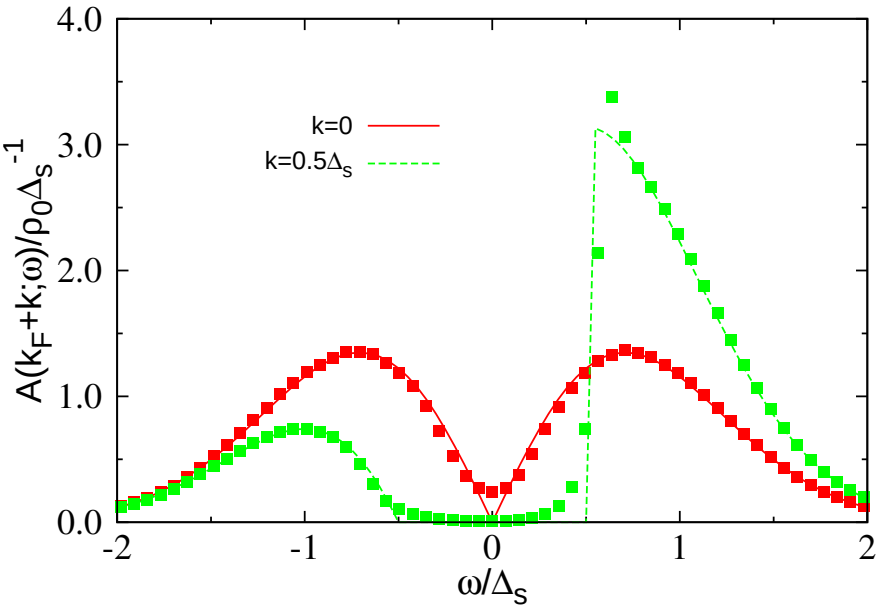

Figure 4.17: The spectral function $A(k_F + k; \omega)$ with $k = 0$ and $k = 0.5\Delta_s$. The red dots are the results for $k = 0, \Delta_s\xi = 100.0$, the blue ones are for $k = 0.5\Delta_s, \Delta_s\xi = 100$. The red line and dashed blue line are exact result for infinite correlation length with $k = 0$ and $k = 0.5\Delta_s$ respectively.

see, the results are very close to the exact results for infinite correlation length.

$$A(k;\omega) = \frac{1}{\Delta_s^2}\theta(\omega^2 - k^2)(\omega + k)e^{-(\omega^2-k^2)/\Delta_s^2}. \tag{4.38}$$

In the result for $k = 0.5\Delta_s$, the deviation at $\omega = k$ is due to the error of the numerical method we used to solve the Fokker-Planck equations. The spectral functions for Gaussian fluctuations with different correlation lengths are plotted in Fig. (4.18) for $k = 0$ and in Fig. (4.19) for $k = 0.5\Delta_s$ separately. In the symmetric case, there is a quasi-particle peak at $\omega = 0$ when the correlation length is small. As the correlation length increases, the peak broadens and finally splits into to peaks, which indicates the break down of the quasi-particle picture. While in the asymmetric case, the peak shifts to ω at around k, and the one close to $\omega = \alpha k$ has larger weight.

We also compare our results to those calculated using second-order Born approximation, which are presented in Fig. (4.20) and Fig. (4.21). For small correlation lengths, the second-order Born approximation gives almost the same result as our calculation, but for large correlation lengths, there is large discrepancy between them, which shows that the second-order Born approximation becomes unreliable in this region, and makes the calculation based on it questionable [2, 60].

non-Gaussian

The results for the non-Gaussian fluctuations are plotted in Fig. (4.22) and Fig. (4.23). From the results, we can see that, at relative large temperature, the spectral function is

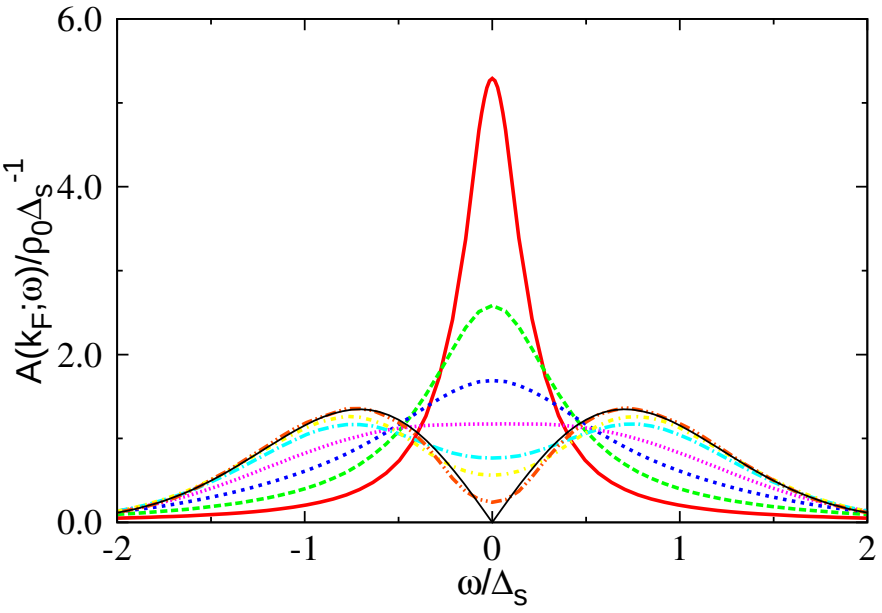

Figure 4.18: The spectral function $A(k_F + k; \omega)$ with $k = 0$ for Gaussian statistics with finite correlation lengths $\Delta_s \xi = 0.2, 0.5, 1.0, 2.0, 5.0, 10.0, 100.0$. The black line is the exact result for the infinite correlation length

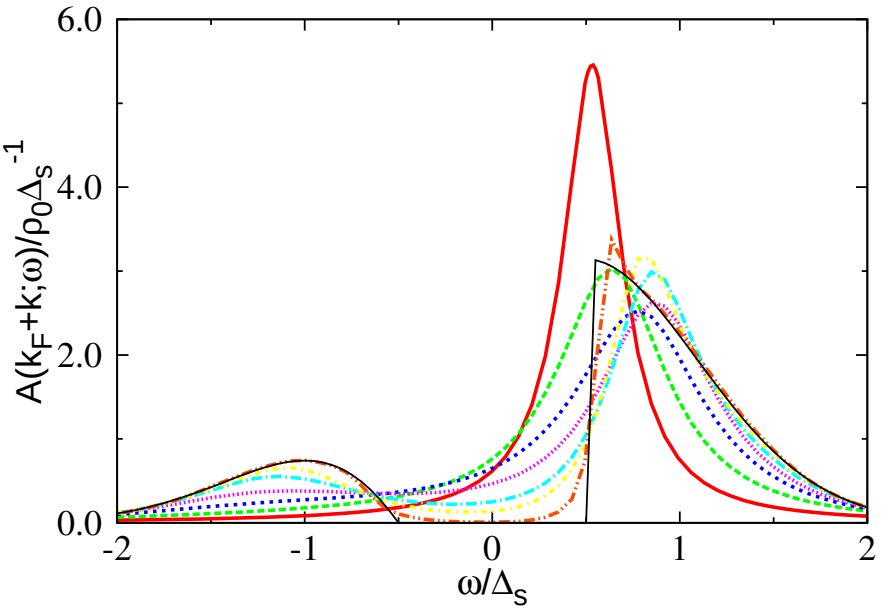

Figure 4.19: The spectral function $A(k_F + k; \omega)$ with $k = 0.5\Delta_s$ for Gaussian statistics with finite correlation lengths $\Delta_s \xi = 0.2, 0.5, 1.0, 2.0, 5.0, 10.0, 100.0$. The black line is the exact result for the infinite correlation length

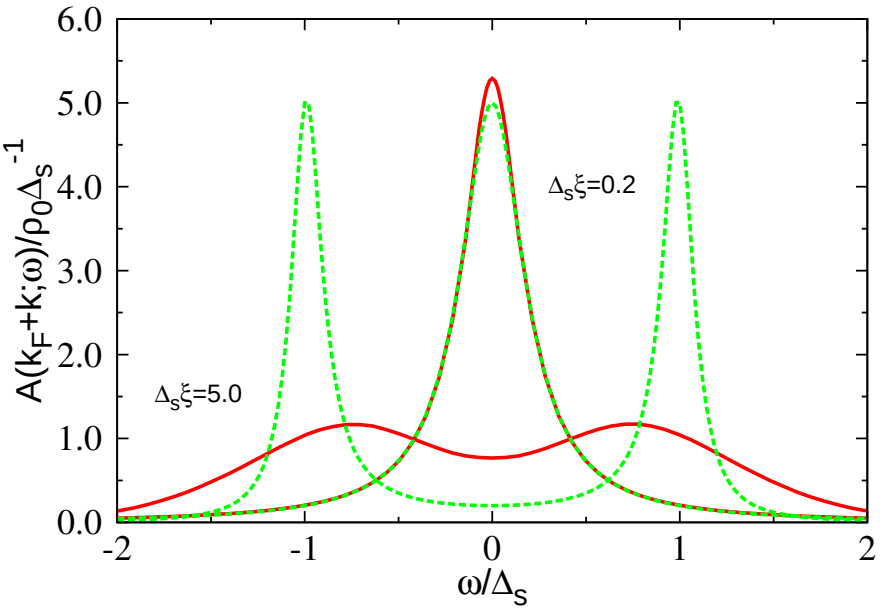

Figure 4.20: The spectral function $A(k_F + k; \omega)$ for $\Delta_s\xi = 0.2, 5.0$ with $k = 0$. The red lines are our calculation and the green dashed lines are results from the second-order Born approximation.

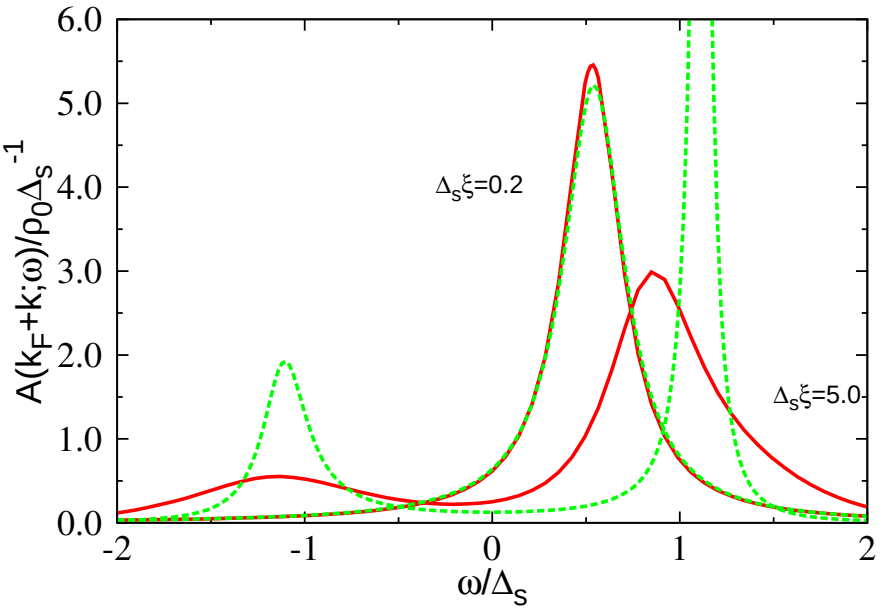

Figure 4.21: The spectral function $A(k_F + k; \omega)$ for $\Delta_s\xi = 0.2, 5.0$ with $k = 0.5\Delta_s$. The red lines are our calculation and the green dashed lines are results from the second-order Born approximation.

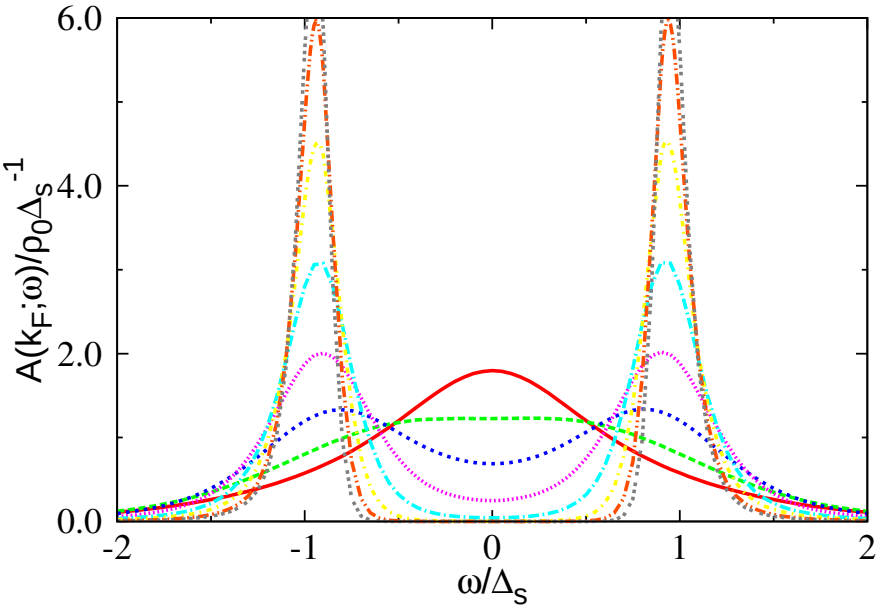

Figure 4.22: The spectral function $A(k_F + k; \omega)$ with $k = 0$ for non-Gaussian order parameter fluctuations and temperature $\tau/\Delta\tau = -7 \ldots 0$ in step of one.

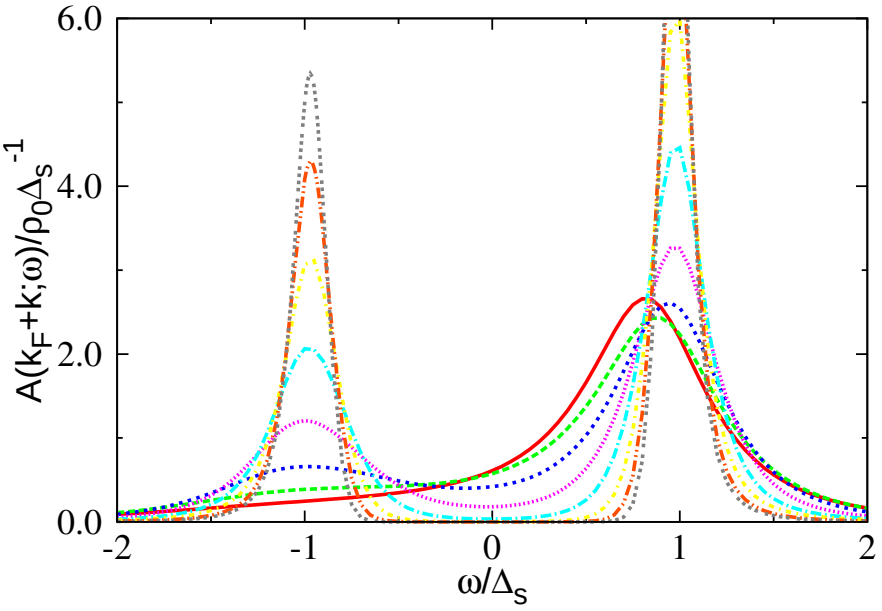

Figure 4.23: The spectral function $A(k_F + k; \omega)$ with $k = 0.5\Delta(T)$ for non-Gaussian order parameter fluctuations and temperature $\tau/\Delta\tau = -7 \ldots 0$ in step of one.

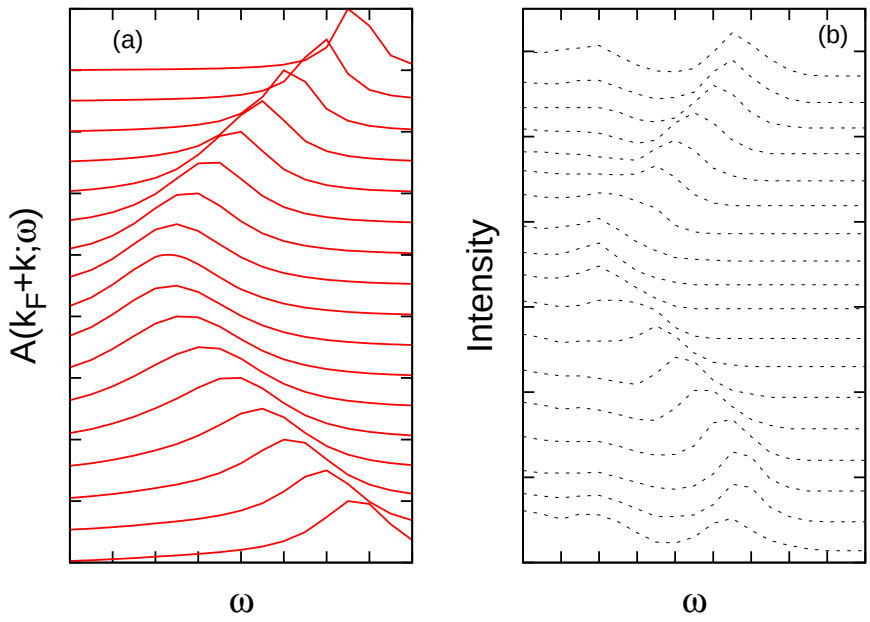

Figure 4.24: (a)The calculated $A^<(k;\omega)$ for $\tau/\Delta\tau = 5$ and $k = -2.0\Delta_s$ to $2.0\Delta_s$ in steps of 0.25.(b) The ARPES data for $(TaSe_4)_2I$ at temperature 60 K (Ref. [35])

similar to the result for Gaussian fluctuations with small correlation length. There is also a single quasi-particle peak, which appears at around $\omega = k$. For lower temperature, the peak also splits into two peaks, different from Gaussian case with large correlation length, the peak becomes much narrower. Also in contrast to the exact results for Gaussian fluctuations with finite correlation, for large correlation length, i.e. low temperature, the spectral function at low energy broadens significantly, and is similar to the results in second-order Born approximation.

4.2.4 Photoemission Spectroscopy

Now we will compare our results with experiments. The angle-resolved photoemission spectroscopy (ARPES) measures the spectral function directly [35, 36, 37, 38, 39]. The conventional interpretation of the ARPES line shape predicts that it is essentially proportional to [61]

$$I(k;\omega) = \sum_{k'\approx k} \sum_{\omega'\approx\omega} A^<(k';\omega'), \tag{4.39}$$

where

$$A^<(k;\omega) = \frac{A(k;\omega)}{e^{\beta\omega}+1} \tag{4.40}$$

is the spectral function multiplied with the Fermi function. In Fig. (4.24), we plot $A^<(k;\omega)$ with different k from -2 to 2 in steps of 0.25 for $\tau/\Delta\tau = -5.0$ in panel (a). As a comparison, we also show the ARPES data from Fig. 1(a) in Ref. [35]. Our results show a very similar patten as the experiments data shows.

4.2.5 Optical Conductivity

The optical conductivity is proportional to the optical absorption of a solid. For the quasi-one dimensional system, it also has been studied extensively both theoretically [62, 63, 64] and experimentally [11, 12]. For a one-dimensional system with Gaussian white noise the optical conductivity is given by the generally accepted Mott-Berezinskii law [63, 64, 65]

$$\sigma_1(\omega) \sim 4\sigma_0(\omega\tau)^2 \ln^2(\omega\tau). \tag{4.41}$$

Here σ_0 is the Drude conductivity, ω is the frequency and τ is the elastic-scattering time. When we consider the Gaussian fluctuations with finite correlation length and non-Gaussian fluctuations, the optical conductivity can be expressed as

$$\sigma_1(\omega) = \pi\omega_P^2 \int_{-\infty}^{+\infty} d\epsilon \frac{f(\epsilon) - f(\epsilon+\omega)}{\omega} F(\epsilon, \epsilon+\omega), \tag{4.42}$$

where

$$F(\epsilon, \epsilon') = 2\int_0^{+\infty} d\Delta \int_0^{2\pi} d\varphi \int_0^{2\pi} d\varphi' \frac{\mathrm{Re}\, p_1(\Delta, \varphi, \varphi') p_0(\Delta, -\varphi, -\varphi')}{P(\Delta)} \tag{4.43}$$

with $p_0(\Delta, \varphi, \varphi')$ and $p_1(\Delta, \varphi, \varphi')$ are stationary solutions to the following Fokker-Planck equations:

$$\partial_x P_0 = \left[\frac{(\partial_\varphi + \partial_{\varphi'})^2}{2\Delta^2} - 2\partial_\varphi(\epsilon + \Delta\cos\varphi) - 2\partial_{\varphi'}(\epsilon' + \Delta\cos\varphi') + \frac{\partial_\Delta^2}{2} - \partial_\Delta a\right] P_0, \tag{4.44}$$

$$\partial_x P_1 = \left[\frac{(\partial_\varphi + \partial_{\varphi'})^2}{2\Delta^2} - 2(\epsilon + \Delta\cos\varphi)\partial_\varphi - 2(\epsilon' + \Delta\cos\varphi')\partial_{\varphi'} - i(\epsilon' - \epsilon + \Delta e^{i\varphi'} - \Delta e^{-i\varphi}) + \frac{\partial_\Delta^2}{2} - \partial_\Delta a\right] P_1 + P_0. \tag{4.45}$$

Solving for the stationary solutions to Eqs. (4.44) and (4.45) is not an easy task. Different from the equations we solved for the density of states and the spectral function, equations here are parabolic partial differential equations. The absence of a diffusion term makes their numerical solutions unstable. However, adding a small but finite diffusion term $\kappa(\partial_\varphi - \partial_{\varphi'})^2$ turns the equations into elliptic partial differential equations which are numerical accessible. When we chose smaller and smaller κ, we can get stable solutions and for sufficiently small κ, the solutions are independent of κ.

Phase Fluctuations Only

First, we will consider a simpler case. We restrict ourselves to the phase fluctuations only, where Δ drops out of all equations and the coefficient of the term $(\partial_\varphi + \partial_{\varphi'})^2$ is $1/\xi$. In Fig. (4.25), we show the optical conductivity calculated for various correlation lengths and zero temperature. Unfortunately, we have not been able to calculate $\sigma_1(\omega)$ for very small ω. Since the dc conductivity of a one-dimensional disordered system is zero [55], we have extrapolated our calculation into low energy part. From Fig. (4.25), we can see that for larger correlation lengths, the optical conductivity has a peak at $\omega/\Delta_s = 2$. In

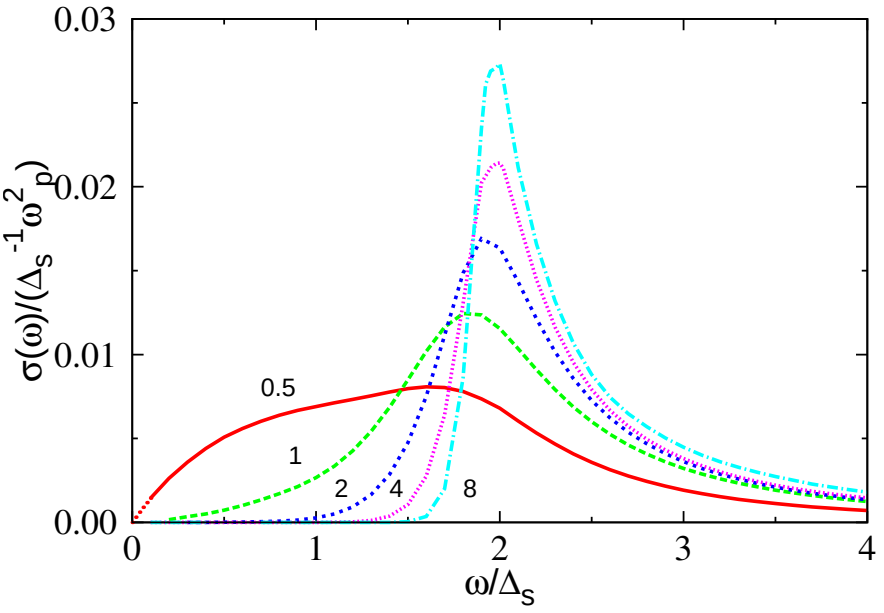

Figure 4.25: The optical conductivity for phase fluctuations only and $\Delta_s\xi = 0.5, 1, 2, 4, 8$. For $\Delta_s\xi = 0.5$ case, we have extrapolated the data between $\sigma(0) = 0$ and our numerical result.

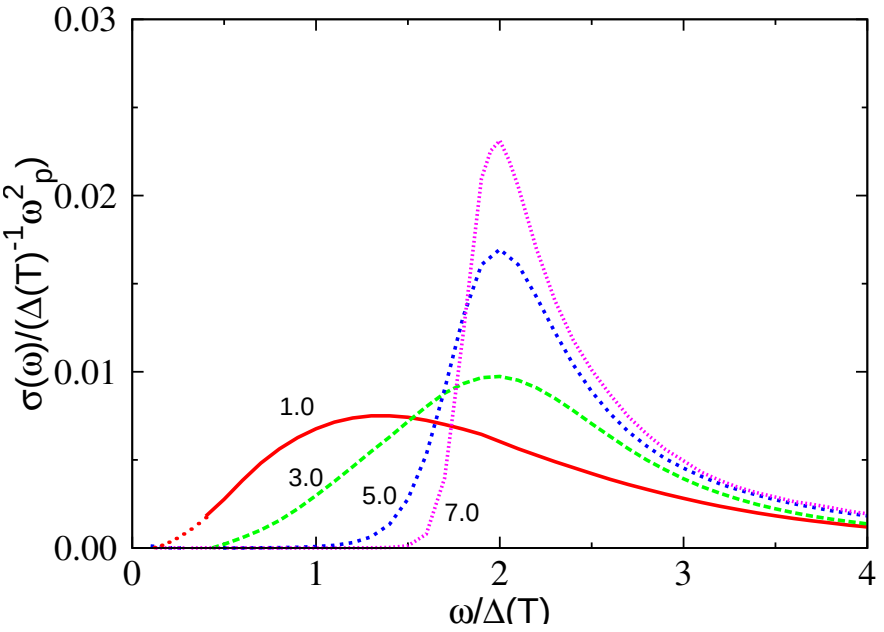

Figure 4.26: The optical conductivity for non-Gaussian order parameter fluctuations and temperature $\tau/\Delta\tau = -1.0, -3.0, -5. - 0, 7.0$. For $\tau/\Delta\tau = 1.0$ case, we have extrapolated the data between $\sigma(0) = 0$ and our numerical result.

the limit $\xi \to \infty$ the optical conductivity approaches the well-known result of a Peierls insulator [62]

$$\sigma_1(\omega) = \frac{\omega_p^2}{2} \frac{\Delta_s^2 \theta(\omega^2 - 4\Delta_s^2)}{\omega^2 \left(\omega^2 - 4\Delta_s^2\right)^{1/2}} \tag{4.46}$$

which has a square-root singularity at $\omega = 2\Delta_s$. As the correlation length decreases, the peak shifts to the low energy region and broadens significantly. In the pseudogap regime, $\sigma_1(\omega)$ shows a strong dependence on the correlation length. At large ω limit, however, all the results have the same asymptotic $1/\omega^3$-decay, which shows that for large ω the perturbation theory is accurate.

Non-Gaussian

We now present our calculation for non-Gaussian fluctuations. In Fig. (4.26), we plotted the optical conductivity for $\tau/\Delta\tau = -1.0, -3.0, -5.0, -7.0$. We also extrapolated our calculation at small ω region in $\tau/\Delta\tau = -1.0$ case. For large temperature, the optical conductivity shows similar behavior to the result with Gaussian fluctuations. When the temperature is lowered, the peak of the optical conductivity moves to the high energy region and $\sigma_1(\omega)$ also approaches to the Peierls insulator result. For large ω, the asymptotic $1/\omega^3$-decay also applies to all results at different temperature. In an early calculation based on the perturbative method [30], a finite dc conductivity was obtained. Our calculation, even though could not be applied to the calculation of the dc conductivity directly, gives a trend to a zero dc conductivity. Thus the finite results of the dc conductivity in the perturbative calculation must be an artifact.

Chapter 5

Conclusion

In this work, we have discussed the Fluctuating Gap Model (FGM) in a wide temperature range. The FGM was first proposed as an effective model to describe the low energy physics of the one-dimensional electron-phonon system. It is also of great interest in other physical contexts: Spin chains can be mapped by a Jordan-Wigner transformation onto the FGM and the higher-dimensional generalizations of the FGM have been used to explain the pseudogap-phenomenon in the underdoped high-temperature superconductors above the phase transition. Although this model is very important and large amount of effort has been made to understand it, all the previous work are restrict to the Gaussian statistics of the order parameters and thus are valid only in relative high temperature region. In order to get a better understanding of the FGM, we have developed an exact method to solve the FGM in a wide temperature range. In our method, the calculation of various electronic properties has been converted into solving a set of multidimensional Fokker-Planck equations. A simple quadrature of the stationary solutions to these Fokker-Planck equations then gives the density of states, the spectral function and the optical conductivity.

We calculated the density of states for order parameters $\Delta_0 + \vec{\Delta}(x)$, where Δ_0 is a static gap potential and $\vec{\Delta}(x)$ are Gaussian white noise with $\left\langle \vec{\Delta}(x)\vec{\Delta}^*(x') \right\rangle = \Delta_s^2 \delta(x-x')$. In the commensurate case, our calculation confirms the Dyson singularity at around the Fermi energy when $\Delta_0/\Delta_s^2 < 1/2$. In contrast, for the complex order parameters, there is no such singularity in any cases, and the fluctuations only lead to a filling up of the static gap. When the order parameters are Gaussian with finite correlation lengths, i.e. $\left\langle \vec{\Delta}(x)\vec{\Delta}^*(x') \right\rangle = \Delta_s^2 e^{-|x-x'|/\xi}$, the density of states at Fermi energy $\rho(0)$ decreases as a function of the correlation length $\Delta_s\xi$, which indicates an opening of a pseudogap, and can be described by the numerical fitting $\rho(0)/\rho_0 = C\left(\Delta_s\xi\right)^{-\mu}$, with the fitting parameters $C = 0.61200 \pm 0.027124, \mu = 0.673449 \pm 0.01822$. The pow-law behavior is similar with those obtained in the second-order Born approximation calculation. We also calculated the density of states for non-Gaussian order parameter fluctuations. However the results show that for small temperature the zero-point density of states vanishes exponentially as $\rho(0)/\rho_0 = C\exp\left(-a\xi/\xi_0\Delta\tau^{1/2}\right)$, where $C = 1.31 \pm 0.15, a = 0.881 \pm 0.028$. This exponential behavior has the same character as in the phase fluctuations only case when $2\Delta_s\xi \gg 1$, which concludes that for small temperature, the amplitude of the order parameter fluctuations get frozen out and only the phase fluctuations contribute. Using the density of states we calculated for the non-Gaussian fluctuations, we also obtained

the static spin susceptibility, and the numerical results shows good agreement with the experimental data.

The spectral functions for different statistics of the order parameter fluctuations also have been obtained. In the case of the Gaussian white noise limit, the resulted spectral function shows two peaks at around $\omega = \pm\sqrt{\Delta_0^2 + k^2}$ for large Δ_0/Δ_s^2, and it approaches the mean-field result as $\Delta_0/\Delta_s^2 \to \infty$. The results for the Gaussian fluctuations with finite correlation lengths show quasi-particle peaks at $\omega = k$ for small correlation lengths. As the correlation length increases, the spectral function approaches the exact result for infinite correlation length limit. The quasi-particle peak at small correlation lengths broadens and finally splits into two peaks, which indicates a break down of the Fermi-liquid picture. A comparison of the perturbative results and our results shows that the perturbative calculation is valid when the correlation lengths are small. However the great deviation for large correlation lengths fails the validity of the perturbation theory in this regime. Our results for non-Gaussian order parameters can be used to explain the experimental angle-resolved photoemission spectroscopy (ARPES) data, which exhibits the common non-Fermi-liquid features and the absence of a Fermi edge.

In the calculation of the optical conductivity, the results for phase fluctuations and non-Gaussian order parameters have been presented. For low temperature or large correlation lengths, the results approach the well-known Peierls insulator result. The asymptotic $1/\omega^3$-decay applies to all of the results at large ω. As the temperature increases, or the correlation length decreases, the peak of the optical conductivity broadens and shifts to the low energy region, and the line shape have a very strong dependence on the temperature or the correlation length ξ. At small ω, our calculation gives a zero dc conductivity which is differ from previous perturbative calculation within the same model. We argue that the finite dc conductivity calculated to the first order in perturbation theory is just an artifact of the perturbation theory.

List of Figures

Bibliography

[1] R. E. Peierls. *Quantum Theory of Solids*. Oxford Univ. Press, Oxford, England, 1955. i, 1

[2] P. A. Lee, T. M. Rice, and P. W. Anderson. Fluctuation effects at a peierls transition. *Phys. Rev. Lett.*, 31(7):462–465, Aug 1973. i, 1, 2, 3, 18, 82

[3] B. Dardel, D. Malterre, M. Grioni, P. Weibel, Y. Baer, and F. Lévy. Unusual photoemission spectral function of quasi-one-dimensional metals. *Phys. Rev. Lett.*, 67(22):3144–3147, Nov 1991. i, 2

[4] J. M. Ziman. Electrons in liquid metals and other disordered systems. *Proc. R. Soc. Lond. A*, 318:401, 1970. i, 2

[5] J. A. Hertz and M. A. Klenin. Fluctuations in itinerant-electron paramagnets. *Phys. Rev. B*, 10(3):1084–1096, Aug 1974. i, 2

[6] D. Waxman. The low-energy, local density of states of an isolated vortex in an extreme type ii superconductor. *Ann. Phys.*, 223:129–148, 1993. i, 2

[7] Nils Schopohl and Kazumi Maki. Quasiparticle spectrum around a vortex line in a d-wave superconductor. *Phys. Rev. B*, 52(1):490–493, Jul 1995. i

[8] Nils Schopohl. Transformation of the eilenberger equations of superconductivity to a scalar riccati equation. *arXiv:cond-mat/9804064*, 1998. i

[9] D. C. Johnston. Thermodynamics of charge-density waves in quasi one-dimensional conductors. *Phys. Rev. Lett.*, 52(23):2049–2052, Jun 1984. 1, 18

[10] L. Degiorgi, G. Grüner, K. Kim, R. H. McKenzie, and P. Wachter. Optical probing of thermal lattice fluctuations in charge-density-wave condensates. *Phys. Rev. B*, 49(20):14754–14757, May 1994. 1

[11] A. Schwartz, M. Dressel, B. Alavi, A. Blank, S. Dubois, G. Grüner, B. P. Gorshunov, A. A. Volkov, G. V. Kozlov, S. Thieme, L. Degiorgi, and F. Lévy. Fluctuation effects on the electrodynamics of quasi-one-dimensional conductors above the charge-density-wave transition. *Phys. Rev. B*, 52(8):5643–5652, Aug 1995. 1, 18, 87

[12] L. Degiorgi, St. Thieme, B. Alavi, G. Grüner, R. H. McKenzie, K. Kim, and F. Levy. Fluctuation effects in quasi-one-dimensional conductors: Optical probing of thermal lattice fluctuations. *Phys. Rev. B*, 52(8):5603–5610, Aug 1995. 1, 87

[13] A. A. Ovchinnikov and N. S. Erikhman. *Sov. Phys. JETP*, 46:340, 1977. 2, 69

[14] M. V. Sadovskii. A model of a disordered system (a contribution to the theory of "liquid semiconductors"). *Sov. Phys. JETP*, 39:845, 1974. 2

[15] M. V. Sadovskii. Exact solution for the density of electronic states in a model of a disordered system. *Sov. Phys. JETP*, 50:989, 1979. 2, 71

[16] Ross H. McKenzie and David Scarratt. Non-fermi-liquid behavior due to short-range order. *Phys. Rev. B*, 54(18):R12709–R12712, Nov 1996. 2, 3

[17] Jörg Schmalian, David Pines, and Branko Stojković. Weak pseudogap behavior in the underdoped cuprate superconductors. *Phys. Rev. Lett.*, 80(17):3839–3842, Apr 1998. 2, 3

[18] Jörg Schmalian, David Pines, and Branko Stojković. Microscopic theory of weak pseudogap behavior in the underdoped cuprate superconductors: General theory and quasiparticle properties. *Phys. Rev. B*, 60(1):667–686, Jul 1999. 2, 3

[19] Oleg Tchernyshyov. Pseudogap in one dimension. *Phys. Rev. B*, 59(2):1358–1368, Jan 1999. 2

[20] A. J. Millis and H. Monien. Pseudogaps in one-dimensional models with quasi-long-range order. *Phys. Rev. B*, 61(18):12496–12502, May 2000. 2

[21] Lorenz Bartosch and Peter Kopietz. Exact numerical calculation of the density of states of the fluctuating gap model. *Phys. Rev. B*, 60(23):15488–15491, Dec 1999. 2

[22] Lorenz Bartosch and Peter Kopietz. Classical phase fluctuations in incommensurate peierls chains. *Phys. Rev. B*, 62(24):R16223–R16226, Dec 2000. 2

[23] Lorenz Bartosch. Fluctuation effects in disordered peierls systems. *Ann. Phys.*, 10:799–857, 2001. 2

[24] Hartmut Monien. Exact results for the crossover from gaussian to non-gaussian order parameter fluctuations in quasi-one-dimensional electronic systems. *Phys. Rev. Lett.*, 87(12):126402, Aug 2001. 2, 19

[25] Bertrand I. Halperin. Green's functions for a particle in a one-dimensional random potential. *Phys. Rev.*, 139(1A):A104–A117, Jul 1965. 2, 3, 55, 58, 60

[26] Lorenz Bartosch. Non-fermi-liquid behavior of quasi-one-dimensional pseudogap materials. *Phys. Rev. Lett.*, 90(7):076404, Feb 2003. 2

[27] L. Bartosch. Optical conductivity of a quasi-one-dimensional system with fluctuating order. *Europhys. Lett.*, 65:68–74, 2004. 2

[28] Ross H. McKenzie. Microscopic theory of the pseudogap and peierls transition in quasi-one-dimensional materials. *Phys. Rev. B*, 52(23):16428–16442, Dec 1995. 2

[29] Nic Shannon and Robert Joynt. Interpretation of photoemission spectra of $(TaSe_4)_2I$ as evidence of charge-density-wave fluctuations. *J. Phys. Condens. Matter*, 8:10493–10509, 1996. 2

[30] N. Shannon and R. Joynt. The spectral, structural and transport properties of the pseudogap system $(TaSe_4)_2I$. *Solid State Communications*, 115:411–415, 2000. 2, 67, 89

[31] A. G. Loeser, Z.-X. Shen, D. S. Dessau, D. S. Marshall, C. H. Park, P. Fournier, and A. Kapitulnik. Excitation Gap in the Normal State of Underdoped $Bi_2Sr_2CaCu_2O_{8+\delta}$. *Science*, 273:325–329, 1996. 2

[32] H. Ding, T. Yokoya, J. C. Campuzano, T. Takahashi, M. Randeria, M. R. Norman, T. Mochiku, K. Kadowaki, and J. Giapintzakis. Spectroscopic evidence for a pseudogap in the normal state of underdoped high-T_c superconductors. *Nature*, 382:51–54, 1996. 2

[33] Andrea Damascelli, Zahid Hussain, and Zhi-Xun Shen. Angle-resolved photoemission studies of the cuprate superconductors. *Rev. Mod. Phys.*, 75(2):473–541, Apr 2003. 2

[34] Y. Hwu, P. Alméras, M. Marsi, H. Berger, F. Lévy, M. Grioni, D. Malterre, and G. Margaritondo. Photoemission near the fermi energy in one dimension. *Phys. Rev. B*, 46(20):13624–13626, Nov 1992. 2

[35] A. Terrasi, M. Marsi, H. Berger, G. Margaritondo, R. J. Kelley, and M. Onellion. Temperature dependence of electronic states in $(TaSe_4)_2\,I$. *Phys. Rev. B*, 52(8):5592–5597, Aug 1995. 2, 86, 96

[36] J. Voit, L. Perfetti, F. Zwick, H. Berger, G. Margaritondo, G. Grüner, H. Höchst, and M. Grioni. Electronic structure of solids with competing periodic potentials. *Science*, 290:501–503, 2000. 2, 39, 86

[37] L. Perfetti, H. Berger, A. Reginelli, L. Degiorgi, H. Höchst, J. Voit, G. Margaritondo, and M. Grioni. Spectroscopic Indications of Polaronic Carriers in the Quasi-One-Dimensional Conductor $(TaSe_4)_2I$. *Phys. Rev. Lett.*, 87(21):216404, Nov 2001. 2, 86

[38] J. Schäfer, Eli Rotenberg, S. D. Kevan, P. Blaha, R. Claessen, and R. E. Thorne. High-Temperature Symmetry Breaking in the Electronic Band Structure of the Quasi-One-Dimensional Solid $NbSe_3$. *Phys. Rev. Lett.*, 87(19):196403, Oct 2001. 2, 18, 86

[39] L. Perfetti, S. Mitrovic, G. Margaritondo, M. Grioni, L. Forró, L. Degiorgi, and H. Höchst. Mobile small polarons and the Peierls transition in the quasi-one-dimensional conductor $K_0.3MoO_3$. *Phys. Rev. B*, 66(7):075107, Aug 2002. 2, 86

[40] J. Fröhlich. On the theory of superconductivity: The one-dimensional case. *Proc. R. Soc. Lond. A*, 233:296, 1954. 3, 4

[41] John W. Negele and Henri Orland. *Quantum Many-Particle Systems*. Addison-Wesley Publishing Company, Redwood City, 1988. 5, 26

[42] Lorenz Bartosch. *Singularities and Pseudogaps in the Density of States of the Fluctuating Gap Model*. PhD thesis. 5, 22

[43] M. Tinkham. *Introduction to Superconductivity.* Mc Graw-Hill, New York, 1996. 12

[44] N. D. Mermin and H. Wagner. Absence of ferromagnetism or antiferromagnetism in one- or two-dimensional isotropic heisenberg models. *Phys. Rev. Lett.*, 17(22):1133–1136, Nov 1966. 18

[45] M.J. Rice and S. Strässler. Effects of fluctuations and interchain coupling on the peierls transition. *Solid State Commun.*, 13:1389–1392, 1973. 18

[46] D. J. Scalapino, Y. Imry, and P. Pincus. Generalized ginzburg-landau theory of pseudo-one-dimensional systems. *Phys. Rev. B*, 11(5):2042–2048, Mar 1975. 18

[47] D. J. Scalapino, M. Sears, and R. A. Ferrell. Statistical mechanics of one-dimensional ginzburg-landau fields. *Phys. Rev. B*, 6(9):3409–3416, Nov 1972. 19, 23, 34

[48] Lorenz Bartosch and Peter Kopietz. Algorithm for obtaining the gradient expansion of the local density of states and the free energy of a superconductor. *Phys. Rev. B*, 60(10):7452–7457, Sep 1999. 22

[49] George Grüner. *Desity Waves in Solids.* Addison-Wiley, Reading, 1994. 23

[50] Josef Honerkamp. *Stochastic Dynamical System : Concepts, Numerical Methods, Data Analysis.* VCH publishers, New York, N.Y., 1994. 27

[51] Barry Simon and A. Dicke. Coupling constant analyticity for the anharmonic oscillator. *Ann. Phys.*, 58:76–136, 1970. 28

[52] Charles Schwartz. A study of some approximation schemes in quantum mechanics. *Ann. Phys.*, 32:277–291, 1965. 28

[53] A. A. Ovchinnikov and N. S. Erikhman. Temperature and frequency dependence of the electron conductivity in a two-band model with impurities. *Sov. Phys. JETP*, 51:728–734, 1980. 52

[54] J. Rammer and H. Smith. Quantum field-theoretical methods in transport theory of metals. *Rev. Mod. Phys.*, 58(2):323–359, Apr 1986. 52

[55] I. M. Lifshits, S. A. Gredeskul, and L. A. Pastur. *INTRODUCTION TO THE THEORY OF DISORDERED SYSTEMS.* Wiley, New York. New York, 1988. 68, 87

[56] Freeman J. Dyson. The dynamics of a disordered linear chain. *Phys. Rev.*, 92(6):1331–1338, Dec 1953. 69

[57] A. A. Golub and Y. M. Chumakov. *Sov. J. Low Temp. Phys.*, 5:427, 1980. 69

[58] D. C. Johnston, M. Maki, and G. Grüner. Influence of charge density wave fluctuations on the magnetic susceptibility of the quasi one-dimensional conductor $(TaSe_4)_2I$. *Solid State Commum.*, 53:5–8, 1985. 78, 95

[59] N. W. Ashcroft and N. D. Mermin. *Solid State Physics.* Saunders College Publishing, Philadelphia, 1988. 79

[60] B. Dumoulin, C. Bourbonnais, S. Ravy, J. P. Pouget, and C. Coulon. Fluctuation effects in low-dimensional spin-peierls systems: Theory and experiment. *Phys. Rev. Lett.*, 76(8):1360–1363, Feb 1996. 82

[61] G. H. Gweon, J. D. Denlinger, J. W. Allen, R. Claessen, C. G. Olson, H. Höchst, J. Marcus, C. Schlenker, and L. F. Schneemeyer. Arpes line shapes in fl and non-fl quasi-low-dimensional inorganic metals. *J. Electron Spectrosc. Relat. Phenom.*, 117-118:481–502, 2001. 86

[62] P. A. Lee, T. M. Rice, and P. W. Anderson. Conductivity from charge or spin density wave. *Solid State Communications*, 14:703–709, 1974. 87, 89

[63] V. L. Berezinskii. Kinetics of a quantum particle in a one-dimensional random potential. *Sov. Phys. JETP*, 38:620–627, 1974. 87

[64] A. A. Abrikosov and I. A. Ryzhkin. Conductivity of quasi-one-dimensional metal systems. *Sov. Phys. JETP*, 44:630–640, 1976. 87

[65] Michael M. Fogler and Ziqiang Wang. Comment on "analytic structure of one-dimensional localization theory: Reexamining mott's law". *Phys. Rev. Lett.*, 86(20):4715, May 2001. 87